THE JOURNAL
OF
CHEMICAL PHYSICS

VOLUME 6 MAY, 1938 NUMBER 5

Chemical Reactions of Organic Compounds with X-Ray Activated Water *

HUGO FRICKE, EDWIN J. HART AND HOMER P. SMITH
Walter B. James Laboratory for Biophysics, The Biological Laboratory, Cold Spring Harbor, L. I., N. Y.

(Received September 18, 1937)

Gas free solutions of carbon monoxide, alcohols, aldehydes, ketones and acids were irradiated in the concentration range 10 μM to 1 M, between pH = 1 to 13 and the reactions studied principally by gas analysis and potentiometric acid analysis. One organic component systems and, to a more limited extent, two organic component systems were investigated. To obtain significant results, foreign organic matter must be strictly excluded from the low concentration solutions and the methods used to accomplish this are described. Organic impurities in the water can be detected by irradiating the water with x-rays and measuring the evolved hydrogen and carbon dioxide. The reactions cannot be briefly abstracted, but oxidation and condensation reactions with the evolvement of gaseous hydrogen are important in the effect of the rays. Carbon dioxide was produced from certain acids, particularly strongly from those having an oxygen containing group in the α-position. No liberation of carbon monoxide, hydrocarbons or oxygen was found. The effect of the rays on all the compounds studied depends on the hydrogen ion concentration, this factor affecting reaction rates as well as the nature of the reactions. The relation of reaction rate to pH can in some cases be represented by

$$[P] = A(1+10^{-p\mathrm{H}+\alpha}/1+10^{-p\mathrm{H}+\alpha}).$$

The rates of the reactions are in many cases independent of concentration, at high concentrations, but generally the rates decrease at low concentrations. The reason for this decrease may be the deactivation of the activated water, although this interpretation would, because of the form of the reaction product concentration curves, lead to the conclusion that the deactivation is approximately monomolecular (rather than bimolecular) during its initial stage. The same conclusion is indicated since the reaction rates are independent of x-ray intensity down to the lowest concentrations used. The x-ray reactions show some similarity to, but they are generally more complex than, the reactions produced by water activated with light inside the absorption band at 1900A. The irradiation of formic acid in the presence of oxygen at pH = 3, results in a smaller decomposition of the formic acid than is produced in the absence of oxygen and a higher production of hydrogen peroxide than is obtained when oxygen is irradiated alone. This increased hydrogen peroxide production can be accounted for as resulting from the reaction of the oxygen with the nascent hydrogen liberated in the organic reaction.

THE chemical effects produced by irradiating dilute solutions with x-rays have been the subject of considerable study.[1–6] To explain the results it was found necessary to assume that the rays produce active derivatives of the water

* This work was supported by grants from the Committee on Radiations of the National Research Council.

[1] O. Risse, Zeits. f. physik. Chemie **A140**, 133 (1929).

[2] H. Fricke and E. R. Brownscombe. Phys. Rev. **44**, 240 (1933).

[3] *a*, H. Fricke and B. W. Petersen, Am. J. Roent. and Rad. Therap. **17**, 611 (1927). *b*, H. Fricke and S. Morse, Am. J. Roent. and Rad. Therap. **18**, 426 (1927). *c*, H. Fricke and S. Morse, Phil. Mag. **7**, 129 (1929). *d*, H. Fricke and E. R. Brownscombe, J. Am. Chem. Soc. **55**, 2358 (1933). *e*, H. Fricke, J. Chem. Phys. **2**, 556 (1934). *f*, H. Fricke and E. J. Hart, J. Chem. Phys. **2**, 824 (1934). *g*, H. Fricke and E. J. Hart, J. Chem. Phys. **3**, 60 (1935). *h*, H. Fricke and E. J. Hart, J. Chem. Phys. **3**, 596 (1935). *i*, H. Fricke, J. Chem. Phys. **3**, 364 (1935). *j*, H. Fricke, J. Chem. Phys. **3**, 365 (1935).

[4] *a*, W. Stenstrom and A. Lohmann, J. Biol. Chem. **79**, 673 (1928). *b*, W. Stenstrom, Radiology **13**, 437 (1929). *c*, W. Stenstrom and A. Lohmann, Radiology **16**, 322 (1931). *d*, W. Stenstrom and A. Lohmann, Radiology **17**, 432 (1931). *e*, W. Stenstrom and A. Lohmann, Radiology **21**, 29 (1933). *f*, W. Stenstrom and A. Lohmann, Radiology **22**, 304 (1934).

[5] R. Glocker and O. Risse, Zeits. f. Physik. **48**, 845 (1928).

[6] *a*, G. L. Clark, L. W. Pickett and E. D. Johnson, Radiology **15**, 245 (1930). *b*, G. L. Clark and L. W. Pickett, J. Am. Chem. Soc. **52**, 465 (1930). *c*, G. L. Clark and K. R. Fitch, Radiology **17**, 285 (1931). *d*, G. L. Clark and W. S. Coe, J. Chem. Phys. **5**, 97 (1937).

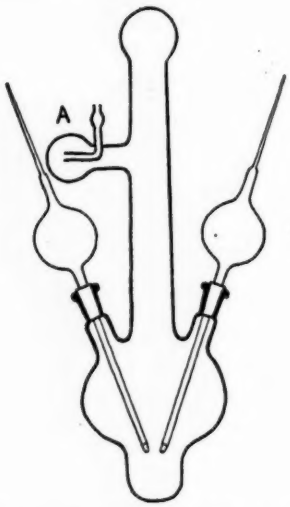

FIG. 1. Evacuation chamber with reaction cells.

molecule which react with the dissolved substances.[4] No decomposition was observed when water was irradiated under the same conditions.[1,2,7] The reactions show a certain similarity to, but they are more complex than, those produced when the water is activated with ultraviolet light inside the absorption band at 1900A.[8] This band is continuous and it is generally connected with the transition $H_2O \rightarrow H + OH$. Nevertheless, as in the case of x-rays, no decomposition was observed when water was irradiated with ultraviolet light in this region of wave-length.[7,8]

The present paper deals with the effect of x-rays on solutions of organic materials. These include carbon monoxide and alcohols, aldehydes, ketones and acids of the aliphatic series. The reactions were studied chiefly by a determination of the gases produced. Electrometric acid analysis was a useful method of inquiry in a number of the reactions.

The greater part of the work is concerned with reactions in solutions containing one organic component. The reactions in systems containing two organic components were studied to a more limited extent and finally, a short account is given of the reactions in the presence of oxygen. Practical interest in studies of the chemical activity of x-rays lies in the effects of the rays on life processes. Since the water content of the biological cell is about 75 percent, it is reasonable to assume that the reactions produced through the activation of the water play an important part in these effects.

EXPERIMENTAL PROCEDURE

The irradiations were carried out with a water-cooled tungsten tube capable of operation at 110 kv and 50 ma. The x-ray intensity produced under these conditions was about 2000 r per minute at a distance of 6 cm, and the effective wave-length as determined by the absorption in aluminum was $\lambda_{eff} = 0.35$A. The x-ray dosage was determined by the irradiation of 1 millimolar formic acid in sulfuric acid at pH of 3.0, using the earlier result (3, f) that 3.2×10^{-6} M H_2 and 3.2×10^{-6} M CO_2 are produced per 1000 r and per 1000 cc.[9]

The solutions were irradiated in flat Pyrex cells 5 cm in diameter and 1 cm deep (see Fig. 1) designed to fit the Van Slyke apparatus into which the contents of the cells were transferred for the purpose of gas analysis. Four cells were usually irradiated at one time, placed at different distances from the x-ray tube so as to give a considerable variation in x-ray intensity.

For the purpose of removing the air from the solutions and introducing other gases, the "evacuation chamber" shown in Fig. 1 is used. It is made of Pyrex and carries six irradiation cells fitted through ground joints. Connection to a water pump and to the gas reservoirs is made at A. The water is transferred directly to this chamber from the purification system described below, the chemicals are added, connection made to the vacuum and the air is removed by simul-

[7] In these experiments small amounts of hydrogen and carbon dioxide were obtained which were ascribed to organic impurities in the water. Recently we were able to produce water so pure that no carbon dioxide was obtained. However, we still obtained a trace of hydrogen (1 or 2 μM H_2 per 1000 cc). We could not be sure whether oxygen or hydrogen peroxide were also produced. The possibility remains that a slight decomposition of the water occurs during the initial period of irradiation. (These experiments were carried out in closed reaction vessels.) This is of great interest since there can hardly be any doubt that the water molecule dissociates under the influence of these radiations. The mechanism whereby the recombination of the dissociation products is accomplished is however, so far, a matter of conjecture.

[8] H. Fricke and E. J. Hart, J. Chem. Phys. **4**, 418 (1936).

[9] The x-ray intensity in r/sec. is defined as the ionization current in electrostatic units produced in 1 cc of air at 76 cm Hg and at 0°C. The x-ray dosage is the average intensity in the irradiated solution, multiplied by the time of irradiation in seconds.

taneous heating and shaking of the solution. At the same time, the evacuation chamber is tilted from side to side to allow removal of the air from the irradiation cells. With gas free solutions the liquid is forced into the cells by slightly increasing the pressure (with air) on the surface of the liquid. Solutions prepared in this manner yield less than 1 micromole of dissolved gases per 1000 cc of solution. When a gas is present, the same method of filling the cells may be used if the pressure is low. At high pressure, the tips of the capillaries of the irradiation cells are broken, the solution forced through, and the tips sealed off.

The water used for preparing the solutions was purified as follows. Water from a Barnstead still was refluxed for extended periods successively in alkali permanganate and in acid dichromate mixtures. The vapor mixed with washed oxygen was then passed through a quartz tube heated to 900°C. This was condensed and redistilled into the evacuation chamber. With this method of purification, the organic impurities in the water are effectively decreased but they are not completely removed. The presence of organic impurities can be shown since they are decomposed by irradiation, with the production of hydrogen and carbon dioxide. In Fig. 2 are shown the results of such a test on (*a*) water from a Barnstead still and (*b*) water purified by the method described. The water can be further purified by irradiating it after it has been transferred to the evacuation chamber. Water thus purified gave on irradiation no carbon dioxide but it did give a small amount of hydrogen, of the order of 1 or 2 micromoles per liter (Fig. 2*c*).

Before irradiating very dilute solutions we usually heated the cells and the evacuation chamber to near the softening point of Pyrex, in order to remove all traces of organic materials. After using the cells for concentrated solutions this heating is especially necessary, since chemical methods apparently never completely remove the organic materials from the walls of the vessels. When the vessels are not heated in this manner an increased amount of hydrogen and carbon dioxide may be found on irradiating otherwise pure water. This may be due in part to traces of organic materials in the water, released from the walls of the evacuation chamber and the cells, and in part to a direct action of the rays on organic materials adsorbed on the walls of the irradiation cells.

The gases produced by the irradiation were analyzed by means of a Van Slyke apparatus. The entire contents of the irradiation cell (usually about 20 cc) were transferred to the 50 cc extraction chamber and the analysis performed in the usual manner.[10] Potassium permanganate was used to liberate oxygen from hydrogen peroxide, sodium hyposulphite for the absorption of oxygen, sodium hydroxide for the absorption of carbon dioxide and ammoniacal cuprous chloride for the absorption of carbon monoxide. The composition of the residual gas could be determined by a combustion analysis.

The change in acid content resulting from irradiation was determined by potentiometric titration. A glass electrode was used for recording the *p*H values.

The hydrogen ion concentration is a factor in all the reactions. Different *p*H values were obtained as follows: *p*H = 1–4, H_2SO_4 or H_3PO_4; *p*H = 5.5–8, H_3PO_4 + NaOH; *p*H = 8–10, H_3BO_3 + NaOH; *p*H = 10–13, NaOH, KOH or $Ca(OH)_2$. The phosphate and borate buffers were usually used in 0.5 and 5.0 millimolar concentrations. The sulfate, sodium, potassium and calcium ions were not found to exert any influence on the reactions. The borate and phosphate ions were not always indifferent.

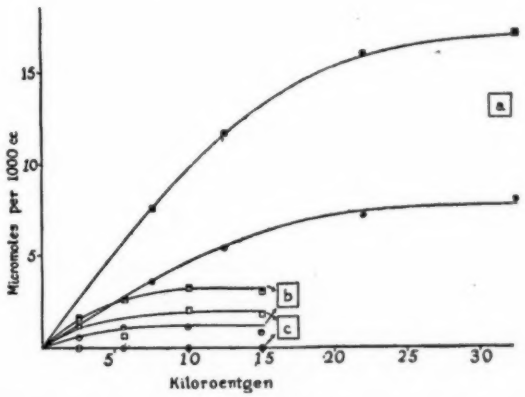

FIG. 2. Decomposition of organic impurities in water by irradiation with x-rays. Square, H_2; circle, CO_2. (*a*) Water from tin still. (*b*) Water purified chemically, as described in the text. (*c*) Water purified by irradiation with x-rays.

[10] J. P. Peters and D. D. Van Slyke, *Quantitative Clinical Chemistry*, II (1932).

Experimental Results

A. One organic component

Gas free solutions of the organic chemicals were irradiated at different concentrations and at different *p*H values. The rate of production of the reaction products is given in micromoles per 1000 cc per 1000 r, the values refer to the initial reactions when nothing else is said. The reactions were studied at x-ray intensities between 500 and 2000 r/min. and within this range the effects were found independent of the intensity when the intensity multiplied by the time of irradiation was kept constant. It should be noted, though, that the measurements are rather inaccurate at the very low concentrations at which the question of a dependence of rates on intensity is of particular interest.

If the absorbed x-ray energy is kept constant, the chemical effect of the rays is probably independent of wave-length, at least over a wide range.[3a, b] Since the ratio of the coefficients of absorption of water and air is slightly dependent on wave-length, the chemical effects would be expected to show a slight wave-length dependence when the rays are measured in terms of r. The wave-length dependence introduced by this factor should be negligible though for wave-lengths longer than about 0.30A. The average wave-length used in the present work was 0.35A.

The solutions were irradiated at room temperature. The influence of temperature on the reactions has not yet been determined, but temperature fluctuations of several degrees were insufficient to affect the reproducibility of the results to any noticeable extent. (Compare also reference 3*d*.)

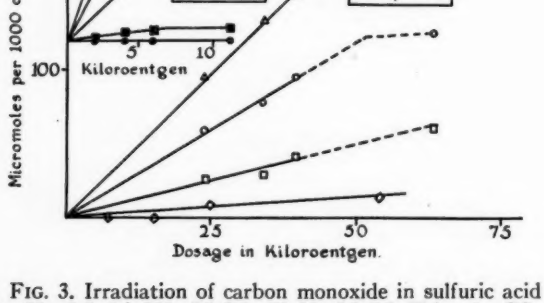

FIG. 3. Irradiation of carbon monoxide in sulfuric acid at *p*H = 3.5. (*a*) 220 μM CO. (*b*) 22 μM CO. Triangle, CO; square, H_2; circle, CO_2; diamond, HCHO. The filled square and circle represent hydrogen and carbon dioxide produced by the irradiation of the sulfuric acid without carbon monoxide.

The change produced in the solutions by irradiation was usually so small that the reaction product-dosage curves remained linear over the whole range of dosages used. A few examples are given of highly dilute solutions irradiated to completion. The end point reached was a complete transformation of the organic compounds to hydrogen and carbon dioxide.

Carbon monoxide

The carbon monoxide was prepared from the reaction of warm sulfuric acid with formic acid. The reaction-dosage curves for solutions of 220 and 22 μM CO in sulfuric acid at *p*H = 3.5 are shown in Fig. 3. Both hydrogen and carbon dioxide were produced but there is less hydrogen than carbon dioxide and the difference between them equals the excess of carbon monoxide consumption over carbon dioxide production. It is concluded that non-gaseous reaction products of the over-all composition of CH_2O are present. The reaction mechanism can be represented by:

$$CO+H_2O(+h\nu)\rightarrow CO_2+H_2^* \qquad (1)$$

with part of the hydrogen reacting according to:

$$CO+H_2^*\rightarrow CH_2O. \qquad (2)$$

The irradiated solutions were tested for formaldehyde by Hehner's method.[11] The amounts could be estimated to an accuracy of 10 micromoles per liter. Formaldehyde was present according to this test (Fig. 3), but the amount was 10 to 20 percent only of the reaction products left unaccounted for by the gases.

The effect of the rays appears to be independent of the concentration of carbon monoxide, in the range of 10 to 800 μM CO. However, the accuracy is only fair at the low concentrations (Fig. 3). The initial reaction rates are 3.9 μM CO, 2.45 μM CO_2, 1.0 μM H_2, and 0.3 μM HCHO (*p*H = 3.5).[12]

[11] C. C. Fulton, J. Ind. and Eng. Chem. (Anal. Ed.) 3, 199 (1931).

[12] All reaction rates are given in micromoles per 1000 cc and per 1000 r, as noted above.

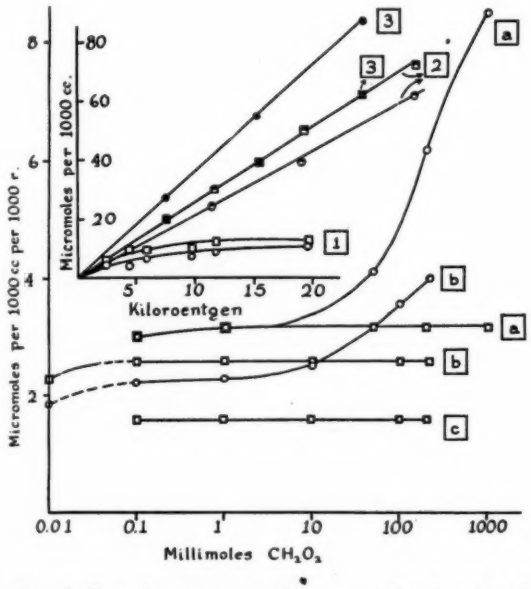

FIG. 4. Reaction concentration curves for formic acid. (*a*) pH = 2.0. (*b*) pH = 3.8. (*c*) pH = 7.2. Square, H_2; circle, CO_2. Inserted: Reaction dosage curves at pH = 3.8. (*1*) 10 μM CH_2O_2 (square, H_2; circle, CO_2). (*2*) 100 μM CH_2O_2 (upper half-filled square, H_2; upper half-filled circle, CO_2). (*3*) 100 mM CH_2O_2 (filled square, H_2; filled circle, CO_2).

A few experiments were carried out to determine the effect of the pH in the reaction. There is no great change in the range of pH = 1 to 7. Possibly the reaction rates increase with decreasing pH but the measurements were not accurate enough to make sure of the form of the relationship. In alkaline solution the character of the reaction changes. The hydrogen and carbon dioxide production decreases while the carbon monoxide consumption greatly increases. Apparently the principal reaction is the combination of the carbon monoxide with water to produce formic acid:

$$CO+H_2O\rightarrow HCOOH. \qquad (3)$$

Acids

Formic acid.—For pH values below pH = 3 and for concentrations of formic acid below 5 mM CH_2O_2, hydrogen and carbon dioxide are produced in equal amounts, indicating a decomposition of the formic acid according to

$$HCOOH\rightarrow H_2+CO_2. \qquad (4)$$

When the pH is increased above pH = 3, the reaction changes (Figs. 4*b*, *c* and Fig. 5*a*). The

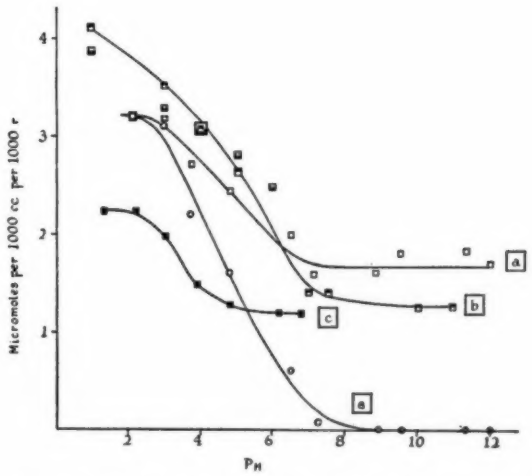

FIG. 5. Reaction pH curves for (*a*) 1.0 mM formic acid (square, H_2; circle CO_2); (*b*) 10 mM formaldehyde (upper half-filled square, H_2); (*c*) 10 mM butyric acid (filled square, H_2). A few observations on 100 mM methyl alcohol are also included (lower half-filled square, H_2).

production of both hydrogen and carbon dioxide decreases. The carbon dioxide decreases more rapidly than the hydrogen and for pH 7 only hydrogen is obtained. The simplest explanation would be that oxalic acid is produced, at these high pH values:

$$2\ HCOOH\rightarrow(COOH)_2+H_2. \qquad (5)$$

The production of hydrogen is independent of the concentration of formic acid, between 1 mM and 1 M CH_2O_2, at all values of pH. The carbon dioxide remains constant over the lower portion of this range of concentrations, while a rapid rise is recorded at the highest concentrations, at small pH values.

These results suggest that reactions (4) and/or (5) are produced at a constant rate between 1 mM and 1 M HCOOH, while an additional reaction liberating carbon dioxide occurs in acid solution, at high concentrations. This reaction may be:

$$2\ HCOOH\rightarrow HCH:O+CO_2+H_2O. \qquad (6)$$

The rate of production of hydrogen varies with pH according to:

$$[H_2]=1.6(1+(10^{5.0-pH})/(1+10^{5.0-pH}))\mu M\ H_2.$$

The effect of the rays was studied in the range of concentrations 100 μM to 1 M HCOOH, at all the different pH values. In acid solution both

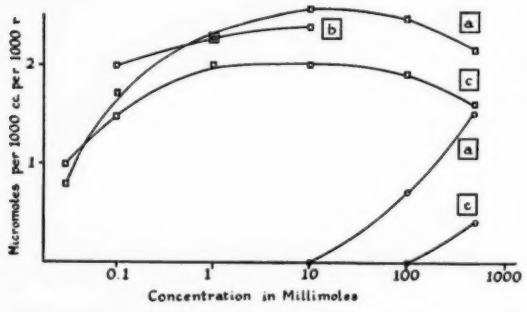

FIG. 6. Reaction concentration curves for (*a*) acetic acid; (*b*) propionic acid; (*c*) butyric acid. Square, H_2; circle, CO_2; pH = 3.

the hydrogen and the carbon dioxide production appeared to decrease slightly at the lowest concentration, but the change was not greater than the experimental error. Measurements were thereafter carried out on 10 μM HCOOH at pH = 3; the reaction-dosage curves are shown in Fig. 4. At the time these measurements were made the water was not as free from organic impurities as it was later possible to make it and it will be seen that all the hydrogen and carbon dioxide is not derived from the formic acid. The measurements do not make it completely certain that there is a decrease in reaction rate even at this low concentration of formic acid; the change, in any case, cannot be great.

Acetic acid.—The gas analytical data for the irradiation of solutions of acetic acid in sulphuric acid at pH = 3 are shown in Fig. 6*a*. At the lower concentrations, hydrogen is the only gas obtained, while at high concentrations carbon dioxide is also produced.

The production of either glycollic acid or succinic acid would be the simplest reactions at the lower concentrations:

$$CH_3COOH + H_2O \rightarrow CH_2OHCOOH + H_2, \quad (7)$$

$$2CH_3COOH \rightarrow (CH_2COOH)_2 + H_2. \quad (8)$$

To decide between these reactions, an unbuffered solution of 500 μM CH_3COOH was irradiated and the change in pH determined. The data are given in Table I. For comparison, pH measurements were made on mixtures of acetic acid with (*a*) glycollic acid and (*b*) succinic acid, as shown in the table. According to these measurements, the reaction could be the production of succinic acid.

Propionic acid.—Irradiations of propionic acid in concentrations between 0.1 and 10.0 mM CH_3CH_2COOH at pH = 3 gave hydrogen as the only gas. The quantities are given in Fig. 6*b*.

Butyric acid.—This acid was subjected to a more extensive study. The results at pH = 3 are similar to those for acetic acid. Hydrogen is the only gas produced at low concentrations, while at high concentrations carbon dioxide is also obtained. The rate of production of these gases as a function of concentration is represented in Fig. 6*c*. The relation of the hydrogen production to the hydrogen ion concentration for a solution of 10 mM C_3H_7COOH is shown in Fig. 5*c*. The reaction rate is represented by:

$$[H_2] = 1.2(1+10^{3.4-pH}/(1+10^{3.4-pH}))\mu M\ H_2.$$

The middle point of this curve is at pH = 3.4, which is 1.6 pH units to the acid side as compared with the corresponding curve for formic acid.

The irradiation of solutions of 1.0 and 10.0 mM isobutyric acid at pH = 3 gave no carbon dioxide. The total gas calculated as hydrogen was produced at the rates of 2.2 μM and 2.7 μM for the two concentrations, respectively.

Valeric and caproic acids.—A few preliminary irradiations of solutions of 1.0 mM concentrations at pH = 3 gave no carbon dioxide, while the total gas calculated as hydrogen was produced in about the same quantity as was obtained for butyric acid.

Oxalic acid.—Figure 7 shows the gas analytical data for the irradiation of different concentrations of oxalic acid at pH = 3. Both hydrogen

TABLE I.

Dosage (kr)	Hydrogen Produced μM/1000 cc [x]	pH			
		Control (500 μM CH_3COOH)	Irradiated Solution	(500 − x) μM CH_3COOH + (x) μM $CH_2OHCOOH$	(500 − x) μM CH_3COOH + (x/2) μM $(CH_2COOH)_2$
23.8	39.8	4.09	4.08	4.015	4.08
56.0	83.0	4.09	4.07	3.95	4.065

and carbon dioxide are obtained. At low concentrations these gases are produced in the ratio of 1 to 2, as they would be if the reaction was a decomposition of the oxalic acid, according to:

$$(COOH)_2 \rightarrow 2CO_2 + H_2. \quad (9)$$

As the concentration is increased, the carbon dioxide increases and finally becomes constant. The hydrogen, however, shows a continued decrease.

Figure 7 shows the productions of the gases as functions of pH for 100 mM $(COOH)_2$. The rate of production of carbon dioxide is represented by:

$$[CO_2] = 3.7(1+10^{5.6-pH}/(1+10^{5.6-pH}))\mu M\ CO_2.$$

At high concentration of oxalic acid and at high acidity, the rate of production of carbon dioxide becomes constant and equal to 7.4 μM CO_2.

Since the gas produced at high concentrations of oxalic acid is mainly carbon dioxide, it might be thought that the principal reaction at these concentrations is the formation of formic acid: $(COOH)_2 \rightarrow CO_2 + HCOOH$. Because of the high value found for the rate of production of the carbon dioxide, we are however inclined to believe that reaction (9) occurs at all concentrations but at higher concentrations the hydrogen is consumed with the reduction of the oxalic acid.

Malonic and succinic acids.—1.0 and 10.0 mM solutions of these acids were irradiated at pH = 3. Both acids yield hydrogen and a trace of carbon dioxide is also obtained for malonic acid. The rate of production of hydrogen, 2.5 μM H_2, is approximately the same for the two acids and for the two concentrations. The reactions may be:

$$COOHCH_2COOH + H_2O \rightarrow COOHCHOHCOOH + H_2, \quad (10)$$

$$COOHCH_2CH_2COOH + H_2O \rightarrow COOHCHOHCH_2COOH + H_2. \quad (11)$$

α-hydroxy isobutyric acid.—Irradiated at pH = 3 and at a concentration of 1.0 mM, carbon dioxide was produced at the rate of 0.8 μM CO_2. The residual gas calculated as hydrogen was produced at the rate of 1.1 μM. The high production of carbon dioxide is characteristic of an α-hydroxy acid.

Tartaric acid.—Irradiated at pH = 3 and at a concentration of 1.0 mM, carbon dioxide was produced at the rate of 1.2 μM CO_2. The residual gas calculated as hydrogen was produced at the rate of 2.5 μM. The carbon dioxide production is considerably greater than it is for α-hydroxy isobutyric acid.

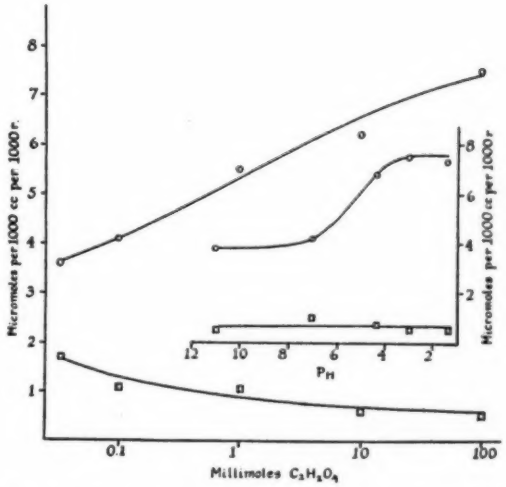

FIG. 7. Reaction concentration curves for oxalic acid at pH = 3. Inserted: Reaction pH curves for 100 mM oxalic acid. Square, H_2; circle, CO_2.

Aldehydes

Formaldehyde.—The data obtained for solutions of formaldehyde at pH = 4 are shown in Fig. 8. The only gas produced was hydrogen. The solutions became acid as a result of the irradiation. The acid is assumed to be formic acid. In concentrated solutions the amount of acid formed is much greater than the hydrogen, but in dilute solutions the two quantities become more nearly alike and they agree at 1.0 mM HCHO. Below this concentration, the acid could not be determined with sufficient accuracy.

These results can be explained by assuming that the hydrogen is liberated in the reaction

$$HCHO + H_2O \rightarrow HCOOH + H_2. \quad (12)$$

At the higher concentrations of formaldehyde an additional reaction liberating formic acid occurs, probably the reaction:

$$2HCHO + H_2O \rightarrow HCOOH + CH_3OH. \quad (13)$$

This reaction is exothermic to the extent of about 11 Cal. and occurs spontaneously in strong basic solution. The rapid increase in the formic

acid production with increasing concentration of formaldehyde, can, therefore, be understood since it may be assumed that reaction (13) has a tendency towards self-propagation outside the ranges of *p*H and concentration at which it occurs spontaneously. Accordingly we find that the excess acid is much greater when alkaline solutions are irradiated. This is shown by the reaction curves for solutions of formaldehyde in sodium hydroxide at *p*H = 10, which are given in Fig. 8.

As evidenced by the hydrogen production, reaction (12) is produced at a constant rate at high concentrations of formaldehyde. The production of hydrogen as a function of the *p*H is shown in Fig. 5*b* for 10.0 mM HCHO. The relationship does not have the same simple form found for the acids. The hydrogen production becomes constant in alkaline solution but continues to rise with increasing acidity.

When we irradiate a mixture containing equal amounts of formic acid and formaldehyde, the formic acid is acted upon to a much greater extent than the formaldehyde, as shown later in this paper. This explains the rather short range of linearity of the formic acid dosage curves obtained in the irradiation of formaldehyde. At higher dosages, carbon dioxide appears, owing to the decomposition of the formic acid. (Fig. 8). For this reason, the determination of the formic acid production is rather difficult in dilute solutions of formaldehyde. This determination could not be carried through at concentrations below 1 mM HCHO.

Acetaldehyde.—Irradiations were carried out on solutions of acetaldehyde in sulphuric acid at *p*H = 4 and in sodium hydroxide at *p*H = 10 (Fig. 9) The reaction products observed were hydrogen and an acid which is assumed to be acetic acid

We consider, first, the reactions in alkaline solution. The results are similar to those obtained with formaldehyde. The hydrogen is constant. The acetic acid is higher than the hydrogen and increases as the concentration of acetaldehyde increases. The increase is, however, less rapid than it is for formaldehyde. We may assume the presence of the two reactions:

$$CH_3CHO+H_2O\rightarrow CH_3COOH+H_2 \quad (14)$$

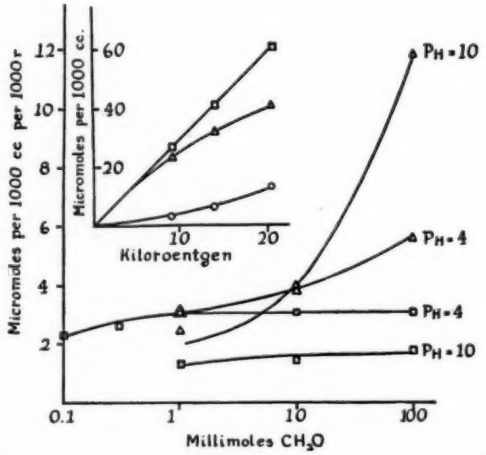

FIG. 8. Reaction concentration curves for formaldehyde at *p*H = 4 and 10. Inserted: Reaction dosage curves for 1 mM formaldehyde at *p*H = 4. Square, H_2; triangle, CH_2O_2; circle, CO_2.

and

$$2CH_3CHO+H_2O\rightarrow CH_3COOH+CH_3CH_2OH, \quad (15)$$

of which reaction (14) is produced at a constant rate, over the whole range of concentrations studied, while the rate of reaction (15) increases as the concentration of acetaldehyde increases. Reaction (15) is exothermic and occurs spontaneously in strong basic solution.

At *p*H = 4 the acetic acid production is constant over a wide range of concentrations of acetaldehyde. At the highest concentration there is a just perceivable rise in the acetic acid probably because of the occurrence of reaction (15).

The constant part of the acetic acid production is probably to be explained by the occurrence of reaction (14). Since the production of hydrogen is greater than that of acetic acid, other reactions yielding hydrogen must occur. The simplest possibilities are:

$$CH_3CHO+H_2O\rightarrow CH_2OHCHO+H_2, \quad (16)$$

$$2CH_3CHO\rightarrow(CH_2CHO)_2+H_2. \quad (17)$$

The hydrogen does not show the usual constancy at high concentrations, but it reaches a maximum and thereafter it decreases, as the concentration increases. This need not mean that the rates of the reactions in which hydrogen is produced

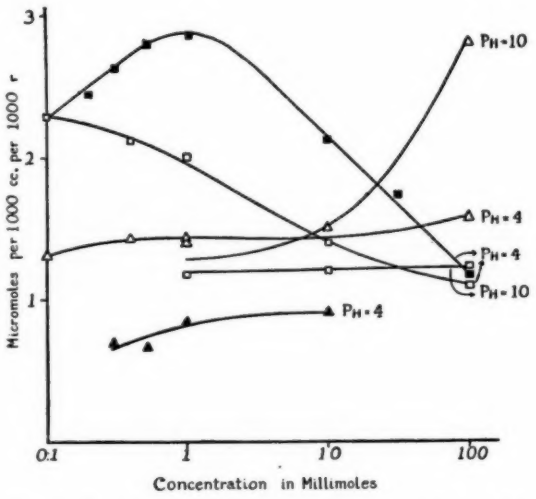

FIG. 9. Reaction concentration curves for (*a*) acetaldehyde at *p*H = 4 and 10 (square, H_2; triangle, CH_3COOH); (*b*) propionic aldehyde at *p*H = 4 (filled square, H_2; filled triangle, C_2H_5COOH).

primarily decrease at high concentrations. The constancy of the acetic acid shows that at least the rate of reaction (14) is independent of concentration. Possibly the decrease in the hydrogen results from the occurrence of a secondary reaction between the hydrogen in its nascent state and the acetaldehyde at the higher concentrations of acetaldehyde.

Propyl aldehyde.—Irradiations were carried out at *p*H = 4. (Fig. 9.) The reaction products observed were hydrogen and an acid, which was assumed to be propionic acid. The reaction concentration curves are similar to those found for acetaldehyde and they may be similarly interpreted. The results indicate that the oxidation of the aldehyde group is a still smaller part of the total reaction than it is in the case of acetaldehyde.

Ketones

Acetone.—The irradiation of unbuffered solutions of acetone produced no acid. The data obtained in the irradiation of solutions of acetone in sulfuric acid at *p*H = 3 are given in Fig. 10. An unusual result was the production of a small amount of hydrogen peroxide. The only gas produced was hydrogen. The hydrogen shows a decrease at high concentrations similar to that observed for acetaldehyde and propyl aldehyde.

Alcohols

Methyl alcohol.—Hydrogen was the only gas produced. Hydrogen reaction curves showing the influence of the methyl alcohol concentration, at *p*H = 1, and for unbuffered solutions, are given in Fig. 11. The irradiated solutions were tested for formaldehyde by Hehner's method.[11] Formaldehyde was found to be present but only to the extent of about 10 percent of the hydrogen. Representative reaction dosage curves are shown in Fig. 11. Measurements of the production of hydrogen in solutions of different *p*H are shown in Fig. 5. The values agree approximately with those obtained for formaldehyde.

Higher alcohols.—Solutions of ethyl alcohol, propyl alcohol and diethyl carbinol were irradiated at *p*H = 3, in concentrations between 0.1 and 10.0 mM. Carbon dioxide was not produced. The total gas calculated as hydrogen was approximately the same as for methyl alcohol.

The rates of the reactions produced by irradiating the organic chemicals decrease generally, at low concentrations. In Fig. 12 we have replotted some of the reaction product concentration curves obtained above. For each particular curve, the reaction rates are given as percentages of the constant reaction rate obtained at high concentrations. The curves can be represented approximately by:

$$[P] = (C/Co)/(1+C/Co) \qquad (18)$$

when C is the concentration and Co is constant for each particular curve. [These curves were obtained at *p*H = 3, but it is interesting to note that the position of the curves (the Co values if the curves are represented by (18)) does not appear to depend on *p*H.]

This decrease in reaction rates may be accounted for by a deactivation of the activated water. However, if this interpretation is correct, then it would appear that the deactivation does not consist in a recombination of the active particles. This conclusion is indicated (1) since the reaction rates show no dependence of x-ray intensity down to the lowest concentrations used (2) because of the form of the reaction concentration curves. On the other hand, it is difficult to believe that active states other than dissociation products of the water molecule could be of suffi-

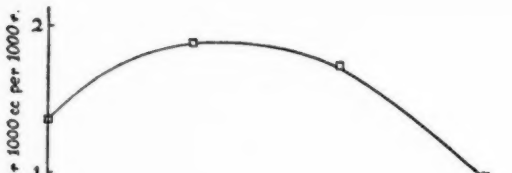

FIG. 10. Reaction concentration curves for acetone at pH = 3. Square, H_2. Diamond, H_2O_2.

cient stability to play a role in the reactions at the low concentrations used.

B. Two organic components

We have irradiated systems containing formic acid or oxalic acid as one of the components. In these systems the effect of the rays can be studied by recording the carbon dioxide production. Usually the hydrogen changes so little with the composition that its measurement is without significance.

The relation of the gas production to the composition of the systems is shown in Figs. 13, 14, and 15. They include mixtures of formic acid with methyl alcohol, formaldehyde, acetone, acetic acid, caproic acid, oxalic acid and benzene, and of oxalic acid with methyl alcohol. These irradiations were all carried out at pH = 3. In most of the curves the transitional region extends over 3 or 4 units in the log concentration ratio. Many of the curves can be represented rather closely by the expression:

$$[P]=\frac{C_1}{C_1+\alpha C_2}[P]_1+\frac{C_2}{C_1+\alpha C_2}[P]_2, \quad (19)$$

where $[P]$ is the rate of production of the reaction product, C_1 and C_2 are the concentrations of the components, and $[P]_1$ and $[P]_2$ are the rates at which the reaction product is produced when the components are irradiated separately at the concentrations C_1 and C_2, respectively; α is a constant.

The position of the transitional region in the reaction curves shows the relative susceptibilities to irradiation of the substances in the mixture.

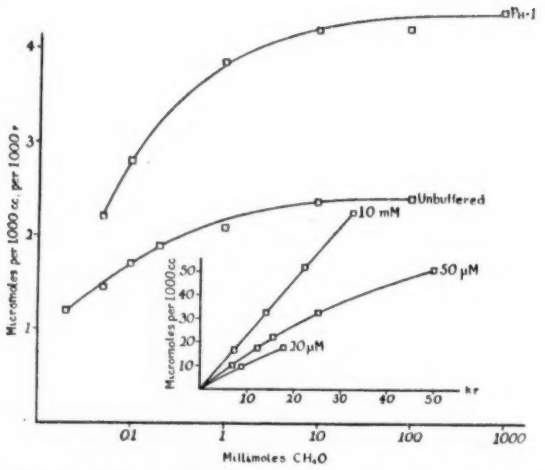

FIG. 11. Reaction concentration curves for methyl alcohol at pH = 1 and in unbuffered solution. Inserted: Reaction dosage curves for different concentrations of unbuffered solutions of methyl alcohol. Square, H_2.

The values of the susceptibility ratios obtained in the different mixtures vary widely. The results for acetic acid-formic acid are of particular interest. The production of gases from this system is independent of the acetic acid even when the concentration of this substance is 100 times that of the formic acid.

C. One organic component—oxygen

When water containing dissolved oxygen is irradiated, hydrogen peroxide is produced.[1, 3d, e] The reaction is:

$$O_2+2H_2O\rightarrow 2H_2O_2. \quad (20)$$

The production of hydrogen peroxide increases when the irradiation is carried out in the presence of organic compounds.[3d] It was suggested that

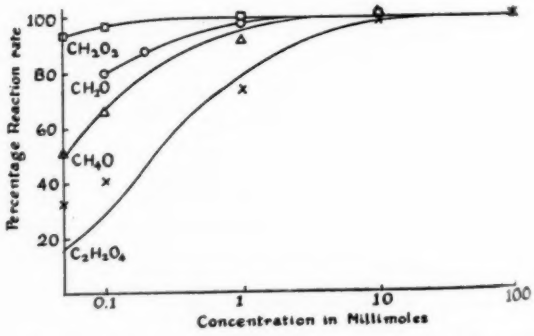

FIG. 12. Reaction concentration curves for (*a*) formic acid; (*b*) formaldehyde; (*c*) methyl alcohol; (*d*) oxalic acid. pH = 3.

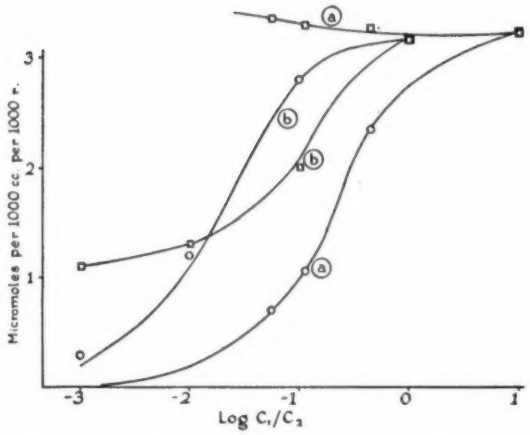

FIG. 13. Reaction log concentration ratio curves for solutions of formic acid and (*a*) formaldehyde; (*b*) acetone. Concentration of formic acid, $C_1=1$ mM. pH = 3. Square, H_2. Circle, CO_2.

this additional hydrogen peroxide results from a reaction of the oxygen with the nascent hydrogen produced by the action of the rays on the organic material. The gasometric studies which we have now carried out confirm this conclusion.

In Table II are shown the data obtained for formic acid irradiated in two concentrations, 0.03 and 1.0 mM CH_2O_2, at pH = 3 and at oxygen pressures of 6 cm and 70 cm of mercury.

Contrasting the results obtained when formic acid and oxygen are irradiated together against those obtained, when these substances are irradiated separately, we notice (1) the production of hydrogen peroxide and the consumption of oxygen increase; (2) the production of carbon

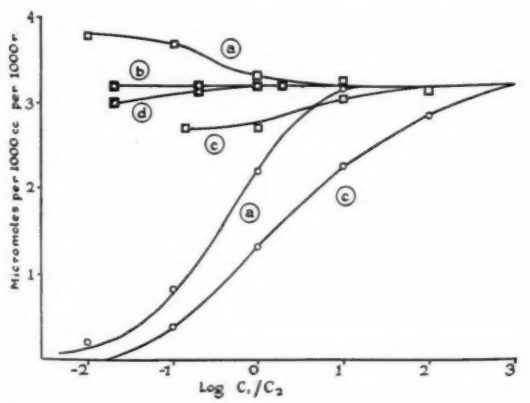

FIG. 14. Reaction log concentration ratio curves for solutions of formic acid and (*a*) methyl alcohol; (*b*) acetic acid; (*c*) caproic acid; (*d*) benzene. Concentration of formic acid, $C_1=1$ mM. pH = 3. Square, H_2. Circle, CO_2.

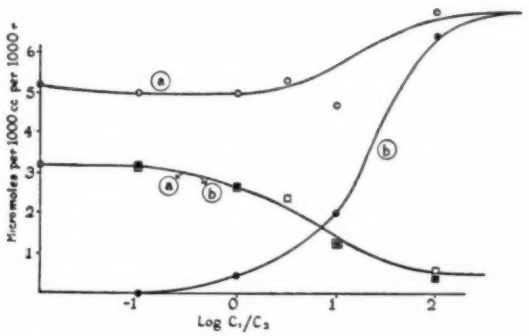

FIG. 15. Reaction log concentration ratio curves for solutions of oxalic acid and (*a*) formic acid (Square, H_2; Circle, CO_2); (*b*) methyl alcohol (filled square, H_2; filled circle, CO_2). Concentration of oxalic acid, $C_1=1$ mM. pH = 3.

dioxide and of hydrogen decreases, but the decrease of the hydrogen is greater than that of the carbon dioxide; (3) the increase in the hydrogen peroxide production ΔH_2O_2, the increase in the oxygen consumption ΔO_2 and the amount by which the hydrogen differs from the carbon dioxide $\Delta H_2=[CO_2]-[H_2]$, are equal, as far as the accuracy of the data allows one to judge. This is shown by the following tabulation:

6 cm O_2 1.0 mM HCOOH $\Delta H_2=2.1-0.8=1.3$ μM; $\Delta O_2=2.2-1.1=1.1$ μM; $\Delta H_2O_2=3.4-2.2=1.2$ μM;

6 cm O_2 0.03 mM HCOOH $\Delta H_2=1.6-0.5=1.1$ μM; $\Delta O_2=2.1-1.1=1.0$ μM; $\Delta H_2O_2=3.2-2.2=1.0$ μM;

70 cm O_2 1.0 mM HCOOH $\Delta H_2=2.0-0.4=1.6$ μM; $\Delta H_2O_2=3.7-2.2=1.5$ μM.

These results can be explained by assuming (1) Reaction (20) takes place at the same rate as when formic acid is not present. (2) Formic acid is decomposed to hydrogen and carbon dioxide but the rate of this reaction is lower than when oxygen is absent. (3) The quantity ΔH_2 of the

TABLE II. *Irradiation of formic acid in the presence of oxygen at 6 cm and 70 cm* Hg *and at* pH = 3. *The initial production or consumption of gases is given in micromoles per 1000 cc and per 1000 r.*

Millimoles HCOOH	Gas Free		Oxygen at 6 cm Hg				Oxygen at 70 cm Hg			
	CO_2	H_2	CO_2	H_2	O_2*	H_2O_2	CO_2	H_2	O_2*	H_2O_2
1.0	3.2	3.2	2.1	0.8	2.2	3.4	2.0	0.4	—	3.7
0.03	2.7	2.7	1.6	0.5	2.1	3.2	—	—	—	
0	—	—	—	—	1.1	2.2	—	—	1.1	2.2

* Consumed.

hydrogen from this reaction combines with oxygen to form hydrogen peroxide according to:

$$H_2+O_2\rightarrow H_2O_2. \quad (21)$$

(4) This reaction (21) accounts for the increased production of hydrogen peroxide and increased consumption of oxygen.

The decrease in carbon dioxide shows us to what extent the effect of the rays on formic acid is suppressed by the presence of the oxygen and it is given in the following tabulation:

6 cm O_2 1.0 mM HCOOH $\Delta CO_2=3.2-2.1=1.1$ μM CO_2,
0.03 mM HCOOH $\Delta CO_2=2.7-1.6=1.1$ μM CO_2,

70 cm O_2 1.0 mM HCOOH $\Delta CO_2=3.2-2.0=1.2$ μM CO_2.

The decrease in carbon dioxide is independent of the formic acid concentration and of the oxygen pressure and equals $\Delta CO_2=1.1$ μM. This value equals the rate at which oxygen is consumed when it is irradiated alone.

Apparently the formic acid decomposition can be only partially suppressed by adding oxygen. This result takes on a special significance when we note that water activated with ultraviolet light causes the decomposition of formic acid, but it has no effect on oxygen. Possibly, therefore, the reason for the inability of oxygen to completely suppress the formic acid reaction may be that the x-ray activated water molecules, which act on formic acid, do not all react with oxygen.

We are indebted to D. M. Gallagher for his assistance during the greater part of this work.

MAY, 1938 JOURNAL OF CHEMICAL PHYSICS VOLUME 6

The Near Ultraviolet Bands of Acetylene

SHO-CHOW WOO, TA-KONG LIU, T. C. CHU AND WU CHIH
National Research Institute of Chemistry, Academia Sinica, Shanghai, China

(Received February 28, 1938)

The present investigation is a part of the program of a series of studies aiming at a satisfactory analysis of the near ultraviolet spectrum of acetylene. The spectrum of C_2H_2 at room temperature and 300°C was taken with a Bausch and Lomb large quartz spectrograph. The spectrum extends from λ2430A down to the ultraviolet limit of the instrument. More than 1000 bands and lines have been measured. Most of the bands revealed intensification at elevated temperature. Some of them have been partially resolved into rotational lines with alternating intensities. Seven main progressions all with frequency difference ~1050 cm^{-1} have been found. Only the bands of three of the progressions showed no intensification at higher temperature. From the differences between these bands, a frequency 580 cm^{-1} has been observed. Weaker bands on the red side of stronger ones have been proved through temperature variation to be due to transitions from the excited $2v_5''(E_g)$ level in the ground state. Through a tentative assignment, $2v_5'=1050$ cm^{-1} and $\nu_4'(E_u)=580$ cm^{-1} and the empirical selection rules, all of the bands in the seven progressions can be satisfactorily explained. Other possible assignments and the nature of the electronic transition have also been briefly discussed.

THE complexity of the ultraviolet spectra of polyatomic molecules usually prevents a complete analysis in the present state of knowledge. Attempts toward simplification have been made by working with those molecules which possess a structure of high symmetry. For this reason, we have recently been working mainly on molecules which are considered to be of the symmetrical and collinear type. Acetylene is particularly suitable in this category since its structure and fundamental frequencies in the ground state have been thoroughly investigated through the infra-red and Raman spectrum measurements. Unfortunately, no satisfactory analysis which makes use of these results in the ground state has been attained, in spite of the numerous investigations[1] made in recent years.

[1] (a) J. Stark and P. Lipp, Zeits. f. physik. Chemie **86**, 36 (1913); (b) H. Hese, A. Rose and R. Gräffin Zu Dohna, Zeits f. Physik **81**, 745 (1933); (c) G. Kistiakowsky, Phys. Rev. **37**, 276 (1931); (d) M. A. Jonesco, Comptes rendus **199**, 710 (1934); (e) M. A. Jonesco, Comptes rendus **200**, 817 (1935); (f) H. Göpfert, Zeits. f. wiss. Phot. **34**, 156 (1935); (g) It is uncertain if the bands beginning at λ2070A found by Herzberg (Trans. Faraday Soc. **27**, 378 (1931)) are a continuation of the system here discussed, since the distances between the main bands were found to be 1365 and 865 cm^{-1}, which are quite different from what we have found here.

A program has thus been planned in this laboratory to investigate this problem in the following three steps. (1) The spectrum of C_2H_2 is to be taken at different temperatures in order to ascertain which of the bands are due to transitions from the vibrationless level, and which are from the higher vibrational levels in the ground state. The frequency differences between these two groups of bands are then compared with the results of infra-red and Raman spectrum measurements. (2) The vibrational isotopic shifts of the bands are to be determined by a study of the spectrum of pure C_2D_2. This will help us not only to identify the (0,0) band, but also to prove the correctness of the assignment of the vibrational levels in both the ground as well as the excited states, since by a simple computation the frequencies of C_2D_2 may be obtained from those of C_2H_2. (3) The rotational structure of some of the bands is to be analyzed with a grating spectrograph of high dispersion, so that the nature of the electronic transition and hence the vibrational selection rules may be clearly understood.

With the above outlined program, we could certainly hope to attain a satisfactory solution of the problem. Unfortunately our work has been interrupted by the Sino-Japanese war just before the beginning of step (2). We are much obliged to Drs. Vaughan and McQuigg of the Union Carbide and Carbon Company for their kindness in offering us the purest calcium carbide available in their company.

Thus only step (1) of the program has been finished. With this part of the data, a complete analysis may not be attained. However, a plausible vibrational analysis may still be made and this part of experimental results may assist in the future investigation of the problem.

Experimental

The acetylene gas used in this investigation was obtained from a commercial tank. It was thoroughly purified by passing through a train of Milligan wash-bottles containing, respectively, water, cupric nitrate in nitric acid, mercuric chloride in hydrochloric acid and chromic acid in sulphuric acid. After being dried with soda-lime and P_2O_5 and collected in a liquid-air trap, the gas was then fractionated under reduced pressure, only the middle portion being taken for use. A large excess quantity of the gas was thus prepared and reserved for use in round-bottomed flasks provided with glass stopcocks and connections with the traps. After the gas had been condensed in the liquid-air traps, the complete system was thoroughly evacuated in order to remove any gaseous impurities which might be present.

The experimental arrangement was as usual. A hydrogen discharge tube, the same as one described before[2] was used as the continuous light source. The spectrum was taken with a Bausch and Lomb large Littrow type spectrograph with a dispersion of 2.1A/mm at 2430A and 1.2A/mm at 2040A. Glass tubes 50 cm and 350 cm long, fitted with quartz windows and connections to traps, manometer and vacuum pump, were used as our absorption cells. The amount of the absorbing gas varied from a few millimeters pressure in the short tube, to 1040 mm in the long tube. Plates were taken at adjusted pressure intervals in order to reveal the bands as completely as possible. Ilford Empress and Eastman 40 plates sensitized with mineral oil were used. Exposure for one hour was usual and in some cases two or three hours were found necessary. Iron arc and copper spark lines were taken as comparison spectra.

For the study of the intensity variation of the bands with temperature, quartz absorption cells with fused-on windows of 10 cm and 100 cm length were used. They were heated with tube-form electric heaters connected to rheostats for temperature regulation. For every amount of the absorbing gas in the cell, two spectra were taken side by side on the same plate with one at room temperature and the other at a higher temperature ($\sim$300°C). By varying the amount of the absorbing gas from a few mm pressure in the 10 cm tube to half an atmosphere in the 100 cm tube, the temperature effect, if any, on most of the bands could be observed. Photo-polymerization was found to become more prominent at the higher temperature. In the case of higher pressures, the product of polymerization was found to deposit on the light-entering window whose transparency was thereby diminished. Conse-

[2] Sho-Chow Woo and Ta-Kong Liu, J. Chem. Phys. **5**, 161 (1937).

TABLE I. *The acetylene bands in the region λλ2430–2050.*

ν(cm⁻¹) (IN VACUUM)	DESIG-NATION	I	ν(cm⁻¹) (IN VACUUM)	DESIG-NATION	I	ν(cm⁻¹) (IN VACUUM)	DESIG-NATION	I	ν(cm⁻¹) (IN VACUUM)	DESIG-NATION	I
41227.1*		00	*v*43490.4*		3	*v*44660.5		7	*c*45993.4		4
41393.9*		00	*c*43502.9*	b_6	4	*c*44672.6		8	*v*45998.7		
41406.1*	a_3	00	*v*43505.1*			*v*44675.0	A_7		46028.6*		5
41456.6*	b_2	00	43524.6		1	*c*44685.0		7	46041.7		5
41644.8	B_0	00	43530.3*		1	*v*44686.8			46046.0	c_{10}	5
41819.2*		0	43610.5		2	44694.4*		4	*c*46060.0*		7
41929.8*		0	43617.1*		1	44707.0		4	*v*46061.9*		
*c*42024.3		1	*c*43660.0		3	*c*44733.8		6	*c*46073.3		8
*v*42029.2			*v*43663.8			*v*44736.0			*v*46074.6		
*c*42041.4*			*c*43674.1	A_5	5	*c*44747.0	B_6	8	*c*46121.6*		6
42044.0*	c_2	1	*v*43676.9			*v*44749.4			*v*46123.7*		
*v*42045.3*			43682.9*		3	44815.2*		2	*c*46133.7*		7
42128.9*		00	43686.7*		3	*v*44830.5*		5	*v*46135.6*		
42142.6*	c_1	1	*v*43719.4		4	*v*44879.2*		00	46173.6		4
42226.6	C_0	00	*c*43730.8	B_4	6	44888.9*		4	46182.7	c_9	4
42335.5*		00	*v*43733.3			44892.5		5	*c*46288.4		6
42376.3*		00	43797.5*		1	*c*45057.2		5	*v*46290.1		
42395.8*		00	*c*43800.8*		1	*v*45058.4			*c*46305.1	C_8	7
42421.2*		0	*v*43803.8*			*v*45059.8*		5	*v*46307.4		
42430.2*	a_5	0	*c*43816.5*		3	45067.9*	c_8	4	46449.0*	b_{12}	4
42432.2*		0	*v*43819.2*			*c*45073.2*		6	46462.2*		6
42472.9		00	43859.9		0	*v*45075.2*			46480.7		4
*v*42476.2*		00	*v*43861.9		0	*c*45103.1		4	46546.5		4
*c*42487.5*	b_4	1	*c*43873.0*		2	*v*45106.2			46558.4		4
*v*42489.4*			*v*43874.8*			*c*45116.9		6	46582.5		5
42631.0		2	43947.7*		00	*v*45118.6			*c*46594.7		5
*v*42632.8	A_3	1	44007.2		3	*v*45191.4*		3	*v*46596.8		7
*v*42646.3		2	*c*44068.3*		5	*v*45193.6*		3	46625.3	A_{11}	7
42656.3*		2	*v*44072.8*			*c*45203.4*	c_7	6	46636.6		7
*v*42683.6		2	*c*44081.0*		2	*v*45206.7*			46655.3		4
*c*42696.4	B_2	3	*v*44082.7*	c_6		45251.7		8	46666.7		5
*v*42697.9			*c*44085.0*		5	45260.5		8	46691.5	B_{10}	10
42762.1*		00	*v*44087.4*			45289.6		6	*c*46703.3		
42829.5*		00	44132.5		1	*c*45300.3		8	*v*46705.2		
42832.1*		00	44157.3		1	*v*45302.4			47009.0		4
42838.4*		0	44193.4		3	*c*45317.6	C_6	10	47026.6		4
42949.9*		00	*c*44205.5*	c_5	5	*v*45319.6			*c*47045.2		5
42961.7*		00	*v*44208.4*			*v*45397.0*		7	*v*47048.3		
*c*43057.0*		3	44213.3*		2	*c*45455.4		5	*c*47057.4		7
*v*43059.0*			44216.1*		3	*v*45457.5			*v*47061.0		
*v*43074.6*	c_4	4	*c*44286.7		5	*c*45472.4*	b_{10}	6	*c*47111.5		5
*v*43169.1*		2	*v*44289.5			*v*45474.2*			*v*47114.8		
43176.9*	c_3	0	*c*44304.8	C_4	5	45596.4*		5	*c*47124.8		9
*v*43184.4*		4	*v*44307.2			*c*45659.3		9	*v*47126.4		
*c*43190.5*		00	44344.3*		2	*v*45660.9			47156.4		4
*v*43192.2*			44415.6*	a_9	5	*c*45670.7	A_9	10	47172.2		5
43203.6*		1	*v*44427.9*		5	*v*45672.4			47204.7		5
*c*43256.9		2	44443.3*		3	45691.4		9	*c*47223.2		6
*v*43257.6			*v*44447.2*		5	45703.1		5	*v*47225.0		
*c*43273.0	C_2	3	*c*44458.7*		3	*c*45725.9		7	47247.8		5
*v*43274.8			*v*44460.9*			*v*45728.0			*c*47258.9		5
43309.0*		00	44480.3*		1	*c*45739.5	B_8	10	*v*47260.4		
43365.7*		00	*v*44485.0	b_8	0	*v*45741.1			*c*47275.5	C_{10}	7
43378.1*		0	*c*44493.5*		5	45814.9*		3	*v*47277.3		
*c*43411.6		3	*v*44497.3*			*c*45827.1		2	47418.3		4
*v*43412.8			44553.4		1	*v*45831.7			47434.3		4
*v*43430.1*	a_7	4	44567.3*		4	45869.4		0	47569.9	A_{13}	5
*v*43442.0*		4	44597.5		3	*c*45881.4		3	47582.4		5
43458.1		1	44611.2		3	*v*45885.4			47676.1		7
43467.7		0				*c*45974.2		4	*c*47692.4		8
						*v*45979.5			*v*47694.7		

* Bands which showed intensification at higher temperature.
† Bands whose intensification at elevated temperature was anticipated, but not observed. Probably the crowding of bands and lines as well as the diminished transparency at 300°C make the observation difficult.

quently after a few exposures, the window had to be cleaned.

Measurement of bands and lines was made with an S.I.P. comparator. The error of measurement for most of the bands was less than ± 1 cm^{-1}.

Results and Discussion

The spectrum of acetylene extends from λ2430A down to the ultraviolet limit of the instrument. More than 1000 bands and lines have beem measured. A number of the bands have been partially resolved into rotational lines with alternating intensities. However, on account of the limited dispersion of the instrument, great accuracy for the rotational lines cannot be claimed. In Table I, are given the wave-lengths and wave numbers of the band heads with their visually estimated intensities. Because of the fact that the bands and lines are so numerous and closely spaced in some cases of weak absorption it was difficult to tell their real nature. Consequently, it may be that some of the weak band heads have been left unlisted in Table I while some of the lines may have been mistaken for band heads. It will be seen that our results agree very well with those of Göpfert.[1f] Most of the bands showed intensification at elevated temperature. Seven progressions with reasonable intensity distribution and all with frequency difference $\sim$1050 cm^{-1} have been found. These are listed in Table II, where the bands without intensification at higher temperature are designated by the capital letters.

All of the bands are double headed and with a degradation toward the red, showing an increase in moment of inertia by the electronic excitation. The separations of the doublets remain almost constant for each progression but vary from one progression to another, the greatest one being that in the bands of progression *C*. This indicates that in the upper levels of the *C* bands, the molecule possesses a moment of inertia nearest to that in the ground state. Hence if we take C_0-B_0 as a vibrational frequency, it must be a deformational one, since it has been shown in the infra-red spectrum that the moment of inertia of acetylene in the ground state is decreased slightly by deformational oscillations[3] and this is probably true also for the excited state.

The second differences in each of the progressions show considerable variations which exceed our experimental error. It is, however, interesting to note that these variations, though irregular, show a general tendency of increasing at first, followed by a decrease. This fact may help us to a better understanding of the nature of these bands, although no definite conclusion could be drawn here from this fact alone.

The complexity of the spectrum results from the fact that the bands are so numerous and crowded that it can hardly be understood how all of their frequency differences can be ascribed to the fundamental frequencies in the lower and upper states. The study of the intensity variation with temperature has simplified the analysis enormously. Thus it can be seen that only three progressions of bands showed no intensification at higher temperature and hence they must be the only ones which arise from transitions from the vibrationless level in the ground state to different vibrational levels in the excited state. Consequently there remain at most only three frequency differences, namely, $\sim$1050 cm^{-1}, $\sim$1000 cm^{-1} (A_3-B_0), and $\sim$580 cm^{-1} (C_0-B_0) which may be ascribed to the fundamentals or their multiples in the excited state. All of the other bands arise from transitions from higher vibrational levels in the ground state. These bands must be on the red side of the *A*, *B* and *C* bands by distances which are multiples of the fundamental frequencies in the ground state.

Before the meaning of $\sim$1050 cm^{-1}, $\sim$1000 cm^{-1} and $\sim$580 cm^{-1}, and the nature of the transitions of these bands can be understood, a reference to the fundamental frequencies in the ground state appears to be necessary. From the infra-red and Raman spectrum measurements, it has been proved that the acetylene molecule is symmetrical and collinear and possesses the following frequencies: ν_1''(Ag) = 1974, ν_2''(Ag) = 3370, ν_3''(Au) = 3288, ν_4''(Eu) = 729, ν_5''(Eg) = 612.[4] Now if the electronic transition is not a forbidden one and the excitation is at the C−C bond, by which the symmetry of the molecule is not altered, the most natural assignment is

[3] K. Hedfeld and R. Mecke, Zeits. f. Physik **64**, 151 (1930); G. Herzberg and J. W. T. Spinks, Zeits. f. Physik **91**, 386 (1934).

[4] Gösta W. Funke and Einar Lindholm, Zeits. f. Physik **106**, 518 (1937).

$\nu_1' \backsimeq 1050$ cm^{-1} and $\nu_5' \backsimeq 580$ cm^{-1}. This assignment encounters, however, several difficulties. First, a frequency of 1050 cm^{-1} is usually to be regarded as a single bond frequency. By a comparison with the isoelectronic molecule, N_2, a reduction from a triple bond to a single bond frequency (1974 to 1050 cm^{-1}) by the electronic excitation does not seem to be probable. Secondly, in the far ultraviolet systems of acetylene studied by Price,[5] it has been found that the ν_1' frequencies for all of the excited states are of the order of 1750–1820 cm^{-1}. According to the selection rules set up by Herzberg and Teller,[6] only bands with $\Delta v_5 =$ even should appear with prominent intensity if the electronic transition be an allowed one. As a matter of fact, this is actually the case with the bands, a's, b's and c's, which are on the red side of the bands A's, B's and C's by a frequency difference of ~ 1240 cm^{-1} or $2\nu_5''$. It can hardly be understood why only one quantum of ν_5' is excited in the case of the C and c bands. Moreover, no satisfactory explanation can be given for the small separation of each pair of A's and B's which cannot be regarded as electronic doublets, since the ground state of acetylene is $^1\Sigma$ and hence its excited state should be either singlet or triplet. Again, the assignment is not able to account for the bands, c_1, c_3, c_5, etc.

The last two difficulties may be removed by assigning $\nu_1' = 1050$ cm^{-1}, $\nu_4' = 580$ cm^{-1} and $2\nu_5' = 1000$ cm^{-1}. However, the other difficulties are still left unsolved. Although the bands, c_1, c_3, $c_5 \cdots$ are situated just in the middle of B_0—A_3, $B_2 - A_5$, B_4—$A_7 \cdots$ with comparatively low intensity as should be expected, it cannot be explained why they should show remarkable intensification at higher temperature. Moreover, the appearance of bands with $\Delta v_4' = 1$ with con-

[5] W. C. Price, Phys. Rev. **47**, 444 (1935).
[6] G. Herzberg and E. Teller, Zeits. f. physik. Chemie **B21**, 410 (1933).

TABLE II. *Main progressions in the near ultraviolet spectrum of* C_2H_2.

A			B			C			
A_1	.....		B_0	41645		C_0	42227		$C_0 - B_0 = 582$
A_3	42633	13	B_2	42684	14	1053	C_2	43258	17	1048	$C_2 - B_2 = 577$
	42646			42698				43275		
A_5	43664	13	B_4	43719	14	1035	C_4	44290	17	1032	$C_4 - B_4 = 574$
	43677			43733				44307		
A_7	44661	14	B_6	44736	13	1016	C_6	45302	18	1013	$C_6 - B_6 = 571$
	44675			44749				45320		
	44687	12								
A_9	45661	11	B_8	45728	13	992	C_8	46290	17	987	$C_8 - B_8 = 566$
	45672			45741				46307		
A_{11}	46625	12	B_{10}	46692	13	964	C_{10}	47260	17	970	$C_{10} - B_{10} = 572$
	46637			46705				47277		
A_{13}	47570	12								
	47582									

1031 (between A_5 and A_7); 1010 (between A_7 and A_9); 985 (between A_9 and A_{11}); 965 (between A_{11} and A_{13}); 945 (after A_{13})

siderable intensity is also in disagreement with the selection rules of Herzberg and Teller.

In order to remove most of the above difficulties, an alternative assignment has to be considered. This assignment, though quite peculiar, may be suitable for a forbidden transition with which we are probably dealing, judging from its low intensity as compared with those in the far ultraviolet. Let us assume $\nu_4' = 580$ cm^{-1} and $2\nu_5' = 1050$ cm^{-1}. Thus the bands in the progressions, A, B, and C are considered as arising from transitions from the vibrationless level in the ground state to levels in the excited state with $v_4' = 0, v_5' = 1, 3, 5 \cdots$; $v_4' = 1, v_5' = 0, 2, 4 \cdots$; and $v_4' = 2, v_5' = 0, 2, 4 \cdots$ respectively. The bands a's, b's and c_{even}'s are on the red side of the corresponding A, B, and C bands by a distance of ~ 1240 which is approximately $2\nu_5''$ (see Table III). The c_{even} bands may as well as considered as being separated from the A bands by $1\nu_5''$ (thus $A_3 - c_2 = 601$; $A_5 - c_4 = 602.3$; $A_7 - c_6 = 599.4$; $A_9 - c_8 = 597.2$). However, the former interpretation is preferred on account of its unique validity for all of the a, b, c_{even} bands.

It will be seen from the above discussion that most of the prominent progressions may be fitted into the last scheme of analysis. The only difficulty which confronts this assignment is, however, its peculiar selection rules which do not quite agree with those of Herzberg and Teller and are not quite consistent among themselves. Despite this fact, if these selection rules be empirically followed, bands due to transitions from $v_5'' = 1$ to $v_5' = 0, 2, 4 \cdots$ (for A group of bands) or to $v_5' = 1, 3, 5 \cdots$ (for B and C groups) should also be expected to appear in the spectrum. This is just the case with the bands, c_1, c_3, $c_5 \cdots$. This may be shown as follows:

The frequencies of the bands, C_0, C_2, $C_4 \cdots$ may be approximately represented by the follow-

TABLE II.—*Continued.*

a	b	c_{even}	c_{odd}
a_1	b_0	c_0	c_1 42129 } 14
			42143 }
			1041
41394 }		42029 }	c_3 43169 } 15
a_3 41406 } 12	b_2 41457	c_2 42045 } 16	43184 }
1026	1032	1030	1024
42421 }	42476 }	43059 }	44193 }
a_5 42432 } 11	b_4 42489 } 13	c_4 43075 } 16	c_5 44208 } 15
1010	1016	1012	999
43430 }	43490 }	44073 }	45194 }
a_7 43442 } 12	b_6 43505 } 15	c_6 44087 } 14	c_7 45207 } 13
986	992	988	976
44416 }	44480 }	45060 }	
a_9 44428 } 12	b_8 44497 } 17	c_8 45075 } 15	c_9 46183(?)
	977	971	
	45458 }		
	b_{10} 45474 } 16	c_{10} 46046(?)	
	988		
	46449 }		
	b_{12} 46462 } 13		

TABLE III.

$A_1-a_1=$——	$B_0-b_0=$——	$C_0-c_0=$——	$C_1-c_1=612$
$A_3-a_3=1240$	$B_2-b_2=1241$	$C_2-c_2=1230$	$C_3-c_3=610$
$A_5-a_5=1245$	$B_4-b_4=1244$	$C_4-c_4=1232$	$C_5-c_5=606$
$A_7-a_7=1245$	$B_6-b_6=1244$	$C_6-c_6=1233$	$C_7-c_7=607$
$A_9-a_9=1244$	$B_8-b_8=1244$	$C_8-c_8=1232$	$C_9-c_9=612$
	$B_{10}-b_{10}=1231$	$C_{10}-c_{10}=1231$	

ing formula if the interaction coefficient between v_4' and v_5' is neglected:

$$\nu=42227.51+529.56v_5'-2.450v_5'^2, v_5'=0, 2, 4\cdots.$$

The term values of the levels, C_1, C_3, $C_5\cdots$ can be obtained by letting $v_5'=1, 3, 5\cdots$. In Table IV are given the calculated term values and the observed frequencies while in the last column of Table III, the calculated differences C_1-c_1, C_3-c_3, $C_5-c_5\cdots$ which, as will be seen, agree well with the ν_5'' found from infra-red and Raman spectrum measurements.

The ground state of acetylene has been identified as $'\Sigma$. In the far ultraviolet systems studied by Price, the electronic transitions have been determined to be of $^1\Sigma\leftarrow{}^1\Sigma$ and $^1\Pi\leftarrow{}^1\Sigma$. From a study of the rotational structure of the bands C_2 (designated by Jonesco as a_1), Jonesco[1d] has suggested a $^1\Sigma\leftarrow{}^1\Sigma$ transition for the near ultraviolet system. On account of the interruption of our research plan, we are not able to judge the correctness of Jonesco's interpretation. However, the numerous mistakes and typographical errors in this author's article make his experimental results doubtful. For example, from the data given in his equation $\nu=44292.20\pm2.236J-0.08J^2$, we cannot obtain his values of moments of inertia, $I''=23.89\times10^{-40}$ and $I'=24.21\times10^{-40}$, but $I''=23.92\times10^{-40}$ and $I'=25.66\times10^{-40}$ instead. We cannot understand why the author's measurements of the band heads should be so different from ours which are in satisfactory agreement with those of Göpfert and Kistiakowsky. This discrepancy may be the reason why our results cannot be represented by his simple formula $\nu=\nu_0+1034.6v'-v'^2$, where, again, the coefficient of v'^2 has been dropped, probably through a misprint. Thus whether the transition involved in this system is $^1\Sigma\leftarrow{}'\Sigma$ is still uncertain. From the low intensity of the system and the small vibrational frequencies we are inclined to consider that it is probably a forbidden transition.

TABLE IV.

		ν calc.	ν obs.
C_0		42227.5	42226.6
	C_1	42754.6	——
C_2		43276.8	43274.8
	C_3	43794.1	——
C_4		44306.6	44307.2
	C_5	44814.1	——
C_6		45316.7	45319.6
	C_7	45814.4	——
C_8		46307.2	46307.4
	C_9	46795.1	——
C_{10}		47278.1	47277.3

It is to be noted that the analysis suggested here is not claimed to be the uniquely correct one. However, we feel that our interpretation may not be far from the truth and that the program we suggested would certainly point to the way for the complete solution of the problem.

In conclusion, the authors of this paper want to express their sincere thanks to Professor Richard M. Badger for his kindness in reading the manuscript before publication.

Infra-Red and Raman Spectra of Polyatomic Molecules

II. Cis- and Transbutene-2

HAROLD GERSHINOWITZ AND E. BRIGHT WILSON, JR.
Mallinckrodt Chemical Laboratory, Harvard University, Cambridge, Massachusetts

(Received March 14, 1938)

The infra-red absorption spectra of gaseous cis- and transbutene-2 have been measured with a prism spectrometer from 435 to 4000 cm^{-1}. The Raman spectra of these compounds as liquids have also been obtained. The accepted identification of the high boiling isomer with the *cis* structure is confirmed by the fact that this compound shows many more coincidences between the Raman and infra-red spectra than the other isomer, as is to be expected if the latter approximates a molecule with a center of symmetry. The observed frequencies below 800 cm^{-1} are sufficiently different for the two isomers so that it is not safe to assume that both isomers have the same vibrational entropy.

THE two isomeric butenes, cis- and transbutene-2, are interesting compounds because of their close relationship, the possibility of free rotation of the methyl groups and the fact that a considerable body of thermodynamic data concerning them has already been accumulated.[1] From the point of view of a vibrational analysis they are rather complicated, so that their spectra are somewhat difficult to interpret with any certainty until some of the simpler molecules of the same type shall have been analyzed. Nevertheless, since pure samples of these butenes were made available to us at this time,[2] we decided to carry out the experimental work and to postpone the analyses until later.

Apparatus and Experimental Procedure

For the infra-red absorption spectra the automatic prism spectrometer described in Part I was used.[3] The rocksalt prism was used to investigate the region from 750 to 4000 cm^{-1} and the KBr prism for the region from 435 to 750 cm^{-1}. The absorption cells were 20 cm long and were made of 48 mm Pyrex tubing. The windows of KBr and rocksalt were cemented to the ends by means of clear glyptal cement. The cement was not baked. The recording was done in the manner described in Part I, with the filled cell and an evacuated dummy cell alternately in the path of the radiation. Blanks, with both cells evacuated, were taken throughout the spectrum. The absorption was recorded at intervals of three Veeder numbers throughout the entire spectrum and at least three records were taken of each band, so spaced that the spectrum was covered in steps of one Veeder number. With the NaCl prism one Veeder number is equivalent to 1 cm^{-1} at 1000 cm^{-1} and to 20 cm^{-1} at 3500 cm^{-1}. With the KBr prism 1 Veeder number corresponds to 2 cm^{-1} at 650 cm^{-1} and to $\frac{1}{3}$ cm^{-1} at 500 cm^{-1}. These intervals are much closer than are usually used. As a matter of fact, they are closer than is justified by the resolving power of the instrument, which has been designed with an eye to future improvement. The large number of points completely eliminates any advantage of the continuous type of recording, and makes more certain the positions of the minima. The slit widths in cm^{-1} are shown on Fig. 1, and varied from 6 cm^{-1} at 450 cm^{-1} to 150 cm^{-1} at 3500 cm^{-1}.

The Raman equipment is being redesigned at the present time, so that only a brief description of the apparatus used for this work will be given. The spectrograph is a rebuilt single glass prism instrument with Bausch and Lomb optics. The aperture is $f:6$ and the dispersion is 100A per mm at 4358A. The Raman tube was illuminated from four sides by four vertical quartz mercury

[1] G. B. Kistiakowsky, J. R. Ruhoff, H. A. Smith, and W. E. Vaughan, J. Am. Chem. Soc. **57**, 876 (1935). L. O. Brockway and P. C. Cross, J. Am. Chem. Soc. **58**, 2407 (1936). S. S. Todd and G. S. Parks, J. Am. Chem. Soc. **58**, 134 (1936). G. B. Kistiakowsky and W. R. Smith, J. Am. Chem. Soc. **58**, 766 (1936).

[2] We are indebted to Professor Kistiakowsky for supplying us with pure samples of these butenes. For their preparation, see reference 1.

[3] H. Gershinowitz and E. B. Wilson, Jr., J. Chem. Phys. **6**, 197 (1938).

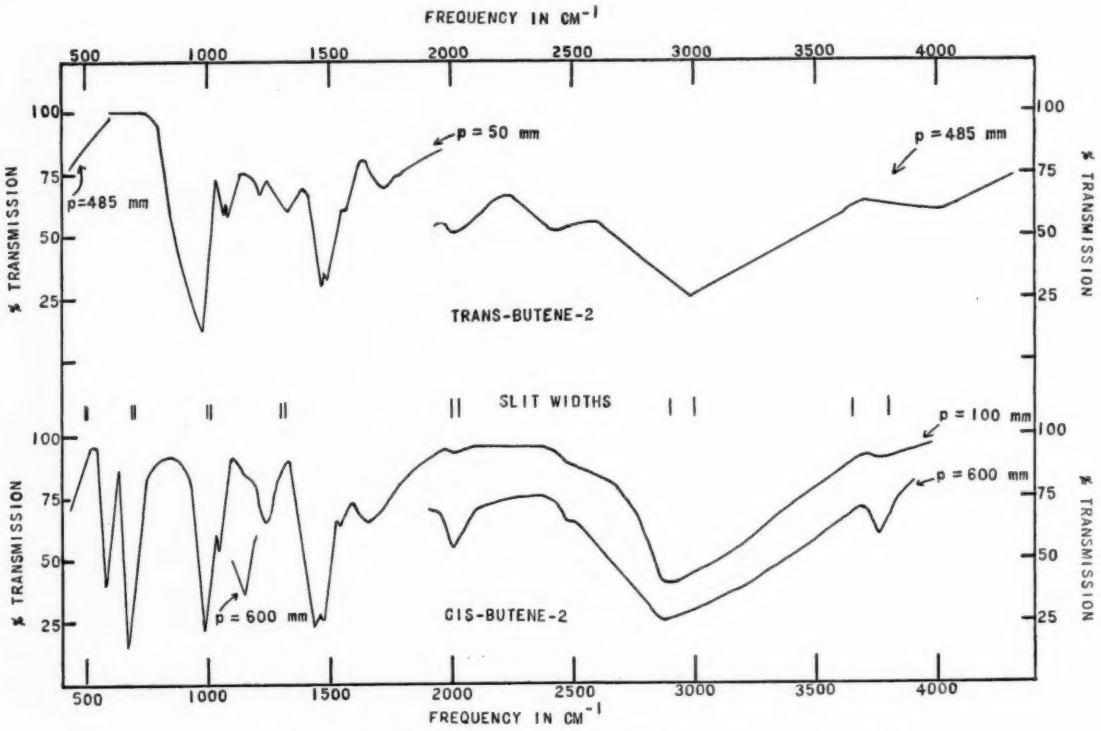

FIG. 1. Percentage transmission of cis- and transbutene-2 in the infra-red.

arcs,[4] each operating on about 4 amp. with 25 v d.c. The lamps were provided with individual parabolic reflectors and were cooled by an air blast from a vacuum cleaner used as a blower. The liquid samples were contained in vertical Pyrex tubes of either 50 or 13 cc capacity equipped with plane Pyrex windows. A double jacketed Dewar tube surrounded the Raman cells. The inner jacket was evacuated, while the filter liquid was circulated by means of a stainless steel centrifugal pump through the outer jacket and then through a copper coil cooled with running water. Dry air was blown through a copper coil immersed in dry ice and alcohol and then up through the inside of the Dewar vessel around the Raman tube. In this way the temperature of the sample was maintained at any desired value (usually about $-15°C$) in spite of the large amount of heat liberated by the lamps.

Two filter solutions were used. One contained 43 g *p*-nitrotoluene and 0.06 g rhodamine 5GDN Extra dye per liter of alcohol,[5] and was very efficient in isolating the lines at 4358A. The other contained the same amount of dye but only 2 g of *p*-nitrotoluene per liter and was used to transmit the 4358 and 4047A lines while cutting out all the ultraviolet. Eastman spectroscopic plates, black backed, emulsions I–O and I–J were used. The slit width employed was usually 0.09 mm. Under these conditions the best pictures required exposures of from 1 to 2 hours.

Polarization measurements were obtained on the *trans* compound with a Polaroid cylinder, by means of the method previously described.[5] To aid in the determination of the polarization, compensating for possible failure of the plates to obey the reciprocity law, a companion plate was taken for each Polaroid plate with weaker exciting light but the same exposure. Circumstances prevented determination of the polarization of the lines of the cisbutene-2, but we hope to have access to a sample of this compound again later, and plan to study the polarization at that time.

[4] Much of the Raman equipment, including the arcs, was constructed by Professor G. B. Kistiakowsky for an earlier investigation.

[5] J. T. Edsall and E. B. Wilson, Jr., J. Chem. Phys. 6, 124 (1938).

Experimental Results

In accordance with the established structures, in the following we shall call the low boiling isomer the *trans* and the high boiling isomer the *cis* form. Fig. 1 shows the transmission curves in the infra-red for both compounds. Table I gives the positions of the minima and the relative intensities. The absorption was measured at several different pressures in order to bring out weak bands and to resolve as much of the structure as possible. The curves show the results at only two pressures for each compound, but the positions (not intensities) in the table are those obtained at the most favorable pressure for each band. The uncertainty in the position of any band is probably equal to the slit width with which it was studied. These slit widths may be estimated from those shown in the figure.

The bands in the transbutene-2 at 1072 and 1080 cm^{-1} are so close together that we are not really sure that they are distinct bands, although they appear to be such on three separate records taken at different times. Also there is some doubt about the existence of the band at 1782 cm^{-1} which appears as just a shoulder on the 1720 cm^{-1} band. The bands at 1214 cm^{-1} and 1560 cm^{-1} which appear only as slight dips in the curves may also not be real, although they are much more definite than that at 1782 cm^{-1}. In the cisbutene-2, the band at 1541 cm^{-1} may be doubtful.

Table II lists the frequencies (in vacuum) of the Raman lines found for each compound, with the shifts from the excitation lines to which they have been assigned. All the lines reported have been observed on at least two plates and in addition have been identified on microphotometer records made of each plate. The polarization of the lines of the *trans* compound is also listed. Table I summarizes the results of both infra-red and Raman measurements, the Raman frequencies being weighted averages of the displacements from the (*k*) and (*e*) lines of Hg.

The Raman line reported at 22728 cm^{-1} for the *trans* compound appears along the side of the 4358A Hg line and may be double. This Hg line is so broadened out that it seems that there may well be other Raman lines of shorter shifts concealed. (The line is broadened only on the lower wave number side.) Fig. 2 shows microphotometric records* of comparable plates for the *cis*

Table I. *Observed frequencies in infra-red and Raman shifts with relative intensities and polarization of the transbutene-2 Raman lines.*

Cisbutene-2		Transbutene-2	
Infra-red	Raman	Infra-red	Raman
<435	304 (double)? (2)	<435	210 (3) (*D*)
583 (60)	402 (7)	978 (90)	507 (7) (*P*)
673 (85)	581 (double)? (1)	1072 } (40)	746 (5) (*D*)
986 (80)	685 (1)	1080 }	870 (4) (*P*)
1047 (45)	881 (7)	1214 (35)	1043 (2) (*D*?)
1149 (15)	978 (4)	1326 (40)	1309 (8) (*P*)
1233 (35)	1018 (5)	1466 (70)	1389 (4) (*D*)
1436 (75)	1044 (4)	1488 (65)	1455 (9) (*D*)
1473 (70)	1267 (8)	1560 (40)	1681 (8) (*P*)
1541 (35)	1389 (4)	1720 (30)	2739 (2) ?
1663 (35)	1462 (7)	1782 (25)	2867 (5) (*P*)
2004 (5)	1669 (8)	2004 (15)	2926 (10) (*D*)
2481 (10)	2671 (½)	2427 (15)	2965 (4) (*P*?)
2874 (60)	2715 (½)	2976 (40)	3011 (2) ?
3759 (10)	2758 (½)	4000 (5)	
	2813 (½)		
	2877 (6)		
	2931 (10)		
	2979 (6)		
	3034 (8)		

Table II. *Observed frequencies (cm^{-1} in vacuum) with displacements from the 4047 (k) and the 4358 (e) lines of* Hg.

Cisbutene-2		Transbutene-2	
ν in cm^{-1}	$\Delta\nu$ in cm^{-1}	ν in cm^{-1}	$\Delta\nu$ in cm^{-1}
23827	878 (*k*)	24197	508 (*k*)
23443	1262 (*k*)	23962	743 (*k*)
23318	1387 (*k*)	23843	862 (*k*)
23243	1462 (*k*)	23665	1040 (*k*)
22634	304 (*e*)	23398	1307 (*k*)
22536	402 (*e*)	23319	1386 (*k*)
22357	581 (*e*)	23251	1454 (*k*)
22253	685 (*e*)	22728	210 (*e*)
22055	883 (*e*)	22432	506 (*e*)
21960	978 (*e*)	22190	748 (*e*)
21920	1018 (*e*)	22065	873 (*e*)
21894	1044 (*e*)	21976	2737 (*k*)
21829	2876 (*k*)	21894	1044 (*e*)
21774	2931 (*k*)	21840	2872 (*k*)
21676	1262 (*e*)	21784	2921 (*k*)
21548	1390 (*e*)	21746	2959 (*k*)
21476	1462 (*e*)	21687	3018 (*k*) ?
21269	1669 (*e*)	21628	1310 (*e*)
20268	2671 (*e*)	21547	1391 (*e*)
20224	2715 (*e*)	21482	1456 (*e*)
20181	2758 (*e*)	21257	1681 (*e*)
20126	2813 (*e*)	20199	2740 (*e*)
20062	2877 (*e*)	20074	2865 (*e*)
20008	2931 (*e*)	20010	2929 (*e*)
19960	2979 (*e*)	19981	2968 (*e*)
19905	3034 (*e*)	19931	3008 (*e*)

* A description of the instrument used for making these records will be published shortly by Professor G. B. Kistiakowsky and Dr. W. H. Avery.

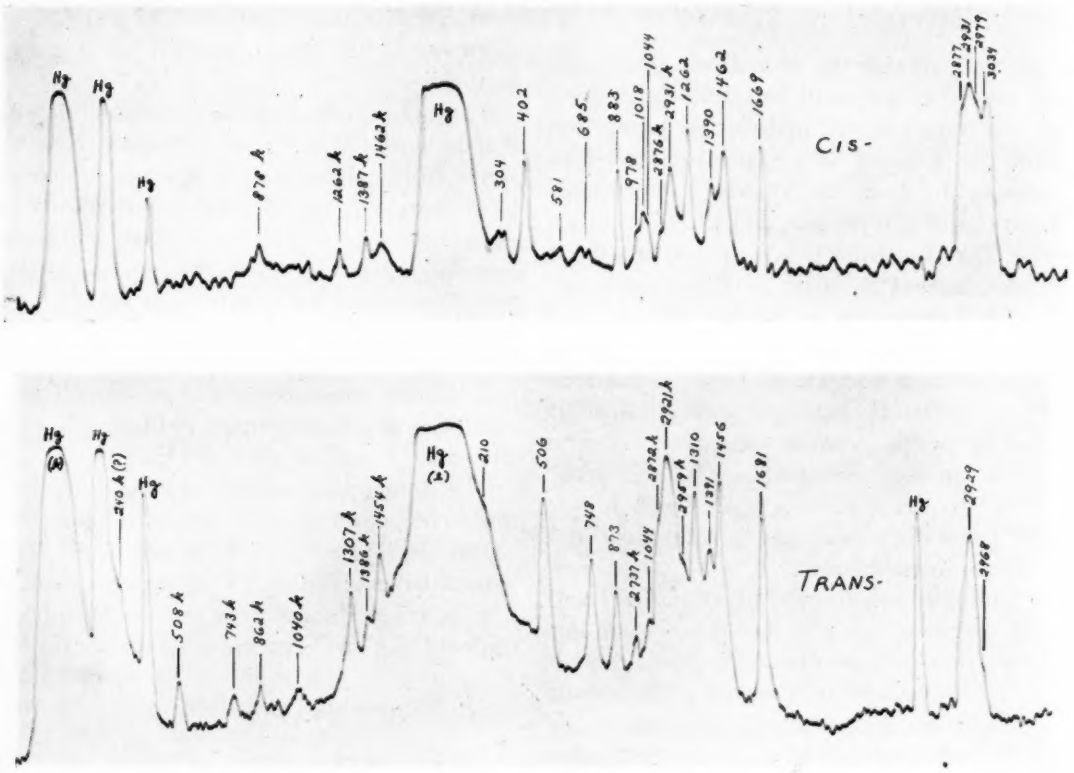

FIG. 2. Upper curve, microphotometer record of Raman spectrum of cisbutene-2. Lower curve, Raman spectrum of transbutene-2.

and the *trans* compounds which clearly show this broadening of the region about 4358A. This would indicate that the *trans* compound may have frequencies lower than 210 cm^{-1}. It can be seen that the mercury line at 4077A is similarly broadened, the line at 210 *k* appearing as a bump along the side. This Raman line has not been reported in the table above (the measured frequency is 24465 cm^{-1}) because it appears only on this one plate, which is the most intense one of this region.

The lines of the cisbutene-2 from 20268 cm^{-1} through 20126 cm^{-1} appear as a very faint series of sharp lines. They have, however, been identified and measured on two plates. We are uncertain whether the line at 21687 cm^{-1} in the *trans* compound is 3018 *k* or 1251 *e*, but tend to believe it is the former. The line at 304 *e* is quite weak but appears distinctly on four plates. The microphotometer records of this line indicate that it may be double. The line at 581 *e* also appears to be double.

DISCUSSION

Even without making a vibrational analysis of these molecules, it is possible to arrive qualitatively at results of interest. The transbutene-2 has a center of symmetry if the methyl groups may be considered as units. In this case there should be no coincidences between the Raman and infra-red spectra, except by accident, because the selection rules would forbid the same frequency being active in the Raman and the infra-red. For the *cis* compound, however, it should be possible to have some frequencies active in both the Raman and the infra-red. From Table I it may be seen that this state of affairs is actually realized, since there are very many more coincidences in the *cis* spectra than in the *trans*. This tends to corroborate the assigned structures.

Recently there has been much discussion about the question of whether or not methyl groups in organic molecules may rotate freely. As evidence on both sides, calculations of the entro-

pies of various molecules have been made.[6] To make these calculations, it is necessary to know the vibration frequencies of the molecules. The isomeric butenes are among the molecules which have been studied and it has sometimes been assumed that the structure of the two isomers is so similar that they may safely be assumed to have the same vibrational entropies, at least for the purpose of such calculations. Although no certain conclusions can be drawn until the spectra of these molecules have been completely analyzed, so that all the vibration frequencies are known, from the available data it would seem that this assumption is of doubtful validity. Table I shows that while the trans- and the cisbutenes have practically identical spectra when one considers the frequencies above 800 cm^{-1}, below that the spectra are quite different. Although this difference may be wiped out by the existence of frequencies which may not have been observed by us, such a possibility is rather remote and it would seem much more probable that there are real differences in these low frequencies. This seems not unreasonable, when one considers that in these low frequencies motions of the entire chain are involved and that these might well be different for the two compounds. It does not seem profitable, therefore, to attempt to draw definite conclusions about the existence of free rotation unless all the vibration frequencies are known.

[6] K. S. Pitzer, J. Chem. Phys. **5**, 473 (1937); L. S. Kassel, ibid. **4**, 144 (1936).

MAY, 1938 JOURNAL OF CHEMICAL PHYSICS VOLUME 6

Separation of Gaseous Isotopes by Diffusion

R. SHERR
Palmer Physical Laboratory, Princeton University, Princeton, New Jersey

(Received February 22, 1938)

The behavior of a set of mercury diffusion pumps has been investigated and the separation factors for a number of isotopic mixtures have been determined. Formulae have been derived which give the dependence of enrichment on the choice of reservoirs. In addition, Barwich's theory for the fractionation process has been extended to the case of finite reservoirs. The solution for this problem is a slowly converging series, but a qualitative picture of the dependence of equilibrium time on various factors is obtained. The separation factors which have been found for the Hertz diffusion pumps for bromine in CH_3Br, carbon in CH_4, oxygen in O_2 and H_2O, Ne, and A are 1.005, 1.107, 1.045, 1.073, 1.198, and 1.154 per unit, respectively. Twelve pumps of the Hertz design, and seventeen modified units were used. The modifications were made in an attempt to improve the original design, but the factors obtained for these units are smaller. Auxiliary experiments indicate that the performance of the new units is seriously impaired by the presence of back diffusion and that increased factors can be obtained by eliminating the latter effect.

1. INTRODUCTION

IN recent years many problems in chemistry, biology, and physics have arisen whose solutions are facilitated by or dependent on the use of fractionated isotopes. There is consequently a growing interest in the more immediate problem of the separation of isotopes. Many fractionating devices, based on physical or chemical principles, have been applied to a number of isotopic elements with varying degrees of success.[1] One of the more promising methods has been that of separation by diffusion.

This method, although historically the first to be employed, gave no marked results until quite recently. The weakness of the earlier diffusion experiments lay in the fact that only one fractionating unit could be employed in a single operation. However, in 1932, G. Hertz[2] announced the invention of porous-walled units, so designed that a number of them could be connected in series, leading to multiple fractionation in one operation. These units have been used by a number of investigators[2, 3] for the fractionation of neon, hydrogen, carbon and nitrogen.

[1] For recent reviews, see F. W. Aston, *Mass Spectra and Isotopes* (Edw. Arnold and Co., 1933). G. Champetier, Bull. Soc. Chem. **3**, 1701 (1936).

[2] G. Hertz, Zeits. f. Physik **79**, 108 (1932).

[3] Harmsen, Zeits. f. Physik. **82**, 589 (1932); Harmsen, Hertz, and Schutze, Zeits. f. Physik **90**, 703 (1934); Wooldridge and Smythe, Phys. Rev. **50**, 233 (1936).

The difficulty of preventing the accumulation of impurities during operation and the possibility of obtaining higher separation factors led Hertz[4] to the development of the mercury diffusion pumps to be described below. The behavior of individual pumps under various conditions has been investigated by Barwich[5] and separation experiments on neon, water vapor, and argon have been made by Barwich,[5] and Kopfermann and Kruger.[6]

The primary object of the present experiments has been a wider study of the potentialities of this method of separating isotopes. The usefulness of a fractionating device is determined by the degree of separation which can be obtained, by the yield,

[4] G. Hertz, Zeits. f. Physik **91**, 810 (1934).
[5] Barwich, Zeits. f. Physik **100**, 166 (1936).
[6] Kopfermann and Kruger, Zeits. f. Physik **105**, 389 (1937).

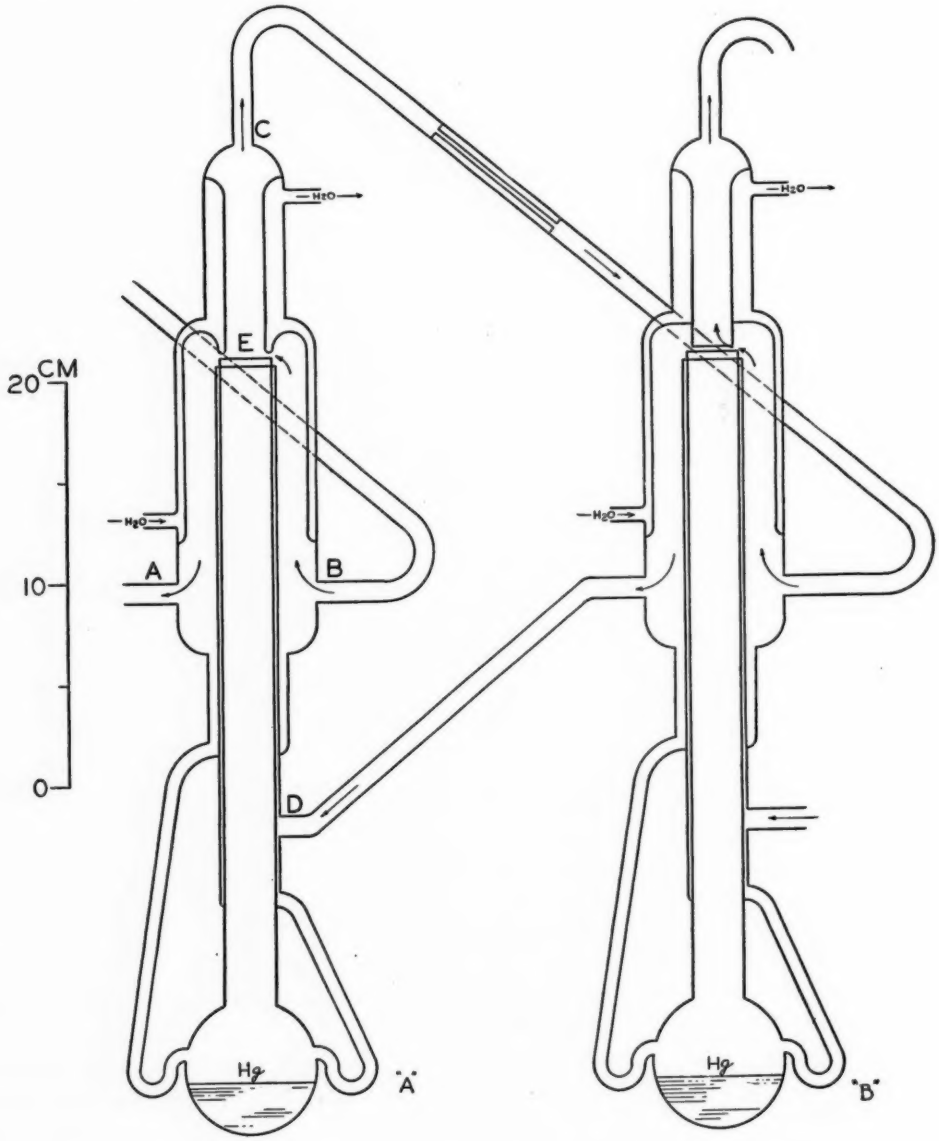

FIG. 1. Mercury diffusion pumps. "*A*" is the Hertz pump; "*B*" is a unit with a modified mercury jet. The pumps are connected in series as shown.

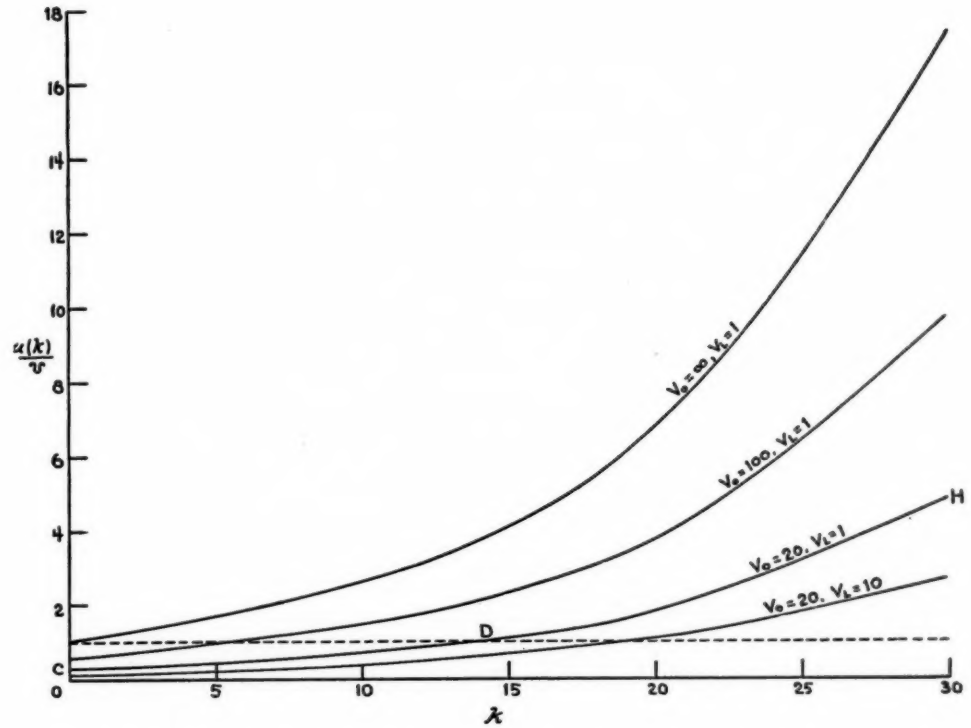

FIG. 2. Equilibrium gradient $u(k)/U$ for various choices of end volumes for small concentration of the heavier fraction. 0 corresponds to the light volume, 30 corresponds to both the Lth pump and the heavy volume. For $L=30$, $s=1.10$, and $V=0.5$. Volumes are expressed in liters.

and by the range of applicability. Since the first two of these requirements are limited by the efficiency of the individual units, the separation factors per pump for a number of gases have been determined.

The pumps are constructed and connected in series as shown in Fig. 1. Mercury vapor streams through the inner cylinder and forms a jet at E. At this point it is intercepted by a parallel cylinder of smaller radius which divides the stream so that only the inner part of it enters the cylinder. The outer portion of the stream acts as the separating agent while the central region serves to pump the gas which has diffused through the separating layer into the neighboring unit on the right. Since the lighter fraction of the gas has a greater diffusion coefficient, the gas pumped through C is enriched in this fraction. There is therefore a transport of the lighter fraction from left to right along the system of pumps through the upper connecting tubes. This is compensated by a flow of the heavier fraction in the opposite direction through the lower connecting tubes.

The action of each pump is to increase the relative concentration of its lighter fraction by a quantity s, which defines the separation factor per unit. When equilibrium is reached, the initially uniform distribution has been transformed into an exponential concentration gradient. The light gas (the gas enriched in the lighter fraction) collects in a reservoir at the right end of the system, while the heavy gas flows into a reservoir at the left end.

2. THEORY

We confine our attention to the heavier fraction and assume for simplicity that its concentration is always much smaller than that of the lighter fraction. Then at equilibrium, by our definition of the separation factor,

$$u(k)=su(k-1), \tag{1}$$

where $u(k)$ is the concentration of the heavier fraction in the kth pump; $k=0$ corresponds to the

reservoir at the "light" end of the system, and $k=L$ corresponds to both the Lth pump and the "heavy" reservoir. Since the total number of molecules is conserved,

$$V_0u(0)+\sum_1^L Vu(k)+V_Lu(L) = U(V_0+V_L+LV), \quad (2)$$

where V_0 and V_L are the volumes of the "light" and "heavy" reservoirs, respectively, V is the volume of each pump, and U is the initial concentration. Transforming (2) by means of (1),

$$u(k)/U=As^k, \quad (3)$$

where A is given by

$$A=(V_0+V_L+LV)/(V_0+V\sum_1^L s^k+V_Ls^L). \quad (4)$$

Equation (3) is represented graphically in Fig. 2. Since A is less than unity, there is an impoverishment of the heavier fraction in pumps near the light end, as is shown by the portion CD of the curve CDH. At D, enrichment begins, reaching a maximum value at $k=L$. The enrichment factor E for the entire system, defined as the ratio of the concentration at the heavy end to the initial concentration, is given by the ordinate of H. The separation factor S, the ratio of the concentrations at the heavy and light ends is given by H/C. By Eq. (3) it is seen that $S=s^L$ and is therefore independent of the choice of end volumes.

In order to obtain the maximum enrichment, A should approach unity. This is accomplished by making the light end volume as large as possible and the heavy volume small. The effect of the variation of volumes on the concentration gradient is indicated by the other curves of Fig. 2. When $V_0=\infty$, it is seen that E and S are identical. The maximum enrichment is therefore limited by s^L.

It is to be expected that an increased enrichment is obtained at the expense of the time required to reach equilibrium, since a greater amount of gas must be circulated through the pumps. Consequently it is of interest to see how the equilibrium time depends on the size of the end volumes, the number of pumps and the separation factor s. Barwich[5] has developed a theory for the time dependence of the separation process for the case of a small concentration of the lighter fraction of gas, with the assumption that the heavy end volume is infinite. It is possible, using Barwich's method, to investigate the case of finite end volumes by introducing more general boundary conditions.

If one assumes that the total volume V of each pump can be considered as concentrated in the immediate neighborhood of the mercury jet, the variation of the concentration $u(k)$ is due to three factors. Heavy gas from the $(k-1)$ pump is transported through D (Fig. 1) into the neighborhood of the jet (E) between the coaxial cylinders. Light gas leaves E through C, and flows into the $(k-1)$ pump. There is in addition a diffusion flow between E and the region $A-B$. If it is assumed that the gas in the latter region undergoes a complete mixing and that the gradient between E and $A-B$ is linear, one obtains the following equation: (cf. reference 5)

$$\partial u(k,\tau)/\partial\tau=(1/s)u(k+1,\tau) -(1+(1/s))u(k,\tau)+u(k-1,\tau), \quad (5)$$

where s is the separation factor, and τ is connected to the time t by the equation

$$t=\tau V(1/av+b/AD_0). \quad (6)$$

D_0 is the self-diffusion constant of the gas, A and b are the cross section and length of the path between E and $A-B$; a is the cross section of the connecting arms, and v is the velocity of flow through these tubes. In general $AD_0/b\gg av$, so that the second term of (6) may be neglected.

Equation (5) must be solved with the appropriate boundary conditions. For the Lth pump, it is assumed that V_L, the heavy end volume is added to V, so that the variation of $u(L)$ is due to the transport of heavy gas from the $(L-1)$ pump through D and the flow of light gas to the $(L-1)$ pump through C. Then

$$\partial u(L,\tau)/\partial\tau=\lambda_L\{u(L-1,\tau)-(1/s)u(L,\tau)\}, \quad (7)$$

where $\lambda_L=V/(V+V_L)$. This equation must be satisfied at all values of τ.

Similarly for $k=0$, that is, for the light volume V_0, the variation of $u(0)$ is due to the flow of

light gas from the first pump and the flow of gas to the first pump. Assuming that the outflowing gas has the same composition as the gas in V_0 and that $AD_0/b \gg av$, one obtains

$$\partial u(0, \tau)/\partial \tau = \lambda_0\{(1/s)u(1, \tau) - u(0, \tau)\}, \quad (8)$$

where $\lambda_0 = V/V_0$.

A third condition which must be satisfied by the solution of (5) is

$$u(k, 0) = U, \quad (9)$$

where U is the initial concentration of the heavier component.

When equilibrium has been reached, $\partial u(k)/\partial \tau$ vanishes. It is seen that $u(k) = su(k-1)$ satisfies Eqs. (5), (7) and (8). This steady state solution agrees with Eq. (1).

If we look for time dependent solutions of the form

$$u(k, \tau) = e^{-\mu\tau}s^k v(k) \quad (10)$$

we obtain from (5), (7), and (8) a set of three equations for $v(k)$ which constitute a boundary value problem which will have solutions for certain values of μ. Since there are $L+1$ points in the system, there should be $L+1$ distinct values of μ to each of which corresponds a function $v(k)$.

It can be shown that

$$v(k) = (1/s)^{k/2}\{Ce^{ik\theta} + De^{-ik\theta}\} \quad (11)$$

is a solution if θ is connected to μ by the relationship

$$\mu = 1 + 1/s - 2/(s)^{\frac{1}{2}} \cos\theta. \quad (12)$$

C and D are constants which must be chosen to satisfy the boundary conditions expressed by (7) and (8). On substituting (10) in these equations, one obtains two homogeneous linear equations whose determinant must vanish in order to give values of C and D other than 0.

L solutions of the determinantal equation are given by the values of θ which satisfy the equation

$$A + B\cos\theta = (\sin(L-1)\theta)/(\sin L\theta), \quad (13)$$

where $$A = \frac{\lambda_L/(s)^{\frac{1}{2}} + \lambda_0(s)^{\frac{1}{2}} - (1+s)/(s)^{\frac{1}{2}}}{\lambda_0 + \lambda_L - \lambda_0\lambda_L}$$

and $$B = 2/(\lambda_0 + \lambda_L - \lambda_0\lambda_L). \quad (14)$$

The additional solution of the secular determinant is the one corresponding to $\mu = 0$.

The complete solution is the sum of the functions corresponding to the different values of μ:

$$u(k, \tau) = \sum_n F_n e^{-\mu_n\tau}s^k v_n(k). \quad (10')$$

The functions $v_n(k)$ can be normalized by means of the orthogonality theorem appropriate to the problem,

$$\sum_{k=0}^{L} X_k s^k v_n(k) v_m(k) = \delta_{nm}, \quad (15)$$

where $$X_k = \begin{cases} 1/\lambda_0 & \text{for } k=0 \\ 1 & \text{for } k=1, 2\cdots, L-1. \\ 1/\lambda_L & \text{for } k=L \end{cases} \quad (16)$$

The coefficients F_n are to be determined with reference to Eq. (9). Application of (15) to (10′) yields

$$F_n = U\sum_k X_k v_n(k). \quad (17)$$

On normalizing the functions $v_n(k)$ and determining the corresponding F_n, one obtains as the complete solution

$$u(\tau, k) = Us^k(\sum_k X_k/\sum_k X_k s^k) + U\sum_n A_n s^{k/2} e^{-\mu_n\tau}\Theta_n(k), \quad (18)$$

where

$$\Theta_n(k) = (1 - \mu_n/\lambda_0)\sin k\theta_n - 1/(s)^{\frac{1}{2}}\sin(k-1)\theta_n$$

and $$A_n = \sum_k X_k s^{-k/2}\Theta_n(k)/\sum_k X_k\Theta_n(k)^2.$$

It is observed that when $\tau = \infty$

$$u(\infty, k) = Us^k(\sum_k X_k/\sum_k X_k s^k)$$

$$= Us^k((V_0 + V_L + LV)/(V_0 + V\sum_1^L s^k + V_L s^k)).$$

This expression is identical with the steady state solution given by Eq. (3).

The determination of the coefficients A_n indicates that in general the series does not converge rapidly, so that a number of them must be calculated. It is difficult to estimate in a simple fashion the time required to reach, for example, 90 percent of the final equilibrium value for various choices of V_0, V_L, s, and L. An indication of the

TABLE I. *Variation of $1/\mu$ with V_0, with $V_L=1$, $V=0.5$, $s=1.235$, $L=30$. (The volumes are expressed in liters.)*

V_0	1	10	20	100	1000	∞
$1/\mu$	55.5	122.	215	666	2175	$\sim\infty$

TABLE II. *Variation of $1/\mu$ with V_L, with $V_0=20$, $V=0.5$, $s=1.235$, $L=30$.*

V_L	0	0.5	1	2	5	10	100
$1/\mu$	205	214	215	219	225	228	231

TABLE III. *Variation of $1/\mu$ with L, with $V_0=20$, $V_L=1$, $V=0.5$, $s=1.235$.*

L	10	20	30	50	100
$1/\mu$	92.5	185	215	223	223

TABLE IV. *Variation of $1/\mu$ with s, with $V_0=20$, $V_L=1$, $V=0.5$, $L=30$.*

s	1.235	1.182	1.119	1.085	1.043
$1/\mu$	215	141	100	90	80

influence of these factors is given by Tables I–IV which present the values of the smallest μ corresponding to different experimental conditions. After sufficient time has elapsed, the progress of equilibration is determined by the term belonging to this μ.

The longest period (corresponding to the smallest μ value) increases rapidly with the magnitude of the light volume, but is relatively insensitive to changes in the other factors. Calculations show that the additional μ values are appreciably larger and fairly insensitive. It is of interest to note that the dependence of the equilibrium time on the number of pumps L is similar to the dependence on the heavy volume V_L. This suggests that the equilibrium time is determined primarily by the volume of the system and by the rate of transport.

It is apparent that the attainment of large enrichment factors is accompanied by a considerable increase in the equilibrium time, since the former demands the use of indefinitely large light volumes. The separation factor, on the other hand, is independent of the choice of end volumes, and is determined experimentally by the ratios of the concentrations in the end volumes. The choice of reservoirs in the present experiments ($V_0=10$–20 liters, $V_L=1$ liter) was therefore such as to insure sufficient gas for analysis and sufficient change in the concentrations at both ends to facilitate the analyses. An attempt to obtain maximum enrichment was made only in the case of methane. Here a twelve-hour run indicated a separation factor for $C^{13}H_4/C^{12}H_4$ in the neighborhood of 13, while the enrichment factor was approximately 5 since the enriched sample contained 5–5½ percent $C^{13}H_4$ (normal 1 percent). A continued run lasting 2½ days was then made, refilling the light reservoir from time to time with normal methane. The final analysis indicated 12.4 percent $C^{13}H_4$, showing that the full value of the separation factor had been obtained.

3. APPARATUS

Our experiments were performed on several sets of pumps. A system of fourteen units of the Hertz design (Fig. 1, "*A*") was used to investigate the separation of the isotopes of neon, oxygen, and bromine. In these pumps the cylindrical tube which divides the mercury stream is approximated by the cusp-like shape of the inner wall of the water jacket. They shall be referred to as type *A*.

An attempt was made to increase the efficiency of operation by securing a sharper division of the mercury stream by means of a cylindrical tube, ring-sealed into the neck of the inner wall of the water jacket (Fig. 1, "*B*"). Nine pumps having a radial clearance of 1 mm between the cylinders (type *B*) and eight with a clearance of 2 mm (type *C*) were constructed and added to twelve units of type *A* to form a final system of 29 units.

The pumps were tested for "pinholes" and thoroughly cleaned before mounting. In order to obviate the necessity of two gas-handling systems, the pumps were mounted around a narrow rectangular frame so that both ends were adjacent. In addition to the usual evacuating system, an automatic Toepler pump, was installed. This was fed by a diffusion pump and made it possible to remove desirable gases from the entire system in a short time.

During operation, it was sometimes necessary to run continuously over periods of several days. The system must therefore be completely "tight" in order to prevent impurities from interfering with the separation process or contaminating the

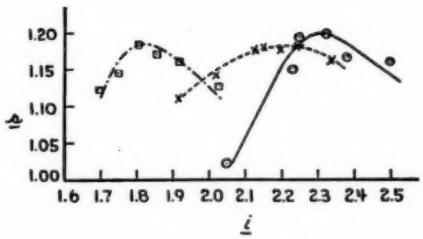

FIG. 3. Variation of separation factor with heater current for the *A*, *B*, and *C* units. Circle, for "*A*" pump; cross, for "*B*" pump; square, for "*C*" pump.

samples. While actual leaks were quickly eliminated, it took several weeks of continued pumping to get the system sufficiently hard. Several flushings with hydrogen, torching of the connectors, and heating of the inner surfaces of the pumps, (by turning off the water through the jackets for a short time), helped to remove adsorbed gases. The chief source of contamination proved to be impurities in the mercury, although this had been cleaned and distilled before using. When operations were begun, the pressure rose to 10^{-4} mm Hg in 24 hours and probably improved as time went on.

Heating was provided by Lavite electrical units whose hemispherical cavities were of the same diameter as the pump boilers. The heaters for a set of pumps were connected in parallel and the current through them was regulated by rheostats in the main leads. It was found that there was a considerable variation in the boiling rates between pumps which were receiving the same current. This variation was eliminated by adjusting the amount of asbestos packing until all of the pumps showed similar mercury streams, as indicated by a leak tester discharge.

Since it was often desirable to run the pumps overnight, safety devices were installed which turned off the heaters in case of failure of the water supply or of sudden increase of pressure in the pumps. The water devices were U tubes filled with mercury, the electrodes being so arranged that contact was maintained as long as there was a sufficient head. The pressure device was a mercury manometer with two tungsten electrodes arranged so that a gas pressure of several centimeters caused the mercury to make contact between them. Breaking of contact in the water gauges or making of contact in the gas manometer opened a heavy duty relay circuit breaker.

4. Procedure and Analysis

The study of many gases is considerably simplified by the fact that the optimum conditions of operation do not vary appreciably from one mixture to another. These optimum conditions were found by observing the degree of separation obtained for various values of heater current and gas pressure.

As the heater current is increased, the over-all separation passes through a maximum. Barwich[5] found that the separation *vs.* current curves for a single pump passed through a maximum, fell to a minimum, and rose again. In addition different pumps exhibited different characteristics. However, if capillary tubes were inserted in the upper connecting arms, (see Fig. 1), the characteristic curves showed single broad maxima which were more or less in the same region for different pumps.

Typical calibration curves are shown in Fig. 3. The experimental data has been reduced to average current and separation factor per unit. The latter is obtained by taking the Rth root of the over-all separation factor for each set of R pumps. The differences exhibited by the three types of pumps is to be attributed largely to difference of design, and partly to natural variations which depend on the packing. These curves were obtained simultaneously from observations on the composite system of 29 units. Analyses were made of samples taken from both ends of each set of pumps. It was found that each set gave a separation factor which depended only on its heater current and was independent of the operation of its neighbors.

Similar curves obtained for different initial gas pressures usually indicated a marked decrease of separation factor with increasing pressure. (Analyses of molecular oxygen failed to disclose such a decrease.) Consequently an initial pressure of 2 mm was found to be most desirable, larger pressures decreasing the separation, and smaller pressures decreasing the yield.

The analyses of the isotopic mixtures were made with mass spectrographs. An instrument of the Dempster type was connected directly to the system of 29 units by a long narrow pipe line. This mass spectrograph required about 0.5 cc of gas for analysis and gave reasonably accurate

relative abundances when the latter were in the region from 1 to 40. Other analyses were made by Dr. J. A. Hipple, Jr., and D. L. G. Smith of this laboratory on mass spectrographs which have been described elsewhere.[7]

5. Results and Discussion

The results of experiments on a number of gases is given in Table V. The first column gives the gas or gases used, while the second gives the mass numbers of the molecules involved. The third and fourth columns show the experimental separation factors s, and log s, for the three types of pumps, A, B, and C. The fifth column gives the radii of the molecules. The radii of Hg and H_2O are those used by Barwich.[5] That of CH_3Br does not appear in the literature, so that a reasonable value has been assumed. The remaining values are taken from viscosity measurements.[8]

According to Barwich,[5] the separation factor s is given by

$$\log s = a\{(r_1+r_Q)^2(m_1)^{\frac{1}{2}} - (r_2+r_Q)^2(m_2)^{\frac{1}{2}}\},$$

where r_1 and m_1 are the radius and mass of the heavier molecule, r_2 and m_2 the corresponding quantities for the lighter molecule, and r_Q is the radius of the mercury molecule. The quantity a is a constant depending on the geometry of the mercury jet and on the rate of streaming of the vapor. If we designate the bracketed expression by F then

$$\log s = aF.$$

The values of F corresponding to the various mixtures are given in the last column of Table V.

The values of the separation factors which have been obtained for type A for Ne, H_2O, and A are to be compared with those obtained by Barwich[5] and Kopfermann and Kruger,[6] who worked with a system of A pumps. If their data is reduced to separation factor per pump, one obtains for Ne, H_2O and A, the values 1.2, 1.085, and 1.126, respectively. The slightly higher factor for water vapor is to be attributed to the lower pressure used by Barwich, 2 mm as compared with 5 mm used in the present work. The factor for argon is smaller than that which we have obtained and may be due to the possibility that equilibrium had not been reached in the experiment of Kopfermann and Kruger. It is of interest to note the high value obtained for the $A-CO_2$ mixture. While diffusion through porous-walled tubes gives the same factor for $A-CO_2$ as for Ne,[3] the present method gives a much larger value for the former mixture.

Barwich[5] found that runs with equal mixtures of the rare gases under identical conditions gave separation factors which agree well with his theoretical formula. The present experimental values of log s do not, however, indicate the predicted linear dependence on F. This discrepancy is probably due to a number of effects.

The formula derived by Barwich is at most only approximate, due to the simplifying assumptions made, especially those concerned with the shape of the mercury stream. The latter was assumed to be cylindrical, whereas actually it is fan-shaped and changes with gas pressure and different gases. The variation of separation factor with pressure and initial concentrations (as found by Barwich by varying the relative concentrations of the mixtures mentioned above) is not unwarranted, although not contained in the theoretical formula. In the present experiments, the initial concentrations ranged from 0.02 percent H_2O^{18} to 50 percent for the bromine isotopes. It is difficult to say whether this variation of concentrations is wholly responsible for the erratic behavior of the separation factors. It is possible that the peculiarities of the gases with respect to interaction with the hot mercury stream, adsorption on the glass walls, and back diffusion may strongly influence the fractionating process.

Observation of the mercury vapor jet of the "A" pumps by means of a leak tester discharge

Table V. *Separation factors for various mixtures.*

Gas	Mass Numbers	Separation Factor			Log s			Radius $\times 10^8$ cm	F
		A	B	C	A	B	C		
CH_3Br	94, 96	1.005			0.005			(1.7)	(1.225)
CH_4	16, 17	1.107	1.105	1.061	.1017	0.0999	0.0592	1.6	1.427
O_2	32, 34	1.045			.0440			1.48	1.879
Ne	20, 22	1.198	1.183	1.183	.1807	.1681	.1681	1.18	1.936
H_2O	18, 20	1.073			.0705			1.4	2.253
A	36, 40	1.154	1.140	1.057	.1432	.1310	.0554	1.49	3.51
$A-CO_2$	40, 44		1.7			.531		1.49 1.70	12.61

[7] W. Bleakney, Phys. Rev. **40**, 496 (1932); Smith, Lozier, Smith and Bleakney, Rev. Sci. Inst. **8**, 51 (1937).

[8] Herzfeld, *Handbuch der Physik*, Vol. 22.

reveals a jet so ill defined that it seems as if its separating efficiency is almost fortuitous. Similar observations on the type *B* and *C* units show jets in which the separating and pumping layers are quite distinct and well defined. Despite the better geometry of the latter pumps, their efficiency is smaller. Furthermore, the *C* units are less efficient than the *B*, although the diffusion path in the former is larger.

Experiments with a fourth type of pump have given the reason for this failure to realize our expectations. The newest unit is essentially the same as the *C* pump except that it is inverted, so that the mercury streams downward. It was observed that in the other pumps large globules of condensed mercury would fall and tear holes in the mercury stream through which gas could pass through the jet without being fractionated. This effect probably accounts to a large extent for the dropping off of the separation factor with high heating current. The new pump was therefore inverted in order to eliminate this.

Tests with a mixture of $Ne-CO_2$ showed that this pump, with improved geometry, was even more inefficient. In addition to the smaller separation factor, the range of current was considerably narrower. These tests were made allowing the gas to circulate freely. The stopcocks in the system were then so adjusted that gas could enter or leave the light volume only by diffusing through the mercury jet. With a current which previously had given no separation a practically complete fractionation was obtained. Neon was run under similar conditions and gave a separation factor for $Ne^{20} : Ne^{22}$ of 1.5 or larger, as compared with the value of 1.2 obtained previously. Because of the extreme slowness with which this separation progressed, it would not be practical despite the fact that the present pump is equivalent to more than two of the other units.

However, these tests show a direction which improvement may take. The transport of the lighter fraction in a fractionation system is insured by the pumping action of each unit. The opposite flow of the heavier fraction through the lower connectors (Fig. 1) is due to the pressure gradient which is established. This latter mass flow is offset by diffusion and unless there is a sufficient pressure gradient, the transport is nullified and the fractionating effect of the jet is not realized. While the "*A*" units pumped so rapidly that capillaries had to be introduced in the upper arms to reduce the transport, the "*B*" and "*C*" units gave rise to much smaller pressure differences. The resulting ill effects of back diffusion should be eliminated by using small capillaries in the lower connectors or by introducing circulating pumps.

This method of separation is applicable to a wide range of elements and gives factors which are favorable compared to those given by other methods. Since the separation factor increases exponentially with the number of pumps, any desired enrichment can be obtained by employing a sufficient number of units. The yield differs for various mixtures, but is of the order of 1 cc of enriched gas at NTP per day.

In conclusion the author wishes to acknowledge his indebtedness to Dr. W. Bleakney under whose direction this work was done, for his continued interest and helpful discussions; to Dr. E. U. Condon for his aid in developing the theoretical considerations; and to Dr. J. A. Hipple, Jr. and Dr. L. G. Smith for analyses of samples.

On the Paramagnetic Conversion of Parahydrogen and Orthodeuterium in the Presence of Nitrous Oxide (The Magnetic Moment of the Deuteron)

L. Farkas and U. Garbatski
Department of Physical Chemistry, The Hebrew University, Jerusalem
(Received February 7, 1938)

THE present communication deals with the comparison of the rates of the two reactions

$$p\text{-}H_2+NO\rightleftarrows o\text{-}H_2+NO, \quad (1)$$

$$o\text{-}D_2+NO\rightleftarrows p\text{-}D_2+NO, \quad (2)$$

in which the *ortho-para* conversion takes place under the influence of the inhomogeneous magnetic field of the NO molecules.[1] According to the theory of Wigner[2] the ratio of the velocities of these two reactions is proportional to $(\mu_H/\mu_D)^2$ where μ_H and μ_D denote the magnetic moments of the proton and of the deuteron.[3] In a previous paper the rate of conversion of light and heavy hydrogen was determined under the influence of O_2[4] and on the basis of a theory of Kalckar and Teller[5] the value $\mu_H/\mu_D=4$ was obtained.

It seemed interesting to determine the ratio of the rates of conversion also under the influence of other paramagnetic substances and the reactions (1) and (2) seemed suitable for such an investigation, the comparison of the two reactions being possible in a wide temperature range.

The reaction vessel had a volume of 50 cc and was kept at constant temperature by means of an electric furnace or suitable cooling bath. First p-H_2 or o-D_2 of 20–40 mm pressure was introduced into the reaction vessel; afterwards NO of known pressure. The pressure was measured with a mercury manometer attached to the glass tube leading to the reaction vessel. p-H_2 and o-D_2 were prepared in the usual way by adsorption on charcoal, cooled with solid air. NO was prepared from a solution of potassium iodide and nitrite and fractionated in vacuum several times. The determination of the concentration of p-H_2 and o-D_2 was carried out according to the micro-thermoconductivity method,[6] extracting small samples from the reaction vessel by means of a capillary lock. The pressure in the reaction vessel did not change more than 1–2 percent during a run, even if several samples were extracted from it for the analysis. Special precaution was taken to prevent NO from coming into the conductivity cell: the hydrogen NO mixture which had to be analyzed passed very slowly through a trap cooled with solid air before it was pumped into the conductivity cell.

The *ortho-para* conversion under the influence of paramagnetic substances is a bimolecular reaction. Since the pressure of the paramagnetic substance remains constant, the progress of the reaction is given by

$$u_t=u_0e^{-k[NO]t}, \quad (3)$$

where u_t and u_0 are the excess concentration of p-H_2 or o-D_2 above the equilibrium concentration at the time $t=t$ and $t=0$ and the temperature $T°$ abs. The half-lifetime τ of the reaction is inversely proportional to the pressure of NO and is independent of the hydrogen pressure. In Fig. 1 one experiment on the conversion of p-H_2 and one on the conversion of o-D_2 in the presence of NO are represented. It will be recognized that the conversion of p-H_2 is much quicker than that of the o-D_2 at the same pressure of NO.

In Table I the data of the experiments on the rate of the reaction (1) at different pressures and temperatures are listed. Table II gives a summary of the results obtained for the reaction (2). Each constant is the mean value obtained from a run. The velocity constants are independent of the pressure and only slightly dependent on temperature. The velocity constants, k_{H_2}* and k_{D_2}*, as listed in column 5 were calculated from the observed half-lifetimes allowing for the fact that only a certain percentage of the NO molecules are paramagnetic in the proper sense. The two

[1] L. Farkas and H. Sachsse, Zeits. f. physik. Chemie **B23**, 1 (1933).
[2] E. Wigner, Zeits. f. physik. Chemie **B23**, 28 (1933).
[3] A. and L. Farkas and P. Harteck, Proc. Roy. Soc. **A144**, 481 (1934).
[4] A. Farkas and L. Farkas, Proc. Roy. Soc. **A152**, 152 (1935).
[5] Kalckar and Teller, Proc. Roy. Soc. **A150**, 520 (1935).
[6] A. Farkas and L. Farkas, Proc. Roy. Soc. **A144**, 467 (1934).

lowest electronic states of NO are $^2\Pi_{1/2}$ and $^2\Pi_{3/2}$, the ground level $^2\Pi_{1/2}$ being diamagnetic and the $^2\Pi_{3/2}$ level, 353 cal. above the ground level, paramagnetic. Consequently only those NO molecules are paramagnetic which are in the $^2\Pi_{3/2}$ state and their concentration varies with the temperature as listed in column 4.

The values for the constants of the reaction (1) differ somewhat from those given in a previous paper;[1] the present determinations seem to be more accurate.

It will be seen that the constants for the parahydrogen conversion are roughly* ten times greater than the constants of the orthodeuterium conversion at the same temperature.

In Table III the velocity constants of the reactions (1) and (2) are compared at different temperatures with the corresponding constants of the parahydrogen and orthodeuterium conversion under the influence of O_2. The ratio of the constants in the case of O_2 is approximately the same as for the conversion with NO but the absolute values of the velocity constants $k^*_{H_2}$ and $k^*_{D_2}$ in columns 3 and 4 are about 5 times greater with NO than with O_2.

The theoretical expressions for velocity constants of the conversion (in mole lit.$^{-1}$ min.$^{-1}$)

TABLE I. p-H_2+NO⇌o-H_2+NO.

T° ABS.	PRESSURE IN MM HG	τ IN MIN.	% NO PARAMAGNETIC	k^* IN MOLE LIT.$^{-1}$ MIN.$^{-1}$	k IN MOLE LIT.$^{-1}$ MIN.$^{-1}$
193	30	29	27.5	34.7	9.6
193	17	47	27.5	37.8	10.4
193	18	45	27.5	37.5	10.3
288	24	43	34.5	34.9	12.0
288	43	24	34.5	34.9	12.0
598	47	39	41.6	33.8	14.1

TABLE II. o-D_2+NO⇌p-D_2+NO.

T° ABS.	PRESSURE IN MM HG	τ IN MIN.	% NO PARAMAGNETIC	k^* IN MOLE LIT.$^{-1}$ MIN.$^{-1}$	k IN MOLE LIT.$^{-1}$ MIN.$^{-1}$
193	80	107	27.5	3.50	0.96
193	80	107	27.5	3.50	0.96
193	112	75	27.5	3.60	0.99
292	80	124	34.5	3.63	1.25
292	94	104	34.5	3.65	1.26
292	131	72	34.5	3.80	1.31
292	192	49	34.5	3.80	1.31
600	150	110	41.6	3.03	1.26
600	189	91	41.6	3.15	1.31
600	216	87	41.6	3.41	1.42
600	237	72	41.6	3.13	1.30

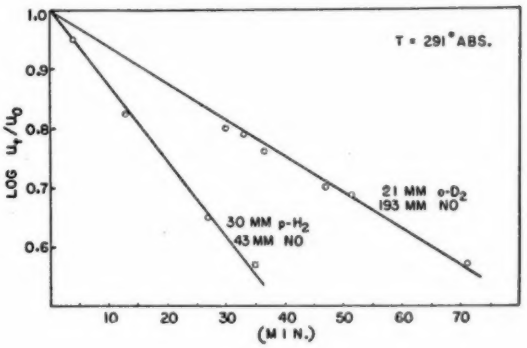

FIG. 1.

is given by

$$k=3.6\cdot 10^{22} d_T^2 \bar{c}\left[\frac{k_{01}a_0+(k_{21}+k_{23})a_2+\cdots}{1+a_2+a_4+\cdots}+\frac{(k_{10}+k_{12})a_1+(k_{32}+k_{34})a_3+\cdots}{a_1+a_3+\cdots}\right], \quad (4)$$

where d_T denotes the distance of nearest approach, $\bar{c}$ the relative velocity of the colliding molecules, k_{lm} the rate constant of the transition $l\rightarrow m$ and a_J the concentration of hydrogen molecules in the rotational state J.

According to Wigner[2] the theoretical expressions for the transition probabilities W_{lm} are as follows:

$$W_{J,\,J+1}=\frac{4\pi^2\mu^2\mu_X^2 I}{h^2 d_T^6 kT}\cdot\frac{1}{18}\,\frac{(2s+1)}{s}\,\frac{J+1}{2J+1}$$

$$=C\mu^2 I\frac{2s+1}{s}\cdot\frac{J+1}{2J+1}, \quad (5a)$$

$$W_{J,\,J-1}=C\mu^2 I\frac{2s+1}{s}\,\frac{J}{2J+1} \quad (5b)$$

for the *ortho→para* transitions,

$$W_{J,\,J+1}=C\mu^2 I\frac{(2s+1)(s+1)}{s^2}\,\frac{J+1}{2J+1}, \quad (5c)$$

$$W_{J,\,J-1}=C\mu^2 I\frac{(2s+1)(s+1)}{s^2}\,\frac{J}{2J+1} \quad (5d)$$

for the *para→ortho* transitions.

In these formulae s denotes the mechanical momentum of the H or D ($s_H=\frac{1}{2}$, $s_D=1$) nucleus, μ_X the magnetic moment of the para-

TABLE III.

	O_2		NO			
T	k_{H_2}	k_{D_2}	$k_{H_2}^*$	$k_{D_2}^*$	k_{H_2}	k_{D_2}
°ABS.	IN MOLE LIT.$^{-1}$ MIN.$^{-1}$					
83	2.7	0.5	—	—	—	—
193	7.1	0.7	37.0	3.50	10.0	0.96
293	8.2	0.83	34.9	3.75	12.0	1.30
600	12.1	—	33.8	3.20	14.1	1.35

magnetic molecule, μ the magnetic moment of the proton or deuteron and I the momentum of inertia of the hydrogen isotope considered. For calculating the rate constants from these transitions probabilities it is the simplest to assume that $k_{lm}=W_{lm}$ if the transition is exothermic and $k_{lm}=W_{lm}\cdot e^{-(E_l-E_m)/kT}$ in case the transition of the energy level E_l to E_m is endothermic.

Introducing the values for a_J and k_{lm} into the formula (4) we obtain for rate constants

$$k_{H_2}=3.6\cdot 10^{22}\frac{2}{9}\frac{\mu_P^2\mu_X^2 I_{H_2}\pi^2}{h^2 d_T^6 kT}\left(\frac{8RT(M_{H_2}+M_X)}{\pi M_{H_2}M_X}\right)^{\frac{1}{2}}\cdot\left[\frac{12(e^{-E_1/RT}+2e^{-E_2/RT}+3e^{-E_3/RT}+\cdots)}{\sum_{J=\text{odd}}(2J+1)e^{-E_J/RT}}+\frac{4(e^{-E_1/RT}+2e^{-E_2/RT}+\cdots)}{\sum_{J=\text{even}}(2J+1)e^{-E_J/RT}}\right], \quad (6)$$

$$k_{D_2}=3.6\cdot 10^{22}\frac{2}{9}\frac{\mu_D^2\mu_X^2 I_{D_2}\pi^2}{h^2 d_T^6 kT}\left(\frac{8RT(M_{D_2}+M_X)}{\pi M_{D_2}M_X}\right)^{\frac{1}{2}}\cdot\left[\frac{3(e^{-E_1/RT}+2e^{-E_2/RT}+\cdots)}{\sum_{J=\text{even}}(2J+1)e^{-E_J/RT}}+\frac{6(e^{-E_1/RT}+2e^{-E_2/RT}+\cdots)}{\sum_{J=\text{odd}}(2J+1)e^{-E_J/RT}}\right]. \quad (7)$$

In the communication of Farkas and Sachsse[1] it was tentatively suggested that the comparatively high rate of conversion in the presence of nitrous oxide is due to resonance between the energy of the 0→1 transition (337.2 cal.) and the energy of paramagnetic $^2\Pi_{3/2}$ level (353 cal.) of nitrous oxide. From the formula (4) it is evident that the contribution of transition 0→1 will be large, were it not counteracted by the endothermicity of this transition. It was suggested that this energy might be preferentially supplied by paramagnetic nitrous oxide molecules.

In the light of the present experiments this view cannot be upheld. In the case of *o*-D_2 such a resonance between the energy of the first rotational state (in this case 170.2 cal.) and the energy of the $^2\Pi_{3/2}$ level of nitrous oxide does not exist and yet the rate of conversion induced by nitrous oxide is five times larger than with oxygen. This is due either to a higher specific activity of the nitrous oxide in inducing the *ortho-para* conversion for which no theoretical reason can be given at present or to the contribution of nitrous oxide molecules in the $^2\Pi_{1/2}$ state. Though this level appears in magnetic measurements as diamagnetic it might be of the same effect for an *ortho-para* conversion as the paramagnetic $^2\Pi_{3/2}$ state. Accordingly, in column 6 of Tables I and II and columns 6 and 7 in Table III the velocity constants are calculated under the assumption that all the NO molecules are equally effective for the conversion. The velocity constants thus obtained are only slightly larger than the corresponding rate constants for oxygen.

As already mentioned, on the basis of the theory of Kalckar and Teller, the value $\mu_H/\mu_D\sim 4$ was obtained from the velocity of the *p*-H_2 and *o*-D_2 conversion in the presence of O_2, according to the general formula

$$\frac{k_{H_2}^{(2T)}}{k_{D_2}^{(T)}}=\frac{\mu_H^2 S_D^2(2S_H+1)[\xi(S_H+1)+S_H]}{2\mu_D^2 S_H^2(2s_D+1)[S_D+1+\xi S_D]}, \quad (8)$$

where $k_{H_2}^{(2T)}$ and $k_{D_2}^{(T)}$ are the velocity constants at the temperatures $2T$ and T and

$$\xi=\frac{\sum_{J=\text{odd}}(2J+1)e^{-E_J/RT}}{\sum_{J=\text{even}}(2J+1)e^{-E_J/RT}}.$$

This formula was derived without making special assumptions on the mechanism of the collision and compares the velocity of the *p*-H_2 conversion at the temperature $2T$ with the D_2 conversion at the temperature T, because under these conditions the momentum distribution of hydrogen and of deuterium are identical. How-

ever, Kalckar and Teller's theory neglects the influence of the kinetic energy of colliding particles on the distance of nearest approach, d_T.

According to Wigner's theory the ratio μ_H/μ_D is obtained by dividing Eq. (6) by (7).

In Tables IV and V the ratio is listed for different temperatures as calculated according to the two theories.

It will be recognized that according to Wigner's theory the same value is obtained for μ_H/μ_D from the experiments with O_2 as from experiments with NO. The formula of Kalckar and Teller gives different values. This result does not, however, invalidate the theory of Kalckar and Teller, since their basic assumptions are not fulfilled in the case of the conversion with nitrous oxide, the energy distribution of the nitrous oxide molecule not being the same at the temperature $2T$ and T.

The difference between the value for μ_H/μ_D obtained in the case of O_2 according to the theory of Teller and Kalckar on the one hand and the value for μ_H/μ_D in the cases O_2 and NO according to the theory of Wigner on the other hand is not very much. It is difficult to decide which of the two theories is the better approximation. We would like to call attention to the fact that Wigner's theory allows for the temperature variation of the distance of nearest approach, which, as pointed out in a previous paper,[7] is quite considerable. On the other hand, the method of Kalckar and Teller allows properly for the variation of the rotational energy of H and D with temperature.

The value 3.8 for the ratio μ_H/μ_D together with the latest value for $\mu_H=2.46$ nuclear magnetons, according to Estermann, Simpson and Stern,[8, 9] gives for $\mu_D=0.65$ nuclear magnetons. These values are markedly different from the results of Kellogg, Rabi and Zacharias.[10] These authors obtained for $\mu_D=2.85$ n.m. and for $\mu_D=0.85$ n.m. and thus for the ratio $\mu_H/\mu_D=3.35$ by measuring the deflection of hydrogen and deuterium atom beams in a magnetic field. Though it is possible that the disagreement between the values for the proton's magnetic moment according to the two methods is due to some experimental error, it is more probable that in Rabi and co-workers' experiments a hitherto unknown spin-spin interaction of the proton-electron is measured as well[11] and is responsible for the higher values for μ_H and μ_D. The present experiments should be compared with the measurements of Estermann and Stern, since they concern the magnetic behavior of the molecule in an external field. If we assume that the present value for $\mu_D=0.65$ n.m. is the magnetic moment of the deuteron without the spin-spin interaction of the proton-electron, then it seems that this effect increases the value of μ_H by 0.4 n.m. and the value of μ_D by 0.2 n.m.

TABLE IV. *According to Wigner.*

T	O_2 μ_H/μ_D	NO μ_H/μ_D
86	3.6	—
195	3.9	3.8
290	3.8	3.6
600	—	3.8
	mean	3.80

TABLE V. *According to Kalckar and Teller.*

T	O_2 μ_H/μ_D	NO μ_H/μ_D
86	3.85	—
195	4.03	3.35
290	4.07	3.2
	—	—

[7] Farkas and Sachsse, reference 1. The variation of d with the temperature is given by

$$d_T=d_{0H_2}(1+C_{H_2}/T)^{\frac{1}{2}}+d_{0X}(1+C_X/T)^{\frac{1}{2}},$$

where C_{H_2} and C_X denote the Sutherland constants of H_2 and the molecule X.

[8] I. Estermann, O. C. Simpson and O. Stern, Phys. Rev. **52**, 535 (1937).

[9] I. Estermann and O. Stern, Phys. Rev. **45**, 761 (1934).

[10] J. M. B. Kellogg, I. I. Rabi and I. R. Zacharias, Phys. Rev. **50**, 472 (1936).

[11] G. Breit, Phys. Rev. **51**, 248 (1937), footnote 14; L. A. Young, Phys. Rev. **52**, 138 (1937).

On the Nature of Ionic Sign Preference in C. T. R. Wilson Cloud Chamber Condensation Experiments

L. B. Loeb, A. F. Kip and A. W. Einarsson
Department of Physics, University of California, Berkeley, California

(Received January 18, 1937)

Experiments made to ascertain if the charge preference in the C. T. R. Wilson cloud method of condensation was due to different hygroscopic impurities brought into the embryonic droplets by capture of ions of different sign proved definitely negative. Since the electrical double layers at liquid-gas surfaces are also incapable of explaining the phenomenon the following hypothesis was evolved and compared to existing experimental data together with results obtained for the first time on $C_6H_5NO_2$, C_6H_5Cl, C_4H_9Br, $C_6H_5CH_3$, $C_6H_5NH_2$ and new results on C_2H_6CO, C_6H_6 and C_2H_5I. It is assumed that the saturated vapor contains *embryonic droplets* of radius insufficient to bring surface tension forces into play. These droplets unlike the larger and more stable visible and invisible droplets are in a *state neither crystalline nor liquid but in a pseudo-crystalline state* having definite space structure. In such pseudo-crystalline or embryonic droplets the orientation of the molecules is determined by van der Waals forces which are directive. As in Thomson's theory at lower supersaturation the nascent surface tension forces preclude growth beyond a certain size. Capture of gaseous ion as in Thomson's theory facilitates condensation by adding dielectric attractive forces. If, the droplet and vapor consist of polar molecules whose dipole moment is oriented in such a direction as to bring approaching vapor molecules to the pseudo crystal surface in an orientation favorable to further structural growth the sign of charge favoring this process will produce visible droplets at a lower supersaturation than will the opposite sign. Once condensation has proceeded to a point where surface tension forces are fully developed the droplet goes over to the *liquid* state having an electrical double layer and neither sign of charge have any further influence on condensation. Using as the directive forces in condensation primarily hydrogen bond formation and dipole attraction the effects observed experimentally can be accounted for on plausible assumptions as to linkage in the embryonic drops. The reason that gaseous ions are not observed to grow to these droplets can be ascribed to the fact that these are already stable complex ions of very few molecules whose orientation is not that of the pseudo-crystals. A capture of such an ion by a pseudo-crystal of 10^2 to 10^5 molecules will not, however, affect the pseudo-crystal other than to facilitate condensation. It is believed possible that it is these pseudo-crystalline droplets or groupings existing in liquids that account for the cybotatic state described by G. W. Stewart from x-ray studies. In gases it is possible that they constitute the intermediate atmospheric ions when large enough to survive the acquisition of a charge. The larger or Langevin ions are then probably the nucleii once formed by supersaturation and condensation to visible size and which have subsequently re-evaporated to invisible liquid droplets with surface tension forces active (10^7 or more molecules) that have acquired a charge. The three groups of ions mentioned exist independently with charged carriers of sizes lying between them entirely absent except during the unstable conditions producing transition.

Introduction

When C. T. R. Wilson[1] made his early studies on the cloudy condensation produced by ions in a gas, he discovered that with water vapor the condensation occurred at lower expansion ratios for negative ions than for positive ions. Przibram[2] later observed that in some substances, for example, ethyl alcohol, the condensation occurred more readily on the positive ion. While the subsequent work confirmed the sign preference, the results were mostly quite discordant.[3–5] The causes of the discrepancy may be sought for in one or several of the following factors:

1. Differences in the degree to which adiabatic expansion was achieved.

2. Failure to correct for the influence of the vapor of the substance in calculating supersaturation.

3. Lack of uniformity and control of the purity of the substance used.

4. No clearly defined common criterion for the appearance of condensation. This is extremely important as the work of Andren[6] and the present work show.

[1] C. T. R. Wilson, Phil. Trans. Roy. Soc. **A189**, 265 (1897); **A193**, 289 (1899). J. J. Thomson, Phil. Mag. **36**, 313 (1893).

[2] K. Przibram, Ber. d. Königl. Akad. Wiss. Wien, **II a 115**, 23, 1906, **II a 118**, 331 1909. Also for later discussion and references see Geiger and Scheel, *Handbuch der Physik*, second edition, Vol. 22, part 1, p. 418 ff.

[3] F. G. Donnan, Phil. Mag. **3**, 305 (1900).

[4] T. A. Laby, Phil. Trans. Roy. Soc. **A208**, 445 (1908).

[5] *International Critical Tables*. Vol. VI (1926), p. 117.

[6] L. Andren, Ann. d. Physik **52**, 1 (1917).

5. Failure to study a sufficient diversity of substances with a uniform technique to enable the nature of the process to be analyzed.

Although the phenomenon of sign preference has thus long been known and utilized in the early determinations of e,[7] its character is completely obscure. In an endeavor to understand the mechanism, investigations suggested by tentative hypotheses were undertaken by us. In these, some of the difficulties in previous work came to light. No attempt was made to make exhaustive or careful redeterminations or to correct the past errors. Enough data, however, have been accumulated, when taken with negative evidence from other fields to lead us to propose a radical but seemingly plausible theory.

The theory for the condensation in the cloud chamber experiments propounded by J. J. Thomson[8] is as follows: Saturated vapor contains numbers of minute nuclei of condensation. Adequate supersaturation causes these to increase by condensation. As they reach a size where the forces of surface tension become fully developed, the curvature of the surface inhibits further condensation, unless the supersaturation exceeds a certain value. For water at room temperatures this occurs at eightfold "supersaturation" as defined by C. T. R. Wilson. Between fourfold and eightfold supersaturation, the droplets do not grow to visible size. If, however, the droplets acquire a negative charge above fourfold supersaturation condensation occurs. Positive charges require about a sixfold supersaturation. The visible droplets must have a diameter of about 10^{-5} cm. This action is due to the forces of dielectric attraction *in* the water droplet, which counteract the effect of the curvature of the surface. It is not open to more than a semi-quantitative verification at the present time.

In its original form, the theory assumed that the water droplets *grew about the ions* by condensation. As early as 1917, Loeb[9] showed that this assumption was purely gratuitous. All that the theory requires is that the embryonic droplets acquire a charge in order that they grow. The charge can be acquired in an ionized gas just as Millikan's oil drops acquired charges.

It must be noted that this mechanism does *not* account for sign preference, since the dielectric action of the charge in the drop is *independent* of its sign. The following hypotheses have been at one time or another considered as accounting for sign preference:

1. That the ions have a specific affinity for vapor molecules which is sign dependent. That the condensation begins *about* the ions and that as ions grow, the one with the strongest affinity grows faster. This implies that the affinity manifests itself for drops that are of considerable size.

2. That there is an electrical double layer in the surface of the drop with one sign of charge outside and the other inside. A charge on the drop which orients approaching vapor molecules so as to combine with this layer will favor the condensation. The opposite charge will hinder this process. The nonpreferential electrostatic forces of the charge acting on the drop in Thomson's equation act independently of the double layer. In his third edition, J. J. Thomson proposes such a double layer. He, however, places one sign of charge *in the gas phase* and the other in the drop.

3. That the gas ions being electrochemical complexes, analogous to complex ions in solution, carry into the embryonic droplets besides the charge some of their companion molecules.[10] If the type of companion carried by one sign of ion into the embryo lowered its vapor tension, more than did the companion carried by the opposite ion, one might expect a difference in condensing power. That is, it was believed possible that the few impurity molecules carried into droplets by ions might add the effect of a concentrated solution in lowering the vapor tension of the droplets.

Since, as will later be seen, there was strong evidence against the first and second of these explanations, experiments were undertaken with a view to ascertaining the real extent of the sign preference and to determining whether hygro-

[7] J. J. Thomson, Phil. Mag. **46**, 528 (1898); **48**, 547 (1899).
[8] J. J. Thomson, *Conduction of Electricity Through Gases*, third edition, Vol. 1 (Cambridge 1928), pp. 320–333.
[9] L. B. Loeb, J. Frank. Inst. **182**, 790 (1917).

[10] L. B. Loeb, Summary in *Kinetic Theory of Gases*, second edition (McGraw-Hill, New York, 1934), Section 106, p. 564 ff. Also Phys. Rev. **32**, 81 (1928); **38**, 549 (1931), and Bradbury, Phys. Rev. **38**, 1716 (1931). See also Tyndall and Phillips, Proc. Roy. Soc. **A111**, 577 (1926); Loeb and Dyk, Proc. Nat. Acad. Sci. **15**, 146 (1929). Herbert Mayer, Physik. Zeits. **27**, 513 (1926); O. Luhr, Phys. Rev. **44**, 459 (1933); **28**, 637 (1927).

FIG. 1.

scopic impurities carried into drops by the ions could be of any influence as suggested under hypothesis 3.

EXPERIMENTAL PROCEDURE AND RESULTS

The technique was essentially that employed by C. T. R. Wilson.[1] The design of the cloud chamber is shown in Fig. 1. Expansion was effected by means of a glass plunger which was floated in the liquid to be tested. On opening the valve to the vacuum tank the air was removed from beneath the glass plunger, causing it to be forced down onto a rubber washer with such speed as to make the expansion process essentially adiabatic. The presence of the metal parts makes realization of adiabatic expansion more difficult. For most of the liquids other than water, the rubber washer was replaced by Thiokol, an artificial rubber which is resistant to many organic substances, including most of those tested. In operation, the gas is ionized by a narrow beam of x-rays in the central section by a flash from the x-ray tube. A lead block B prevents the x-rays from striking the central electrode A. A thin aluminum window is provided for the entrance of the x-rays. The two copper plates, P and N, are respectively positive and negative with respect to A to a degree sufficient to draw the negative ions out towards P and the positive ions out towards N. At the proper time the measured adiabatic expansion is effected, giving a nearly nonturbulent region between A, N, and P. The nature of the expansion ratio for the condensation on positive and negative ions and that for general cloudy condensation can then be determined. For if the time interval between ionization and expansion and the electrical field are correct, only positive ions exist in the region near N and negative ions in the region near P. For water, the potential required between the center plate and N and P was ± 1.5 volts; for other substances such as C_2H_5I it was as high as 50 volts. The potentials on P and N were reversed to avoid any errors due to lack of symmetry of the x-ray beam. The time interval between x-ray flash and expansion for most complete separation of positive and negative ions used at these voltages was about one second. *The criterion for onset of condensation was taken as the lowest expansion ratio which gave a definite cloud, as contrasted to the 5 or 10 scattered drops which are nearly always present near the critical expansion ratio.* The measurements on pure water in hydrogen and air are detailed below. The measurements made on other substances are summarized in Table I.

Most of the substances used were of the best C.P. grade available. Earlier results indicated no essential effect of impurities on sign preference, while impurities did change the values of the expansion ratios. Hence, greater purity was not sought. Subsequent results on C_6H_6 showed that where high expansion ratios and slight or no sign preference occur, impurities can materially alter the supersaturation needed and give a sign preference. Accordingly the greater precautions were used in the C_6H_6 and $C_6H_5CH_3$ experiments. Filtered air and tank H_2 were used, and later tank N_2, two months old, replaced air, since it was free from all nuclei. The chamber was also rebuilt to permit of ready and complete cleaning. For some substances N_2 cannot be used as N_2 does not give negative ions and electrons are swept out too rapidly.

The expansion ratios were calculated in the standard manner, care being used in each case to correct for the vapor pressure of the substance used as given in the *International Critical Tables*. These values were not available to earlier workers and may account for some of the dis-

crepancies. The values for pure water agree fairly well with those of other workers, notably Przibram. For all other substances except acetone, the ratios observed were in general higher than those obtained by previous workers. While this could be attributed to a slower adiabatic expansion or greater warming by the metal parts, the agreement in water seems to preclude an instrumental effect. The chamber used should in fact have given a more rapid expansion than those used by other workers. In some cases the gradual increase in the number of droplets with expansion ratio was sufficiently slow so as to cause a considerable latitude in the choice of the expansion ratio for condensation. For alcohol this is not the case, and the higher ratio observed here might be ascribed to a higher purity of alcohol in view of the fact that water lowers the expansion ratio materially. This is clearly shown by pure benzene, C_6H_6, b.p. 80.2°, which gave an expansion ratio on ions of both signs, of 2.15. When contaminated with 20 percent commercial C_6H_6, the ratio was 1.89 on ions with a negative charge.*

In view of the various factors influencing the absolute values of the observed expansion ratios too much emphasis cannot be placed on the significance of the absolute values in any work of this sort. It is, however, believed that the relative values especially for different signs of charge are correct and most significant.

Reality of Sign Preference and the Effect of Ionic Contaminations

Very carefully purified and boiled water was introduced into the clean chamber and the expansion ratios for condensation on positive and negative ions were determined in air and in pure H_2. While the ratios obtained in H_2 for condensation on positive and negative ions differed slightly from the values in air, it was found that in both cases condensation occurred at lower expansion for negative ions than for positive ions. The difference in the expansions in air and H_2 can be attributed entirely to the difference in the specific heats of the two gases. That is, the necessary supersaturation was very likely the same in the two cases, though this cannot be accurately verified. Since in air it is known that the positive and negative ions pick up different chemically active impurities formed by x-rays, while in H_2 no such substances other than H_2O_2 and perhaps O_2 can be formed, it seems reasonably sure that the sign preference was *not alone* due to a difference in hygroscopic impurities picked up by the positive and negative ions.

This was further confirmed by a study of mixtures of HCl and water. HCl vapor is hygroscopic and HCl is soluble in water. It lowers the vapor pressure of H_2O and makes definite complexes with the *negative* ion presumably containing more than one molecule.[11] Even positive ions make smaller complexes with HCl. Yet none of the solutions of HCl up to concentrations of 23 percent, (i.e., above the constant boiling mixture concentration) that were used showed a decrease in the expansion ratio required for either sign of ion. It was found, however, that mixtures of acetic acid and water did condense on both ions at *lower ratios* than did either vapor separately. A similar effect had been observed in the case of alcohol—water mixtures, initially by Przibram[2] and later by others.[12] These effects are thermodynamically to be expected for acetic acid and alcohol.[12] The effects in alcohol are greater than those observed in acetic acid although the latter are pronounced. In mixtures of acetic acid and water vapors, the former showing sign preference for positive the latter for negative ions, no sign preference is observed since the general lowering of the expansion ratio by mixing probably masks the small differences observed.

It was observed that both acetic acid and HCl were made particularly troublesome by the formation of nuclei *after ionization and a condensation of droplets on the ions*. These nuclei were in a large measure uncharged and persisted after being formed until diffusion and repeated expansion removed them. The character of these nuclei was pointed out by J. J. Thomson.[8] If through ionization and condensation by adequate expansion droplets are formed, they re-evaporate to an invisible size on warming up. The size reached corresponds to the bottom of the second

* This has since been shown to be due to water. 10 percent of C_6H_6 saturated with H_2O causes such an effect.

[11] L. B. Loeb, Proc. Nat. Acad. Sci. **12**, 35, 42 (1926).
[12] Volmer and Flood, and H. Flood, Zeits. f. physik. Chemie **A170**, 273 and 286 (1934).

minimum in the surface tension supersaturation curve of Thomson. Here the droplets remain as stable but invisible droplets. Due to the ambient ionization they in time lose their charges but do not further evaporate for at this size the drop is stable without charge. In fact, charges only influence the growth at much *smaller* sizes. On the slightest increases of supersaturation by adiabatic expansion, these invisible stable droplets again quickly grow to visible size. If ions all of one sign were present about these drops, they would persist as large ions, and it is probable that the Langevin ions found in the atmosphere are of this character. The *persistence* of the nuclei in the presence of HCl and C_2H_5COOH is notable and doubtless due in the case of the HCl to the concentrated solutions of HCl in the larger but invisible droplets (lowered vapor pressure) while in C_2H_5COOH water mixtures it is due to the fact that the expansion ratio for all condensations is less, as shown by Vollmer and Flood.[12] It is clear, however, that *the few HCl molecules or active hygroscopic molecules introduced into embryonic nuclei before the first condensation through diffusion or gaseous ions does not materially influence the condensation process*. In other words, as will appear probable later, the elementary condensation nuclei or *embryonic droplets* are in a different physical state and thus act differently from the larger stable nuclei which have their surface tension forces fully active.

The signal failure of the third proposed mechanism led the writers to cast around for a more plausible theory. J. H. Hildebrand in conference suggested that in addition to the surface layer structure of liquids and the dipole moments, one must study the type of linkages resulting from secondary valence forces between molecules in the condensation processes. The writers then undertook a program of the study of sign preference among a varied assortment of condensable liquids. The scope of such a study is small in that the experiments must be limited to liquids capable of being condensed by realizable expansion ratios in the gases used. Up to the time of this study, water was the only substance showing a negative sign preference. This work has added $C_6H_5NH_2$, CH_3I, C_6H_5Cl, and $C_6H_5CH_3$ to the molecules showing negative sign preference. The results observed are summarized in Table I, which is largely self-explanatory. The symbols E and E_0 are the *expansion ratios* observed for condensation with ions of *both* signs, and for general cloudy condensation in the absence of ions respectively. The symbols E_+ and E_- are the expansion ratios for condensation with positive and negative ions. The *ratios* are given since the rather unusual definition of "supersaturation" introduced by C. T. R. Wilson has little significance. The temperature was 22°C throughout.

Discussion of Proposed Theories

1. The idea that molecules condense about the ions on supersaturation can be led back to the old notion of the ion cluster, as a bulky group of molecules attracted by dielectric forces. Work in the last ten years has conclusively shown that ions are not such agglomerations.[10, 13] They consist in the main of a few (one to four) molecules showing marked sign preference for the charge on the ion and are akin to the well known complex ions in solution. Thus, for example, the negative ion has an affinity for alcohols ROH, Cl_2, HCl, etc., while the positive ion has a strong affinity for NH_3, RNH_2, ethyl ether, etc.[10] With various partial pressures of vapors, including water vapor, only one ionic mobility is observed which shows no indications of being a cluster that alters with the partial pressure of the vapor. Similar results are observed in the unique mobility peaks produced in spraying and bubbling of liquids. Hence one is forced to conclude that ions do not "grow" into drops and that the presence of charge on droplets that condense is due to the picking up of the ions by the drops.

The conclusion based on observation is to be expected since there is no *a priori* reason for believing that molecular affinities for ions of one sign are in any way related to the van der Waals forces linking molecules in condensation. This is strikingly illustrated in a few cases by reference to the tables. CH_3I has no specific ionic affinity yet it shows negative sign preference in condensation. H_2O shows negative sign preference and the alcohols show a marked positive sign preference while all of them have a strong affinity for nega-

[13] Powell and Brata, Proc. Roy. Soc. **A138**, 129 (1932).

tive ions. Amines have a strong affinity for positive ions yet $C_6H_5NH_2$ condenses more readily on negative ions. Finally, it seems unlikely, even did the charge affinity exist, that it would extend over sufficient drop radii to influence condensation.

2. Studies of spray electrification by Lenard[14] and his pupils, cataphoresis of gas bubbles,[15] direct potential measurements by Frumkin,[16] static charge production on separation of surfaces by Coehn,[17] and surface adsorption experiments by Langmuir[18] and others are all in agreement in establishing the existence of the electrical double layers at the surface of liquids. The character of these double layers is not definitely known and the best information comes from spray electrification and bubbling. Coehn and Mozer[17] have studied these layers in liquids other than water by bubbling, as have Blüh[19, 20] and recently Chapman[21] in this laboratory. Chapman's results are in general agreement with those of Blüh but the correlation of his results with the results of Coehn and Mozer is doubtful because of the rather primitive nature of the earlier measurements and due to the fact that he studied the more recently formed carriers. From their own results Coehn and Mozer believe they have proved the law of Coehn that each pure liquid has an electrical double layer at the surface the *negative charge being outward*. The intensity of the field increases in proportion to the dielectric constant. Thus Coehn explains surface electrification on contact or friction as the result of a contact potential the substance with the highest dielectric constant always being positive. Chapman's recent results on spray

[14] P. Lenard, Ann. d. Physik **47**, 463 (1915). See also H. W. Gilbert and P. E. Shaw, Proc. Phys. Soc. (London) **37**, 195 (1925).
[15] McTaggart, Phil. Mag. **27**, 297 (1914); **28**, 367 (1914). Also T. Alty, Proc. Roy. Soc. **A106**, 313 (1914).
[16] Frumkin, Zeits. f. physik. Chemie **109**, 34 (1914); **111**, 190 (1914); **116**, 485 (1920); **123**, 321 (1926).
[17] A. Coehn, Wied. Ann. **64**, 217 (1898). Coehn and Mozer, Ann. d. Physik **43**, 1048 (1914).
[18] I. Langmuir, J. Frank. Inst. **218**, 143 (1934).
[19] Blüh, Kolloid Zeits. **59**, 346 (1932).
[20] Blüh and Stark, Zeits. f. Physik **43**, 575 (1927).
[21] S. Chapman, Phys. Rev. **52**, 184 (1937).

TABLE I. *No ± effect.*

NAME	FORMULA	E	E_0	DIPOLE MOMENT $\times 10^{18}$	FIELD NECESSARY
Benzene (pure)	C_6H_6	2.15±.04		2.2	±1.5v Very sensitive to impurities.
Benzene	C_6H_6	1.73		0	±1.5v
Nitrobenzene	$C_6H_5NO_2$	1.45		3.9	±1.5v
Chloroform	$CHCl_3$	1.83		1.05	±4.5, ±1.5v
Acetone	$(CH_3)_2CO$	1.88	2.06	2.80	
Acetic acid	$+H_2O$	1.24	1.33	same for 50 per cent and 6.2 percent solutions	±4.6v
Negative ion first					
		E_-	E_+	E_0	
Water	H_2O	1.25	1.31	1.32	1.85	±1.5v
Ethyl iodide	C_2H_5I	1.82	2.11		1.66	±50v
Analine	$C_6H_5NH_2$	1.44	1.48		1.56	±25v
Chlorobenzene	C_6H_5Cl	1.53	1.6	1.8	1.52	±4.6v
Toluene	$C_6H_5CH_3$	1.60	1.69	1.73	0.4	±4.6v
$HCl+H_2O$		1.27	1.3	1.37	same for all conc.	17.5 percent 19 ±1.5v 23 (fuming) very weak
Positive ion first					
		E_-	E_+	E_0	
Ethyl alcohol	C_2H_5OH	1.29	1.26		1.70	±1.5v
Methyl alcohol	CH_3OH	1.37	1.33		1.68	±1.5v
Acetic acid	$C_2H_4O_2$	1.54	1.45	1.58	1.4	±3.0v
n-butyl bromide	C_4H_9B		1.48		1.85	±25v

electrification throw some doubt on this interpretation. Both spraying and bubbling experiments show that many very mobile negative ions are found as well as definite groups of slower ions, while sometimes two and perhaps three groups of slower positive ions appear. Both positive and negative carriers as well appear in an added very broad band of large charged droplets. In ethyl alcohol similar results are observed to those in water but with nearly ten times the number of charged carriers. In a heavy saturated pure hychrocarbon, Nujol, no charged carriers are observed to any extent. Both nitrobenzol and aniline show no carriers of high mobility of either sign but both show a continuous band of large ions with equal numbers of positive and negative ions. These results are not such as one would expect on Lenard and on Coehn's predictions. Since Coehn's general law seems well established on other grounds the apparent contradiction of Chapman's results with the conclusions of Lenard and Coehn may be ascribed to faulty conclusion as to the origin of spray electrification rather than to the nonexistence of double layer. However, as will be seen from the table of results for sign preference, the very definite and widely differing behavior of the various substances studied allow of *no correlation with either Chapman's results or with Coehn's law*. Thus, with Chapman alcohol and water show similar behavior and aniline and water differ radically, while water and aniline act in a similar fashion in condensation and water and alcohol show opposite sign preference on condensation. If Coehn's law gave a clue to the surface orientation active in condensation it would be expected that the condensation would always occur preferentially on negative ions, since the negative outer layer of all liquids would more readily bind the positive ends of dipoles. These data definitely indicate that the usual electrical double layer existing at the surface of liquids is not responsible for sign preference in condensation. There is still the possibility envisaged by Thomson[8] that the charge itself causes an orientation at the surface of the liquid, which differs with the sign of charge. If it did occur, however, the orientation by the charge on the liquid surface and of approaching gaseous dipoles outside the liquid surface would for both charges be in a proper sense to *aid* condensation, giving no sign preference.

3. The third alternative was shown by our experiments to be untenable.

The Explanation of Sign Preference

It is clear that sign preference depends on the sign of the charge on the droplet. It appears unlikely that this will materially alter the character and orientation of molecules bound by van der Waals forces in the drop. If it did so, the action unless unusual in its character would not lead to sign preference. The electrical fields existing at the surface of the charged embryonic droplets are of the order of 10^5 to 10^4 volts per cm. Such fields are definitely capable of orienting the *approaching* vapor molecules if they have in them strong permanent dipole moments. If then the structural aspect presented by such an oriented molecule is favorable to linkage with surface molecules, it is clear that such a vapor molecule is in a favored condition for condensation. The oppositely oriented molecule will *not be so favorably situated if the surface is unchanged by the charge*. To utilize this orientation of the vapor dipoles in the field of the drop for an explanation of sign preference, two things are required: 1. that the *axes of the dipole moments have definite directions in the molecules relative to the atomic configurations which determine the linkage elements in the van der Waals binding forces*; 2. that the *surface molecules of the embryonic droplets have definite orientations which will insure the outward propagation of the drop structure on the addition of molecules from the vapor*.

The studies of dipole moments and chemical structure have given us considerable knowledge as to the general relation of the dipole axis to the molecular structure in some cases.[22] More information can be had at will. As to linkage elements in the van der Waals forces little unfortunately is known. The excellent studies of solubilities as reported by Hildebrand[23] in his recent book are beginning to give us some information. It is clear that the hydrogen bond

[22] P. Debye, *Polar Molecule* (Hirzel, Leipzig, 1929). C. P. Smyth, *Dielectric Constant and Molecular Structure* (Chemical Catalog Co., New York, 1931). H. A. Stuart, *Molekulstructur* (Springer, Berlin, 1934).

[23] J. H. Hildebrand, *Solubility* (Chemical Catalog Co., New York, 1936). Also Science **83**, 21 (1936).

formation is one of the most powerful forces active. This occurs especially in the cases of F, O, and N atoms combined with H. Whether it occurs in smaller measure for other halogens remains an open question. Next to bond formation as active agents in linkage Hildebrand lists dipole linkages. In these cases the orientation of the dipoles linking is antiparallel. For most organic dipoles the substituent group is in general negative. A third group of forces active according to Hildebrand is the London forces. In this the linkage of dipoles is parallel and the linkage is strongest for the alkyl iodides. As regards the condensation studies it is probable that the London forces are not of great importance since they are not such as to propagate a structure. Where it is possible, there is no doubt but that the hydrogen bond will predominate. In its absence the antiparallel dipole linkage in chain structures may occur. The lack of specific knowledge of the relation between linkage axes and dipole axes for most molecules leave the specific interpretation of results open only to speculation. On the basis of solubilities Hildebrand did predict that nitrobenzol would show no sign preference and that amines would show a negative sign preference.

As regards the molecular orientation in drops, little can be said. Drops which are *large enough to have a well defined surface layer will show the ordinary statistically conditioned electrical double layer with little surface orientation.* Such a layer it was seen, cannot be of any significance. It is at this point that we must make a radical assumption. It must be assumed that the sign preference occurs on *embryonic droplets which are too small to take on the thermodynamical character of an aggregate with a regular surface layer.* It must also be assumed that these *embryonic droplets have a pseudo-crystalline structure* such that linkages inside the structure are manifest at the surface, and that these are unaffected by the charge that is picked up from the gas. The linkages are thus more of the nature of crystalline structures than of liquids. These droplets presumably do not pick up foreign molecules that do not enter into the structure. Where they can do so as in acetic acid and water, or alcohol and water mixtures, they are picked up and contribute to the lowering of the condensation ratio. Indications that such aggregates exist even in the liquid state might be seen in the cybotactic structure revealed by the x-ray liquid diffraction studies of G. W. Stewart.[24] The existence of a pseudo-crystalline state of possibly similar character has been observed in the case of very minute Bi crystals by Goetz.[25] The size of such aggregates must run from 5×10^{-8} to 10^{-6} cm and contain 100 to 10^6 molecules. When the droplets exceed this size, the structure breaks down and a regular liquid droplet results. This picture will require a slight modification of the Thomson theory for the effect of charge on the growth of the droplets, over the first hump in the curve to the first minimum, in that ordinary thermodynamical considerations are inapplicable to the smaller embryonic drops with few molecules. The breakdown of this part of the theory is in any case indicated by sign preference. The reason why *ions* do not themselves grow to droplets is that they are already a stable complex of few molecules which do not share the structure of the larger embryonic pseudocrystals. It must be emphasized that this discussion *does not preclude* the action of the usual electrical forces, which Thomson and others show important in later stages. It does indicate that there is an earlier stage of the process where sign preference occurs in which ordinary electrical attraction does not suffice.

Rules Governing Charge Preference in Condensation

On the basis of these general considerations one may make certain definite predictions as to the condensation phenomena.

1. Where there is no permanent dipole moment there will be no sign preference on condensation.

2. Where the dipole moment is so oriented that the field of an embryonic pseudo-crystalline droplet is able to orient the approaching vapor molecules into a position favorable for a given type of surface linkage with the oriented molecules in the surface one sign of charge will

[24] G. W. Stewart, Phys. Rev. **37**, 9 (1931).

[25] A. Goetz, Papers and Discussions, International Conference on Physics, London, Vol. 2 (Cambridge Press, 1934), p. 65. Anniversary volume of Science Reports. Tohoku Imperial University, Series I. Sendai, Japan (1936).

facilitate condensation more than the other. Condensation will occur at lower expansion ratios on the ion of one sign than the other.

3. The presence of a strong permanent dipole moment in a molecule may not insure sign preference in condensation. It must in addition fulfill the following conditions

a. The dipole direction in the molecule must be structurally so oriented as to facilitate the binding linkage in the molecules. Thus, for instance, a dipole moment axis perpendicular to the linkage groups would be of no advantage in condensation.

b. The dipole moment must not be so buried in a highly polarizable structure as to lose its influence in orienting the molecule in the divergent field near the surface of the embryo droplets.

c. The surface molecules must be oriented in sufficient numbers materially to affect the rate of condensation, a condition which obtains only in the minute pseudo-crystalline embryonic droplets.

4. The orientation produced by the field must be such as to cause linkages which are already present in the surface structure. That is, they must act to facilitate the addition of successive layers of molecules on the subjacent ones with the same structure as the subjacent ones. Thus it is conceivable that a field could orient molecules so as to saturate the linkage possibilities of the outer layer and thus prevent further growth. Hence dimer formation which occurs for many dipolar molecules in solvents (e.g. in the case of acetic acid where molecules link in pairs) cannot be of any value in the processes envisaged.

Application of Theory to Specific Vapors

It is now possible to turn specifically to the results reported in the table under the heads of: *a*, no sign preference, *b*, preference for negative ions, *c*, and preference for positive ions. The application to specific vapors can only be speculative; accordingly only illustrative examples will be given for each class.

a. No sign preference

As expected, benzene C_6H_6 having no dipole moment shows no preferential condensation. Nitrobenzol and acetone both have very strong dipole moments but neither shows any sign preference. The behavior of nitrobenzol was predicted by Hildebrand from solubility data on the basis of its dipole being unrelated to its structural binding points. Acetone was tried before its solubility characteristics had been investigated. Its behavior is found to be in agreement with what the solubility data led one to expect. Chloroform has a dipole moment but shows no sign preference for the reason that its dipole is so effectively buried in the highly polarizable Cl_3 structure as to be ineffective.

CS_2, a nonpolar substance, was found by Przibram to show no sign preference.

b. Negative sign preference

The first case of sign preference observed in condensation was the negative sign preference shown by C. T. R. Wilson to hold for water vapor. Since the structure of the pseudo-crystalline state is not known, one is free to choose a structure consistent with condensation data. Since hydrogen bond formation is known to be the linkage and preference in condensation is for negative ions, one must conclude as follows: The O molecules in the pseudo-crystals must be outward. Then a negative charge on the pseudo-crystal will orient approaching H_2O molecules with the protons towards the surface favoring hydrogen bond linkage. Molecules striking a positively charged pseudo-crystal will have to rearrange themselves on impact with the surface to be bound. There is some indication of this orientation in the structure of ice crystals.

At the time the present investigations were undertaken water was the only vapor showing preference for condensation on negative ions. Owing to the use of low sweeping fields in the condensation chamber in working with vapors where the ions have a low mobility ethyl iodide was reported erroneously by an earlier investigator as having a sign preference for positive ions. By using adequate fields to separate the ions it was clearly shown that ethyl iodide has a distinct sign preference for negative ions. Data for the orientation of ethyl iodide in surfaces is not at hand. According to Hildebrand the London forces are powerful in alkyl iodine compounds. As these are probably not active here it might be suspected that in general the molecule will

have some sort of tetrahedral symmetry about the carbon atom holding the I. In a surface both the C_2H_5 group and the I because of space occupation might be expected to orient outward. Since linkage on condensation will presumably occur with the one of the two hydrogens of the carbon atom attaching to the iodine atoms at the surface, a negative charge on the ion will facilitate such combination. Aniline was found to have negative sign preference. Toluene and chlorobenzene were also observed to favor the negative ion. These three substances are characterized by organic chemists as being strongly *ortho-para* directive and it may be that this tendency is also manifested in the condensation process. It is, however, more profitable to speculate further as follows:

The structure of aniline is pyramidal and presents many possible methods of combination. The bulky C_6H_5 group might be thought of as projecting outward from the surface in which case it is possible that the C_6H_5 may be the linking group. However, the fact that hydrogen bond formation is possible makes it more likely that the N atom is outward in the droplet surface with the protons of the NH_2 inward. Then the hydrogens of the NH_2 of the condensing molecules which will be oriented downward by the field of a negative ion will favor linkage of the H with the nitrogen at the surface.

c. Positive sign preference

Perhaps the greatest difficulty at first encountered in interpreting these phenomena came in the behavior of the alcohols and fatty acids. On the basis of the action of H_2O the alcohols should be expected to show negative sign preference. Reflection will at once show why this is not the case. Hydrogen bond linkage is active here. However, the alcohols will orient with the organic radical or carbon chain outward where possible. In this case it is clear that the negative oxygen will point inward while the carbon chain and the H group are oriented outward. Thus the linkage will be facilitated by condensation on the positive ion, which orients the oxygen group of the approaching vapor molecule downward favoring hydrogen bond formation.

MAY, 1938 JOURNAL OF CHEMICAL PHYSICS VOLUME 6

The Inhibition of Homogeneous Organic Decompositions

F. O. RICE AND O. L. POLLY
Department of Chemistry, Johns Hopkins University, Baltimore, Maryland

(Received February 24, 1938)

A free radical mechanism is proposed to account for the inhibition of organic decompositions by nitric oxide, based on the assumption that the nitric oxide can both start and stop reaction chains in the substrate. Propylene inhibits organic decompositions and a free radical mechanism appears to account for this effect also. Ethyl nitrite completely inhibits the oxygen promoted chain in acetaldehyde at 300°C but has only a relatively small effect at 500°C.

(1) INTRODUCTION

A FREE radical mechanism such as that proposed by one of us[1] leads to the conclusion that two organic compounds when mixed do not decompose independently of each other and consequently we would expect the experimental result that the rate of decomposition of a particular compound would be either accelerated or retarded by addition of another compound. Acceleration of reaction rate has been observed in a large number of examples[2] but retardation of the rate is much less common; Hinshelwood and his co-workers have found that nitric oxide inhibits

[1] (a) Rice, J. Am. Chem. Soc. **53**, 1959 (1931); (b) Rice and Herzfeld, ibid **56**, 284 (1934); (c) Rice and Rice, *The Aliphatic Free Radicals* (The Johns Hopkins University Press, 1935).

[2] (a) Frey, Ind. Eng. Chem. **26**, 200 (1934); (b) Sickman and Allen, J. Am. Chem. Soc. **56**, 1251 (1934); (c) Echols and Pease, J. Am. Chem. Soc. **58**, 1317 (1936).

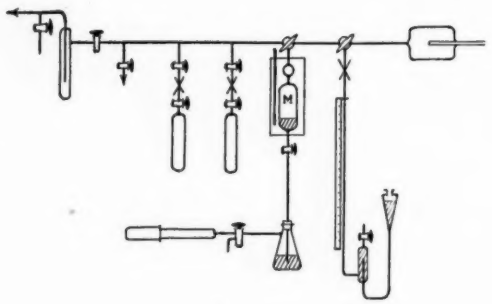

FIG. 1.

the decomposition of some organic compounds but not others[3] and sometimes the products of a reaction have a slight but definite retarding influence.[4]

On the basis of our work in this laboratory we have concluded that, from the chemical standpoint, retardation of the rate of a reaction can occur in two ways according to the nature of the added material. In the first way it probably combines or reacts with the chain radicals to produce molecules[3] according to the equation,

$$R+NO\rightarrow R-NO. \quad (1)$$

We have found that alkyl nitrites also show inhibition which may be ascribed to a dual action:

$$R+CH_3-O-NO\rightarrow RH+CH_2-O-NO \quad (2)$$
$$\rightarrow RH+HCHO+NO.$$

The molecules themselves inhibit and also the nitric oxide produced inhibits according to Eq. (1). On the other hand, earlier experiments[1(e)] in this connection showed that nitrosyl chloride did not slow up the reaction rate of butane[5] and certain other organic compounds; possibly the reaction,

$$R+NOCl\rightarrow RCl+NO, \quad (3)$$

requires too high an activation energy for nitrosyl chloride to be an effective inhibitor.

The second kind of inhibition may occur when the addition of a second substance causes the substitution, in greater or less degree, of the chain radical by another radical which is not so efficient for continuing the chain process. We have found that propylene inhibits the decomposition of hydrocarbons, ethers, acetone and acetaldehyde. The action is probably due to replacement of the chain carrier R by the allyl radical according to the equation,

$$R+CH_3CH=CH_2\rightarrow RH$$
$$+CH_2{=}{=}{=}CH{=}{=}{=}CH_2. \quad (4)$$

The addition of propylene therefore is an example of the second kind of inhibition since probably the allyl radical is not a very efficient chain carrier as compared with methyl or ethyl radicals which are the most common carriers in the above reactions.

The addition of small quantities of either nitric oxide, alkyl nitrites or propylene, to a paraffin hydrocarbon or an ether, causes usually a reduction in rate which is very marked with nitric oxide; in all cases the rate diminishes, rapidly at first until a point is reached where further additions have very slight effect.[6] On the other hand, in the case of acetone or acetaldehyde, there is a sharp contrast between the action of nitric oxide or alkyl nitrites and propylene. Whereas propylene has the normal inhibiting effect, nitric oxide or alkyl nitrites do not show any inhibition.

From the kinetic standpoint no such difference would be expected for the different inhibitors if we assume that the effect of all of them is, essentially, to reduce the concentration of the chain radicals. The disagreement in our experimental results between the action of propylene and the other two inhibitors, indicated the desirability of studying the efficiency of chain breaking in the temperature range 500–550°C, in which many organic compounds decompose at a conveniently measurable rate.

TABLE I. *Effect of small quantities of* O_2 *and ethyl nitrite on acetaldehyde at 300° C. Acetaldehyde pressure = 380 mm.*

I mm O_2	II mm EtONO	III λ	IV Error
0.17	0	94	±12
0.34	0	68	± 5
0.94	0	37	± 2
0	0.19	0	±10
0	1.04	0	± 2
0	1.05	0	± 2
0	1.05	0	± 2

[3] This work is summarized by Staveley and Hinshelwood, J. Chem. Soc. 1568 (1937).

[4] Hinshelwood, Proc. Roy. Soc. **A114**, 84 (1927).

[5] Compare Echols and Pease, J. Am. Chem. Soc. **59**, 766 (1937) who found that NO inhibits the butane decomposition.

[6] Very large addition of NO causes oxidation. See Section (4) and reference 3.

(2) Experimental

The work described in this paper was done in a static system and the rate was followed manometrically. Fig. 1 shows a sketch of the apparatus. The reaction vessel consisted of a 200 cc transparent silica bulb which fitted in a furnace constructed of a graphite cylinder surrounded completely by thin Nichrome sheet to prevent oxidation. The graphite cylinder was heated electrically and lagged in the usual manner and gave a uniform temperature inside our reaction bulb to ±1°C.

The mixing bulb, M, is the most significant part of the apparatus. Using this bulb we could make up accurately known mixtures and displace the whole of the gas into the furnace. This gave us a method of measuring P_0 by displacing an equal volume of a nonreactive gas from the mixing bulb to the furnace, the initial and final conditions of temperature and pressure being the same as with the substrate. Since we were interested in measuring the expansion caused by an initial very rapid reaction, an accurate estimate of P_0 was essential and we prefer the displacement method to one of connecting the mixing bulb with the empty reaction bulb and measuring the initial and final pressure in the mixing bulb. If this method is used, it should be noted that the pressures in the mixing bulb and reaction bulb should not be allowed to equalize because the reaction mixture expands very rapidly during the first few seconds and some of the partly decomposed gas may be driven back into the mixing bulb.[7]

The manifold accommodates two sample bulbs, one containing the substrate and the other the inhibitor; it is also fitted with a McLeod gauge and is connected to a pumping system consisting of a two-stage mercury vapor pump backed by an oil pump.

Table II. *Inhibition of the oxygen promoted chaim decomposition of acetaldehyde by ethyl nitrite. Temperature = 300°C. Pressure* CH_3CHO *= 380 mm.*

I mm O_2	II mm EtONO	III λ	IV Error
0.47	1.05	0	± 4
1.05	2.1	0	± 2
0.94	0.49	27	± 2
0.94	1.0	0	± 2
0.94	1.9	0	± 2
0.94	2.8	0	± 2
0.17	0.37	0	±12
0.34	0.70	0	± 6

[7] Equalization of pressure is satisfactory if there is no rapid initial rate and has been used by Schultz and Kistiakowsky, J. Am. Chem. Soc. **56**, 395 (1934).

Table III. *Effect of small quantities of oxygen or ethyl nitrite on acetaldehyde. Temp. = 502°C. Acetaldehyde pressure = 500 mm.*

I mm O_2	II mm EtONO	III λ	IV Error
0.24	0	555	±8
0.27	0	520	±7
0.62	0	269	±3
0.225	0	606	±9
0	0.66	24	±3
0	1.28	15.6	±2
0	2.7	6.7	±1

(3) Inhibition with Ethyl Nitrite

The first series of experiments described in this section was performed at 300°C with acetaldehyde. Pure acetaldehyde is stable at this temperature and gave no initial increase in pressure; the measured P_0 using acetaldehyde was the same as that obtained by using the same amount of an inert gas after correcting for gas law deviations. However, if the acetaldehyde is mixed with small measured quantities of oxygen (0.1–0.3 percent) in the mixing bulb and then transferred to the reaction bulb, there is considerable decomposition of the acetaldehyde, far more than could be accounted for on the basis of simple oxidation; the decomposition is completed in the first few seconds before any measurements could be made and was measured by the difference in the observed and calculated P_0, after making a small correction for the added oxygen. The number of acetaldehyde molecules decomposed per molecule of oxygen (λ) was calculated on the assumption that the acetaldehyde decomposed into two product molecules.

The results of our experiments are shown in Table I; since the value of λ depends on the difference of two pressure measurements, the error will vary considerably and we have therefore included in column IV, values for the error in λ assuming that the difference between the calculated and measured pressure is subject to an error of ±2 mm. Table I also contains some measurements on acetaldehyde containing small

TABLE IV. *Inhibition of the oxygen promoted chain decomposition of acetaldehyde by ethyl nitrite at 502°C. Acetaldehyde pressure = 500 mm.*

I mm O_2	II mm EtONO	III λ	IV Error
0.23	0.24	496	±9
0.23	0.51	440	±9
0.23	0.93	379	±9
0.225	0.94	361	±9
0.23	1.72	283	±9
0.24	2.55	267	±9
0.23	2.95	217	±9
0.225	3.3	209	±9
0.225	4.9	205	±9
0.225	8.5	227	±9

quantities of ethyl nitrite. The ethyl nitrite had no detectable effect either by inducing an initial rapid acceleration or any subsequent decomposition. Except for a small correction for the decomposition of the nitrite, the mixture behaved like pure acetaldehyde.

In Table II we show the results for mixtures of ethyl nitrite and oxygen with acetaldehyde; within the limits of our measurement, the ethyl nitrite inhibits the oxygen induced chain completely if its concentration is equal to or greater than that of oxygen.

These results are similar to those obtained by Mitchell and Hinshelwood,[8] who found that at 300°C, chains induced photochemically in acetaldehyde could be shortened from over 100 to 1 by the addition of small quantities of nitric oxide.

We then performed a second series of experiments exactly similar to the first but at 500°C. Since acetaldehyde decomposes at a slow but measurable rate at this temperature, it was necessary to make an additional correction for its decomposition. This was done by plotting the pressure-time curve and extrapolating back to zero time. The difference between this P_0 and the calculated P_0 (obtained from the pressure measurement in the mixing bulb) gave the amount of induced decomposition; a small correction was necessary to take care of the oxygen or ethyl nitrite added. The results obtained when acetaldehyde is mixed with either oxygen or ethyl nitrite are shown in Table III. The chain length of the oxygen sensitized reaction is greatly increased and in addition a new phenomenon appeared in the experiments with ethyl nitrite

[8] Mitchell and Hinshelwood, Proc. Roy. Soc. **A159**, 32 (1937).

TABLE V. *Decomposition of acetaldehyde in presence of small amounts of nitric oxide. Temp. = 478°C. Initial pressure acetaldehyde = 250 mm.*

Press. NO	0	0.6	1.2	2.4	6.1	12.0
$100\times(dp/dt)_0 \div P_0$	1.60	1.79	2.05	2.28	3.30	3.83

Pressures in mm Hg., time in min.

since it actually induced a short chain decomposition in the aldehyde. The effect of mixtures of oxygen and ethyl nitrite on the decomposition is shown in Table IV.

The results show that ethyl nitrite is a very inefficient inhibitor at 500°C as might be expected from the experimental result that ethyl nitrite itself actually induces short chains in acetaldehyde. The effect of ethyl nitrite on the oxygen induced chain is to reduce the length to a minimum value of about two-fifths, when the ethyl nitrite is present in about tenfold excess over the oxygen. Addition of one molecule of nitrite per molecule of oxygen has very little effect on the chain length at 500°C although at 300°C there is complete inhibition.

In view of these experimental results it seemed desirable to examine the effect of small quantities of pure nitric oxide on the rate of decomposition of acetaldehyde in the neighborhood of 500°C especially since our method would show up any rapid initial acceleration that occurred. We did not find any such effect as in the case of ethyl nitrite but we did however find that even very small amounts of nitric oxide accelerated the rate of decomposition of acetaldehyde. The results of these experiments are shown in Table V and prove that quantities of nitric oxide of less than 0.5 percent accelerate the reaction rate appreciably at 478°C.

(4) Discussion of Nitric Oxide Inhibition

It seems reasonable to conclude from our experimental results that nitric oxide can both start and stop chains when introduced into acetaldehyde. This is probably true also for other organic compounds and the following mechanism[9] may be proposed for decompositions in presence of nitric oxide.[10]

[9] See in this connection reference 1 (c), pp. 86–90.

[10] When large amounts of nitric oxide are present, a complicated oxidation process predominates. See Gay and

$$M_1 \rightarrow 2R_1 \qquad k_1, \qquad (5)$$

$$M_1 + NO \rightarrow HNO + R_2 \qquad k_2, \qquad (6)$$

$$R_1 + M_1 \rightarrow R_1H + R_2 \qquad k_3, \qquad (7)$$

$$R_2 \rightarrow R_1 + M_2 \qquad k_4, \qquad (8)$$

$$R_1 + NO \rightarrow R_1NO \qquad k_5, \qquad (9)$$

$$2R_1 \rightarrow R_1 - R_1 \qquad k_6, \qquad (10)$$

$$R_2 + NO \rightarrow R_2NO \qquad k_7, \qquad (11)$$

$$R_1 + R_2 \rightarrow R_1 - R_2 \qquad k_8, \qquad (12)$$

$[M_1]=x_1$, $[NO]=y$, $[R_1]=x_2$, $[R_2]=x_3$, k_1x_1 and $k_6x_2^2$ are the respective rates for the appearance and disappearance of *one* radical. According to this, organic compounds decompose in two ways according as the chain ends by reactions (9) and (10) or reactions (11) and (12).

Scheme I

In this scheme reaction (8) has a very low activation energy, so that x_3 may be neglected and Eq. (7) written,

$$R_1 + M_1 \rightarrow R_1H + R_1 + M_2. \qquad (13)$$

Acetaldehyde follows this scheme and reaction (7) in this case would be,

$$CH_3 + CH_3CHO \rightarrow CH_4 + CH_3 + CO. \qquad (14)$$

Since R_2 is present in very low concentration, the chain must end by reactions (9) and (10). Setting up the usual steady state conditions and solving for x_2 we obtain:

$$k_1x_1 + k_2x_1y = k_5x_2y + k_6x_2^2 \qquad (15)$$

$$x_2 = -(k_5/2k_6)y + [(k_1x_1 + k_2x_1y)/k_6 + k_5^2y^2/4k_6^2]^{\frac{1}{2}}. \qquad (16)$$

If the chain length is greater than 10, the rate of the reaction is given by,

$$dx_1/dt \leqq k_3x_1x_2,$$

and if the concentration of nitric oxide is very small this becomes,

$$\frac{dx_1}{dt} = k_3x_1\left[\left(\frac{k_1x_1 + k_2x_1y}{k_6}\right)^{\frac{1}{2}} - \frac{k_5}{2k_6}y\right]. \qquad (17)$$

Travers, Nature (a) **137**, 906 (1936); (b) **138**, 546 (1936). Our mechanism applies only when the NO concentration is sufficiently small that this is negligible.

As the concentration of nitric oxide increases we have,

$$dx_1/dt \leqq k_3x_1[(1/k_5)(k_2x_1 + k_1x_1/y)] \qquad (18)$$

and finally at higher values of y,

$$dx_1/dt \leqq k_2k_3x_1^2/k_5. \qquad (19)$$

Scheme II

In this scheme reaction (8) has a high activation energy and Eqs. (11) and (12) represent the chain terminating reactions. We then have,

$$k_1x_1 + k_2x_1y = k_7x_3y + k_8x_2x_3, \quad k_3x_1x_2 = k_4x_3,$$

$$x_2 = -k_7y/2k_8 + [(k_1k_4 + k_2k_4y)/k_3k_8 + k_7^2y^2/4k_8^2]^{\frac{1}{2}}. \qquad (20)$$

For small concentrations of nitric oxide, we have,

$$\frac{dx_1}{dt} = k_3x_1\left[\left(\frac{k_1k_3x_1 + k_1k_4y}{k_3k_8}\right)^{\frac{1}{2}} - \frac{k_7}{2k_8}y\right] \qquad (21)$$

and for large concentrations

$$dx_1/dt \leqq k_2k_4x_1/k_7. \qquad (22)$$

It seems unwise at present, to attempt an exact discussion of the application of these mechanisms to the phenomenon of inhibition by nitric oxide, because we are uncertain as to what extent the oxidation reaction affects the experimental results. Indeed Verhoek found[11] that the decomposition of acetone by nitric oxide at 600°C was predominantly an oxidation process. However, it is clear that the addition of small quantities of nitric oxide would be expected first to diminish the rate until finally further additions would have no effect. This relation[3] has been found for a number of organic compounds. Furthermore the inhibiting effect of the nitric oxide should increase as the concentration of substrate diminishes according to scheme I whereas according to scheme II the inhibiting effect would be independent of the substrate concentration. Propaldehyde, butaldehyde and ethane behave[3] according to scheme I whereas dimethyl ether and diethyl ether behave[3] according to scheme II; this is what may be expected for the aldehydes and ethers but not for ethane which is exceptional in that it should fall into scheme II.

[11] Verhoek, Trans. Faraday Soc. **31**, 1534 (1935).

(5) Inhibition with Propylene

The peculiar effect of propylene on organic decompositions was discovered accidently in the course of some experiments in which we were trying to catalyze decompositions by adding small amounts of cyclopropane. We were testing to see if the cyclopropane ring would open, thus supplying radicals which would be expected to accelerate the rate. Instead, the rate decreased considerably and further investigation showed that this effect was most probably due to propylene into which cyclopropane isomerizes on heating.[12]

The decomposition of pure propylene was first investigated by heating it in a 12-liter Pyrex flask at 530°C, and pumping out and analyzing the products; the initial pressure was 334 mm and after 40 min. the pressure had only increased by 3 mm. About 15 percent of the propylene had decomposed, giving equal quantities of ethylene and methane and a smaller amount of a C_6 hydrocarbon which was not identified. We assume that the mechanism of the propylene decomposition is,

$$CH_3CH=CH_2 \rightarrow CH_3+CH_2=CH-, \quad (23)$$

$$CH_3+C_3H_6 \rightarrow CH_4+CH_2{=}{-}{=}CH{=}{-}{=}CH_2, \quad (24)$$

$$CH_2=CH-+C_3H_6 \rightarrow CH_2=CH_2+ CH_2{=}{-}{=}CH{=}{-}{=}CH_2, \quad (25)$$

$$2CH_2{=}{-}{=}CH{=}{-}{=}CH_2 \rightarrow CH_2=CHCH_2CH_2CH=CH_2. \quad (26)$$

Table VI. *Effect of propylene on rate of decomposition.*

Substrate	Temp. °C	P_0 Substrate	P_0 Propylene	$100\times(dp/dt)_0 \div P_0$
Propane	497	204	0	0.57
Propane	497	204	102	0
n-Butane	512	290	0	1.1
n-Butane	512	290	13	0.8
n-Butane	512	290	25	0.57
n-Butane	512	290	53	0.53
n-Butane	512	290	102	0.27
n-Butane	512	290	107	0.33
n-Butane	512	290	163	0.17
Acetaldehyde	500	206	0	5.1
Acetaldehyde	500	201	102	2.3
Acetone	550	182	0	5.5
Acetone	550	150	50	1.6
Acetone	550	137	54	1.5
Dimethyl ether	508	203	0	3.4
Dimethyl ether	508	199	108	1.0
Trimethyl amine	470	203	0	7.5
Trimethyl amine	470	194	103	4.3
Ethylene oxide	408	405	0	0.72
Ethylene oxide	408	465	104	0.09

[12] Trautz and Winkler, J. prakt. Chem. **104**, 53 (1922).

This would lead to no change in pressure for the decomposition and appears to account satisfactorily for the products. Propylene is appreciably more stable than the organic molecules whose decomposition it inhibits.

We have completed only some preliminary experiments on the effect of propylene in which we have varied the substrate, and in one example the concentration of the propylene also. The results obtained are shown in Table VI.

We did not continue with this phase of the experimental work because our apparatus was not adapted to measuring rates of reaction in the very early stages. After a few percent decomposition has occurred, the reaction becomes very complex because the substrate frequently yields propylene or some other unsaturated molecule which can inhibit and the decomposition of the propylene yields presumably diallyl which would be expected to diminish the inhibiting effect of the propylene by easily dissociating into allyl radicals. A further difficulty lies in the fact that minute traces of oxygen exert a profound effect on the initial rate of decomposition and it seemed best to examine the oxygen effect before continuing this investigation.

(6) Discussion of Inhibition by Propylene

We shall assume that propylene is sufficiently stable as compared with the substrate molecules investigated, that we can neglect any radicals produced by its decomposition according to Eq. (23). The effect of propylene is to remove some of the chain radicals R by reacting to give RH and the allyl radical which combines with itself to form diallyl instead of continuing the chain. We shall also neglect any chain propagation by the allyl radical. Essentially the propylene functions as a third body for removing radicals, and other unsaturated molecules might be expected to act similarly.[13] The following scheme may then be used to represent organic decompositions in presence of propylene:

$$M_1 \rightarrow 2R_1 \qquad k_1, \quad (27)$$

$$R_1+M_1 \rightarrow R_1H+R_2 \qquad k_3, \quad (28)$$

[13] Recently Staveley, Proc. Roy. Soc. **A162**, 557 (1937) has reported that ethylene inhibits the ethane decomposition.

$$R_2 \rightarrow R_1 + M_1 \qquad k_4, \qquad (29)$$

$$R_1 + R_2 \rightarrow R_1R_2 \qquad k_8, \qquad (30)$$

$$2R_1 \rightarrow R_1R_1 \qquad k_6, \qquad (31)$$

$$R_1 + CH_3CH{=}CH_2 \rightarrow R_1H + 0.5(CH_2{=}CHCH_2)_2 \qquad k_5, \qquad (32)$$

$[M_1]=x_1$, $[R_1]=x_2$, $[R_2]=x_3$, $[C_3H_6]=x_0$.

If the chain ends by (31) and (32) we have

$$k_6x_2^2 + k_5x_2x_0 - k_1x_1 = 0; \qquad (33)$$

$$\therefore \quad x_2 = [k_1x_1/k_6 + k_5^2x_0^2/4k_6^2]^{\frac{1}{2}} - k_5x_0/2k_6. \qquad (34)$$

If the chain length is greater than 10 (at maximum inhibition),

$$dx_1/dt \leqq k_3x_1x_2$$

$$= x_1^{\frac{1}{2}}k_3\left(\frac{k_1}{k_6}\right)^{\frac{1}{2}}\left[\left(1+\frac{k_5^2x_0^2}{4k_1k_6x_1}\right)^{\frac{1}{2}} - \left(\frac{k_5^2x_0^2}{4k_1k_6x_1}\right)^{\frac{1}{2}}\right]. \qquad (35)$$

The corresponding equation for the chain ending by (30) and (32) is,

$$dx_1/dt \leqq k_3x_1x_2$$

$$= x_1\left(\frac{k_1k_3k_4}{2k_8}\right)^{\frac{1}{2}}\left[\left(1+\frac{k_4k_5^2x_0^2}{8k_1k_3k_8x_1^2}\right)^{\frac{1}{2}} - \left(\frac{k_4k_5^2}{8k_1k_3k_8}\right)^{\frac{1}{2}}\frac{x_0}{x_1}\right]. \qquad (36)$$

The decomposition of *n*-butane follows Eq. (35) if as seems probable, the large chain radicals are very unstable. Writing

$$y = (k_5^2x_0^2/4k_1k_6x_1)^{\frac{1}{2}}. \qquad (37)$$

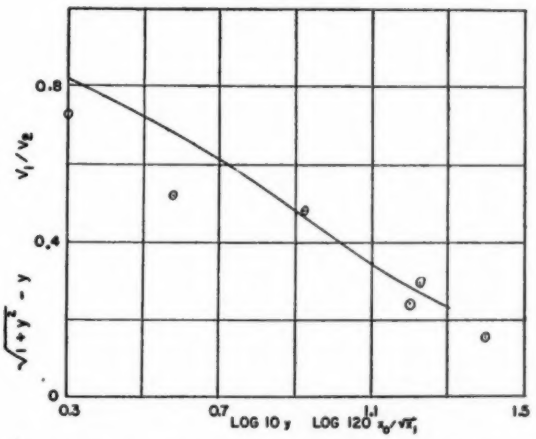

FIG. 2. Inhibition of *n*-butane decomposition by propylene. The curve is obtained by plotting log 10 y against $(1+y^2)^{\frac{1}{2}}-y$. The points are experimental (Table IV) and are obtained by plotting log $120(x_0/(x)^{\frac{1}{2}})$ against the ratio of the inhibited to uninhibited reaction (V_1/V_2); x_0 and x_1 are the concentrations of propylene and butane, respectively, relative to normal pressure and temperature (reference 1(b)).

The inhibition for constant substrate concentration may be represented by a plot of y against $(1+y^2)^{\frac{1}{2}}-y$. This is shown in Fig. 2 which also contains the experimental points taken from Table IV. This gives a value for

$$(k_5^2/4k_1k_6)^{\frac{1}{2}} \leqq 10$$

assuming an activation energy corresponding to k_5 of 22 cal. which seems reasonable. E_1 was taken as 65.4 cal.[14] and E_6 as 8 cal.[1(b)]

The authors wish to express their sincere thanks to Professor Karl Herzfeld for his help and advice throughout this work.

[14] Rice and Johnston, J. Am. Chem. Soc. **56**, 214 (1934).

Arrangement of Molecules in a Single Layer and in Multiple Layers

L. H. GERMER AND K. H. STORKS
Bell Telephone Laboratories, Inc., New York, N. Y.

(Received February 25, 1938)

Electron diffraction studies have been made upon layers of molecules of barium stearate and of stearic acid built upon surfaces by the Langmuir-Blodgett method. Upon clean metal surfaces odd numbers of layers have been built, and investigated by the reflection method; upon thin organic supporting foils even numbers of layers have been built, and investigated by the transmission method. On foils of Resoglaz the molecules are regularly arranged. The hydrocarbon chains of barium stearate molecules form hexagonal arrays with their axes normal to the supporting surface and separated by distances of 4.85A. Stearic acid molecules form crystals of monoclinic form with $a=8.27$A, $b=4.96$A, $\beta=70°$, the a and b axes lying in the plane of the supporting surface. In built-up films we previously observed a different polymorphic form of stearic acid; a correction to the data on this earlier structure is given here. On a clean metal surface molecules of the first layer stand with the axes of the hydrocarbon chains normal to the surface and the chains closely packed together laterally but irregularly arranged. The precision of alignment of the axes normal to the surface is greater for barium stearate than for stearic acid. In layers on top of the first, molecules of barium stearate and of stearic acid are regularly arranged in the way the same molecules are arranged on organic foils. In the case of barium stearate, the arrangement is random about the surface normal, although large single arrays are often formed; in the case of stearic acid, crystals are built with the axes of the hydrocarbon chains approximately in the plane defined by the surface normal and the dipping direction and pointing *upward* from the surface. Two applications or continuations of these experiments are suggested. 1. The methods of the experiments can probably be applied to fundamental studies of boundary lubrication. 2. Interpretable diffraction patterns can be obtained from single layers of molecules which are considerably shorter than stearic acid, and comparable in scattering power with films of adsorbed gas; thus studies of films of adsorbed gas can be carried out as soon as adequate vacuum technique is available.

THE first investigation of a surface film by means of electron diffraction was described in the first comprehensive paper on electron diffraction by Davisson and Germer.[1] In this investigation they determined the arrangement of a single layer of gas atoms (or gas molecules) upon a crystal surface. Since these early experiments the use of low speed electrons in the study of surface structure has been entirely superseded by the use of fast electrons. The technique of experimentation with high speed electrons is vastly easier, and there seems now no likelihood of return to the use of slow electrons as a tool for studying surfaces. There is, however, an unfortunate consequence of this change; it is accompanied by greatly decreased sensitivity to small quantities of superficial material. It seems that with fast electrons one cannot detect the diffraction pattern of a single layer of adsorbed atoms. We are limited to the study of somewhat thicker layers.

It is one of the purposes of this paper to point out that this decrease of sensitivity, serious as it really is, is not quite so bad as it may have seemed. Although we are still unable, with electrons of wave-length in the neighborhood of 0.07A, to study the arrangement of a single layer of atoms adsorbed on a metal surface, we can get interpretable patterns from a single layer of long chain organic molecules.

In a recent paper[2] we described the structure of films built from many layers of stearic acid molecules by the Langmuir-Blodgett technique.[3] The methods used in studying these films have now been applied to a single layer of stearic acid molecules, and to a single layer and to multiple layers of barium stearate.[4]

It has been discovered that the structure of the films sometimes varies with *p*H of the water,

[1] Davisson and Germer, Phys. Rev. **30**, 705–740 (1927). A more extended account of the surface film studies appeared somewhat later, Germer, Zeits. f. Physik **54**, 408–421 (1929).

[2] Germer and Storks, Proc. Nat. Acad. **23**, 390–397 (1937).

[3] Blodgett, J. Am. Chem. Soc. **57**, 1007–1022 (1935).

[4] We have no intention of implying that the experiments described here constitute the first studies, by means of fast electrons, of arrangements of single layers of organic molecules upon surfaces. Havinga and de Wael [Rec. Trav. Chim. **56**, 375–381 (1937)] have carried out such investigations successfully. Finch and Wilman [Trans. Faraday Soc. **33**, 337–339 (1937)] also have reported a diffraction pattern which they believe to be that of a single layer of molecules.

and with other experimental conditions. That an alteration of structure of *barium stearate* films with *p*H would be observed could have been predicted from the fact that the barium content of these films changes[5] with *p*H. In regard to stearic acid films, we suggested at the conclusion of an earlier paper[2] the possibility of obtaining different polymorphic forms under different conditions; this has now been accomplished.

A detailed investigation over a wide range of experimental conditions seems to be called for, but this has not yet been made. The experiments described here are concerned chiefly with the extension of the experimental method from the study of films made up of many layers of molecules to films composed of one layer only. Justification for publishing our experiments at this time rests upon the interesting nature of some of the conclusions, upon a possible application of the methods to the study of lubrication, and upon the probability that considerable time will elapse before comprehensive results are available.

Preparation of Films

A monomolecular film of stearic acid is spread upon commercial distilled water, and compressed in the usual fashion. Layers of molecules are transferred to the surface of a block by dipping the block one or more times through the film on the water surface. Built-up films of stearic acid are formed from water which has been made acid by the addition of HCl. Barium stearate built-up films are obtained from water to which $BaCl_2$ has been added to make a 7×10^{-5} molar solution, and which has been adjusted to suitable *p*H by the addition of $KHCO_3$.

The block upon which the layers of molecules are deposited has a highly polished chromium plated surface, about 5 mm wide. Immediately before dipping this block is cleaned by polishing on levigated alumina to remove the last layer of greasy organic compounds, according to a technique very similar to that described by Hardy and Nottage.[6] The block is always wetted by water on its first immersion, and the first layer of molecules is deposited upon it as it is withdrawn from the water.[3] Upon each subsequent dip two layers of molecules are deposited. Thus any odd number of layers of molecules can be built upon the chromium surface, and all of the reflection experiments reported here have been made upon odd numbers of layers.

The reflection experiments have been supplemented by transmission experiments. For these, layers of molecules are prepared upon thin foils of Resoglaz by dipping through monomolecular layers upon water surfaces.[7] The Resoglaz foil is not wetted as it first passes into the water, and two layers of molecules are deposited upon its front surface on each dip, including the first. Thus any even number of layers of molecules can be built upon the Resoglaz, and the transmission experiments reported here have been made upon even numbers of layers.

One must consider whether or not layers of molecules are built upon the rear surface of a Resoglaz foil at the same time they are being built upon the front. The knife edges, across which the foil lies, support a large drop of water at the rear. Thus successive dips do not add successive layers on this side of the foil, although a single layer may be built upon the rear on the first dip. After the last removal of the knife edge from the water the adhering drop is always removed by blotting paper. It seems highly doubtful that a second layer can be deposited upon the rear surface at this time. A foil dipped once through a barium stearate layer on water, or once through a stearic acid layer, sometimes shows a diffraction pattern characteristic of a single array of molecules (Figs. 2 and 10, respectively); this would be a rare occurrence if two layers had been deposited upon the rear as well as upon the front. None of the conclusions reached in this paper would be altered, however, if each diffraction pattern made by the transmission method were due to one or two layers of molecules on the rear of the foil as well as to the layers upon the front.

Barium Stearate Molecules in a Single Layer and in Multiple Layers

One layer of molecules

The diffraction pattern at the left of Fig. 1 was produced by a single layer of barium stearate

[5] Langmuir and Schaefer, J. Am. Chem. Soc. **58**, 284 (1936).
[6] Hardy and Nottage, Lubrication Research Technical Paper No. 1, H. M. Stationery Office.
[7] A photograph of the foil support used in these experiments appears as Fig. 4 in reference 2, and also as Fig. 1 in a paper by Germer, J. App. Phys., **9**, 143 (1938). Resoglaz is the trade name of a polystyrene resin.

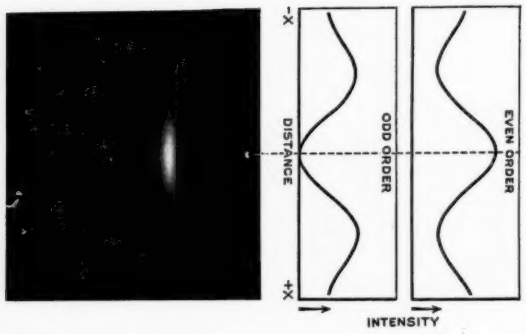

FIG. 1. Electron diffraction pattern from a single layer of barium stearate molecules on a chromium surface. ($\lambda = 0.070$A.) The curves represent intensities along the diffuse vertical bands, calculated on the basis of some simplifying assumptions.

molecules upon a block of chromium. Separations of the diffuse vertical bands of this figure correspond to a spacing of 2.50A normal to the supporting block. Observation of this spacing seems conclusive proof that the bands are due to planar hydrocarbon chains standing approximately normal to the support.[8]

There are no well-defined diffraction features upon the diffuse bands of Fig. 1. Their absence suggests that the molecules are not built into well-defined crystals. Diffraction spots from crystals might, however, be smeared out beyond recognition if, for the various crystals, the axes which are approximately normal to the surface are not strictly so but are distributed over small angles about the direction of the normal. That the axes of the hydrocarbon chains, and of the hypothetical crystals into which they might be built, do really deviate appreciably from parallelism with the surface normal is proved by the slight curvature of the bands of Fig. 1; if the axes were strictly parallel and normal to the support the diffuse bands would be sensibly straight. From the shapes of the bands we have estimated rather crudely that the axes of most of the hydrocarbon chains deviate from parallelism with the surface normal by less than about five degrees. Distribution of the axes of various crystals over such angles would result in broadening diffraction spots by about 2 mm on the first-order band, 4 mm on the second-order band, etc. This would probably cause all diffraction spots to escape observation.

Although from the pattern of Fig. 1 we cannot determine whether or not the barium stearate molecules in a single layer are formed into well defined crystals, evidence will be presented later which suggests strongly that regular arrangements are not formed. It is thus worth while to calculate the diffraction pattern to be expected from unrelated planar hydrocarbon chains, each standing with its axis normal to the surface but with the planes of the chains lying in randomly distributed azimuths about the surface normal, and to compare this calculated pattern with Fig. 1.

To describe the diffraction pattern we adopt Cartesian coordinates on the photographic plate, with the origin at the primary beam position and the x axis parallel to the specimen surface. Other quantities are defined as follows:

λ = electron wave-length,
L = distance from specimen to photographic plate,
s = separation between alternate carbon atoms in the zigzag hydrocarbon chain,
φ = angle between the line joining two adjacent carbon atoms and the axis of the chain,
θ = inclination of the plane of a hydrocarbon chain to a plane normal to the primary beam.

The simplifying assumption is made that each carbon atom of a chain scatters electron waves equally, that there is, in other words, no shielding of atoms near the surface of the metal by those further removed. It is then easy to show that the intensity of electron scattering from an entire chain of $2N$ carbon atoms to any point (x, y) on the plate is greater than the scattering from a single carbon atom to that point by a factor proportional to

$$\frac{\sin^2 NBy}{\sin^2 By} \cos^2 \left\{ \frac{B}{2} (y + x \tan \varphi \cos \theta) \right\}, \quad (1)$$

where $B = \pi s / L\lambda$. Since it is assumed that various chains are unrelated, except in the common direction of their axes, the intensity of scattering from many chains is obtained by adding the

[8] The pattern of Fig. 1 resembles one which we previously obtained from the saturated glyceride, tristearin. From it we concluded [J. Chem. Phys. **5**, 131–134 (1937)] that the hydrocarbon chains of this glyceride orient themselves with their axes normal to a supporting metal surface. Finch and Fordham [Chem. and Ind. **56**, 632–639 (1937)] have recently stated that glycerides orient themselves upon metal surfaces with the axes of the chains inclined. Our experiments indicate (J. Chem. Phys., reference 8) that this may be, and probably is, true for unsaturated glycerides. It is not, however, true for tristearin, and is probably not true for other saturated glycerides.

intensities due to the separate chains. This total intensity, for hydrocarbon chains the planes of which lie randomly distributed in azimuth about the surface normal, is proportional to the quantity obtained by multiplying (1) by $d\theta$ and integrating with respect to θ from 0 to π. The total intensity[9] is proportional to

$$\frac{\sin^2 NBy}{\sin^2 By}\{1+J_0(Bx \tan \varphi) \cos By\}. \quad (2)$$

The principal maxima of the factor $\sin^2 NBy/\sin^2 By$ occur at those values of y for which $sy/L\lambda=1, 2, 3$, etc.; at values of y considerably removed from these the factor is negligibly small. These values of y correspond respectively to the diffuse bands, and from the separation between adjacent bands, $D=11$ mm, one calculates $s=2.50$A ($L\lambda=2.73\times10^{-6}$ mm^2, as determined by calibration against a foil of metallic silver. The electron wave-length is 0.070A in all of the experiments described in this paper).

Along a diffuse band expression (2) is proportional to

$$1\pm J_0(Bx \tan \varphi), \quad (3)$$

the plus sign applying to bands of even order and the minus sign to bands of odd order. At the right-hand side of Fig. 1 are plotted intensity values calculated from (3), vertical distances representing positions along the bands and horizontal distances values of (3) in arbitrary units. In calculating these values $B=\pi s/L\lambda=\pi(2.50\times10^{-7})/(2.73\times10^{-6})$ mm$^{-1}=0.288$ mm^{-1}, and tan φ is assumed equal to $1/\sqrt{2}$ which is its value in the carbon chains in the diamond lattice.

The calculated curves give intensity distributions resembling those of the diffuse bands, but the most intense parts of the bands of odd order are definitely nearer to the horizontal center line than are the maxima of the corresponding curve. In the calculated curves a number of factors have been neglected, including variation with direction of intensity of scattering from each atom and effects produced by waviness of the polished metal surface; but it seems to us that these cannot account for the discrepancies between theory and observation. Although fair agreement would be obtained if we assumed tan φ to be about 1.3 instead of $1/\sqrt{2}$, such an assumption is entirely untenable. We believe that the discrepancies must be attributed to the fact that the lateral spacings between hydrocarbon chains are not entirely random as assumed in the calculation. Packing of the chains closely together would result in diffuse spots located on the bands. Mean lateral spacing of the hydrocarbon chains of 5*A* would correspond to diffuse spots at a distance of $L\lambda/5\times10^{-7}=5.5$ mm from the center line. Such spots are clearly observable on the first-order band; on the third-order band they can account for the fact that the intensity maxima are nearer the center line than the simple theory indicates.

Considerations are presented below (at the end of the section "Three layers of molecules"), which indicate that molecules of a single layer have no regularity of lateral arrangement. On the basis of this evidence and the above calculation, we conclude that the hydrocarbon chains of a single layer of barium stearate molecules on a chromium surface are closely packed together but irregularly arranged, with the axes of the chains normal to the surface within a tolerance angle of a few degrees.

Two layers of molecules

In Fig. 2 is reproduced a diffraction pattern from *two layers of molecules*, obtained by the transmission method. The regular spacing of the hydrocarbon chains of both layers of molecules, which one deduces from this pattern, is in striking contrast to the closely packed but irregular arrangement which accounts for the pattern of a single layer upon chromium. One naturally wonders whether the molecules of the first layer were arranged immediately upon deposition or whether they acquired their arrangement only when the second layer was added. The former seems much more likely, although our experiments offer no direct proof. Such proof is, however, apparently supplied by the experiments of Havinga and de Wael[4] who have obtained an electron diffraction pattern from a single layer of barium stearate molecules deposited upon nitrocellulose by a modification of the Blodgett

[9] The evaluation of the integral was given to us by Dr. S. A. Schelkunoff. A calculation similar to that just carried out here has been published by Murison, Phil. Mag. **17**, 201–225 (1934). It is easy to show that the elaborate expression which he obtains is equivalent to (2).

method. The pattern which they obtain from a single layer resembles that of Fig. 2, and suggests strongly that the first layer of molecules on Resoglaz is arranged before the second is added.

The pattern of Fig. 2 seems to indicate the arrangement of barium stearate molecules in simple crystals having hexagonal symmetry. The smallest separation between diffraction spots of this figure is $R_0=6.50\pm0.10$ mm, which corresponds to a unit cell in hexagonal coordinates with $a=b=2L\lambda/R_0(3)^{\frac{1}{2}}=4.85$A. The cross-sectional area of this cell normal to the c axis is $a^2(3)^{\frac{1}{2}}/2=20.4$A^2. Since this value is in good agreement with the known cross section of a single hydrocarbon chain,[10] one is tempted to conclude that the barium stearate molecules form a hexagonal crystal with its c axis parallel to the axes of the chains and with the cross-sectional area of each unit cell containing one chain only. In a true hexagonal crystal such an arrangement is, however, impossible; the arrangement of *planar* chains to give a diffraction pattern with hexagonal symmetry cannot be accomplished in a structure in which the cross section of the unit cell contains one chain only. We infer that although the axes of the chains intersect the corner points of an extended two-dimensional hexagonal net, the planes of the individual chains are randomly distributed in azimuth about the direction of the normal to the supporting foil. If the distribution is not entirely random, at least the regularities are so slight that the molecules do not build up unit cells which give rise to diffraction spots sufficiently clear to be observed. The diffuseness of the spots of Fig. 2 suggests that each of them may, perhaps, be made up of a number of unresolved spots occurring close together.

The pattern of Fig. 2 was selected for reproduction here because most of it arises from a single hexagonal array of molecules. Some of the patterns which we have obtained from two layers of molecules are obviously composite patterns arising from two or more hexagonal array rotated with respect to each other about the normal to the film. These are less well adapted to exhibit clearly the symmetry of the arrangement.

[10] See, for example, Adam, *The Physics and Chemistry of Surfaces*, p. 50.

Three layers of molecules

The pattern of Fig. 3 was produced by *three layers* of barium stearate molecules. This pattern shows diffuse vertical bands like those of Fig. 1, but in addition there are well-defined features which are not produced by a single layer. It is evident that, in three layers as in two, there occur marked regularities in lateral spacings between molecules.

There is also another difference between Fig. 1 and Fig. 3; the diffuse bands obtained from three layers of molecules are sensibly straight, whereas those from a single layer are slightly curved. One concludes that in the second and third layers the axes of the hydrocarbon chains are strictly normal to the supporting surface.

The horizontal features of Fig. 3 are so diffuse that precise measurements of distances from the center line cannot be obtained. The best estimates of these distances which we have been able to make are given in the first two columns of Table I. One naturally postulates hexagonal arrays of hydrocarbon chains like that which accounts for the pattern of Fig. 2, with, however, many different arrays randomly oriented with respect to the surface normal. Such an arrangement would produce lines at distances from the center line given by $R=6.5(H)^{\frac{1}{2}}$mm where $H=m^2+mn+n^2=1, 3, 4, 7, 9, 12, 13\cdots$, m and n representing any whole numbers. (6.5 mm represents here the smallest spacing between diffraction spots in Fig. 2). Calculated values of R in the fourth column of Table I are in fairly good agreement with observed values, with the single exception of the extra observed spacing of 5.3 mm.

One might guess that the diffuse spots occurring at 5.3 mm have the same origin as those observed in Fig. 1 at about the same locations, that they are due to the first layer of molecules which are closely packed but irregularly arranged. The spots in Fig. 3 are, however, much better defined than those in Fig. 1. Furthermore, in a diffraction pattern which we have obtained from five layers of barium stearate molecules, all of the features are sharper and clearer than in Fig. 3; the "extra" spots are also stronger, and are as clear and sharp as any of the others. These observations have led us to the belief that the extra spots from three and from five layers of molecules may have a

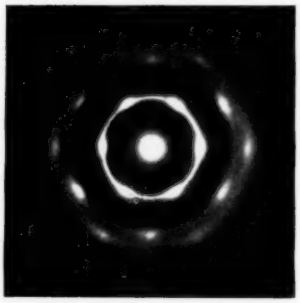

FIG. 2. Diffraction pattern from two layers of barium stearate molecules on a Resoglaz supporting foil.

different origin; they may be due to the breaking up of each of the spots at 6.5 mm into two components. This phenomenon has been observed in transmission patterns, for example in Fig. 4. If this interpretation is correct it proves that in three layers of molecules the planes of the chains have some regularity of arrangement, so that ill-defined true crystals are formed which have hexagonal symmetry.

It seems to us probable that the regularities which account for the features of Table I are confined to the two top layers of molecules, the layer next to the metal having the closely packed but irregular arrangement characteristic of a single layer by itself. Although there is no experimental evidence for this in the case of layers of barium stearate, tests on stearic acid layers described below do indicate rather clearly that this is the situation in layers of the acid.

The thus far unverified conclusion that barium stearate molecules in a *single* layer on chromium have no regularity of lateral arrangement can be reviewed at this time. The differences between Figs. 1 and 3 seem to us to offer convincing evidence in favor of this conclusion. If, in the first layer, the molecules were arranged in some regular fashion, we would expect that two additional layers would continue the regularity of the first; the pattern from three layers would then exhibit curved diffraction bands. That the bands from three layers are sensibly straight proves that any possible regularity which might have existed in the first layer is not continued in the second and third, and suggests very strongly that there was no regularity in the first.

Four layers of molecules

Four layers of barium stearate molecules

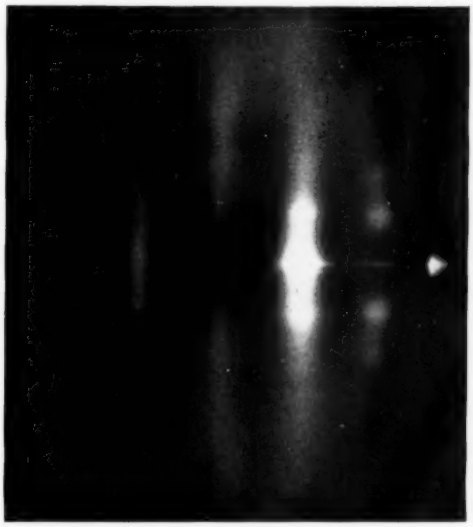

FIG. 3. Pattern from three layers of barium stearate molecules on a metal surface.

sometimes give a diffraction pattern like that of Fig. 2, but often a much more complex pattern is produced. An example of such a pattern appears as Fig. 4.

Most of the features of Fig. 4 belong to a single array which has hexagonal symmetry; the main part of the pattern appears to be that of a single crystal. (This pattern was chosen for reproduction from a number of others each of which was obviously due to two or more crystals). The strongest features correspond to the hexagonal array of diffuse spots of Fig. 2, and determine the same arrangement of molecular axes. The elaborate details of Fig. 4 appear to prove that the planes of the chains of the various molecules are related to each other in such a fashion that a true crystal is built up having a large unit cell. We have, as yet, been unable to determine the

TABLE I.

Distances of Streaks from Center Line in Fig. 3			
First-Order Band	Second-Order Band	H	Calculated Distances $6.5(H)^{\frac{1}{2}}$
5.3 mm			
6.7	6.5 mm	1	6.5 mm
11.8	11.4	3	11.3
13.2		4	13.0
17.5		7	17.2
		9	19.5

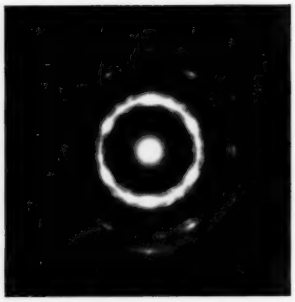

FIG. 4. Pattern from four layers of barium stearate molecules on a Resoglaz foil.

arrangement of the planes of the carbon chains or even the size of the cell. The complexity of the pattern of Fig. 4 makes it obvious that any attempt to draw significant conclusions from "extra" features in the pattern from three layers of molecules (Fig. 3), or from five layers, was doomed to failure.

One notes that the diffraction pattern of Fig. 4 appears to be rotated with respect to that of Fig. 2 through an angle of about 30°. This is fortuitous and is consistent with the observation that the orientations of hexagonal patterns from built-up films of barium stearate molecules are unrelated to direction of dipping when the films were formed. This fact has already been implied in the statement that a transmission pattern is often obviously due to two or more hexagonal arrays of molecules rotated with respect to each other about the surface normal

Multiple layers of molecules

All diffraction patterns which we have obtained by the reflection method have been examined for reflections from crystal planes parallel to the specimen surface. In no case are the horizontal diffraction lines resolved into sharp spots which are prominent. On different plates a total of 34 spots can, however, be seen more or less clearly. As one cannot assign indices to any of these unambiguously a reliable value of the c spacing cannot be obtained. We are able to show that this spacing is of the order of 50A, but the precision of this value is very low. The reason for this uncertainty becomes quite clear when we consider the very slight penetrating power of the electron waves; in the following section of this paper we have shown that in the diffraction pattern from three layers of stearic acid molecules the scattering is predominantly from the two top layers. Thus most of the scattering is always from a surface layer which is only one unit cell thick, and good resolution of different orders of this spacing is never obtained.

Although the variation of structure with pH which was mentioned earlier has not been investigated extensively, some simple observations have been made. All of the barium stearate patterns reproduced here were made at pH in the neighborhood of 7. At high pH, around 10, large single arrays of molecules have not been observed; transmission patterns consist of continuous rings, instead of spots as in the patterns of Figs. 2 and 4. The radii of the rings seem to be the same as radii of spots in Fig. 4, but relative intensities are greatly altered.

STEARIC ACID MOLECULES IN A SINGLE LAYER AND IN MULTIPLE LAYERS

Reflection experiments

One layer of molecules.—The pattern of Fig. 5 was produced by a single layer of stearic acid molecules on a chromium surface. Adjacent diffuse bands of this figure have a separation of 11 mm, as do the bands of Fig. 1. The two patterns have other similarities also; bands of odd order are weak along the center line and bands of even order strong; there are diffuse spots on the first order band which correspond to mean lateral spacings of about 5A. The diffuse bands of Fig. 5 are, however, markedly more curved than those of Fig. 1. We have obtained many diffraction patterns from single layers of barium stearate and from single layers of stearic acid, and have established the fact that these similarities and this difference are characteristic of the molecules of the layer. In both cases, barium stearate and stearic acid, the diffraction pattern from a single layer is the same for different directions of the primary beam relative to the dipping direction.

After the consideration which has already been given to Fig. 1 we are able to interpret the pattern of Fig. 5 readily. We conclude that stearic acid molecules are arranged in a single layer upon chromium with the axes of the hydrocarbon chains approximately normal to the

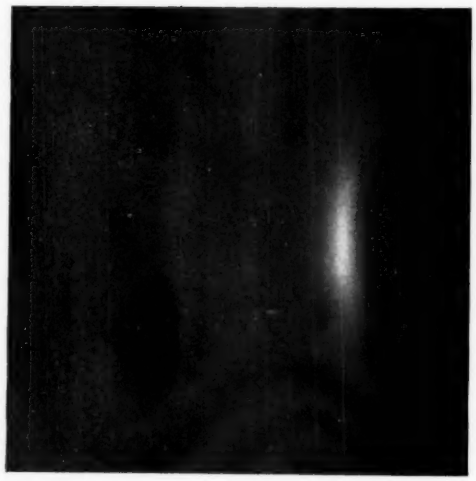

FIG. 5. Pattern from a single layer of stearic acid molecules on a metal surface.

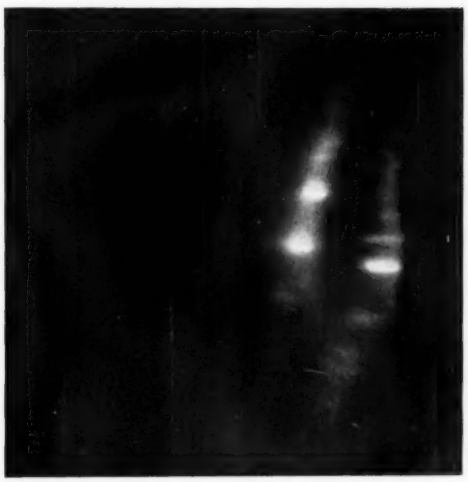

FIG. 6. Pattern from three layers of stearic acid molecules on a metal surface. Primary beam normal to direction of dipping, and dipping direction *downward* as the pattern is reproduced here.

surface. The precision of this alignment is considerably less for stearic acid than for barium stearate; we estimate from the curvatures of the bands of Fig. 5 that the axes of many of the molecules of stearic acid deviate from parallelism with the surface normal by as much as 10°. The molecules of stearic acid are closely packed together laterally but irregularly arranged. In this connection it is interesting to compare the approximate value of 5A for the mean separation of hydrocarbon chains in one layer of stearic acid, and in one layer of barium stearate, with 4.85A which was discovered to be the distance between chains in the regular arrangement of barium stearate molecules in two layers on Resoglaz.

Three layers of molecules.—The diffraction pattern of Fig. 6 was obtained from three layers of stearic acid molecules on a chromium block, with the primary electron beam normal to the dipping direction and the block mounted in the camera just as it was held during dipping. The dipping direction is thus downward as Fig. 6 is reproduced here.

Adjacent diffuse bands of this figure are separated by 11 mm and correspond to a repeated spacing of 2.50A along a direction normal to the bands. We conclude that the hydrocarbon chains of the stearic acid molecules of the second and third layers stand with their axes normal to the bands and thus inclined *upward* from the metal surface. The sharp features upon the bands prove that the molecules are arranged in some regular fashion.

One can see very weakly traces of diffuse *vertical* bands of the second and fourth orders, produced probably by the first layer of molecules standing directly on the metal surface. The relative weakness of these vertical bands proves that the electrons are scattered chiefly from the two top layers of molecules, indicating that the penetrating power of the electons is very slight at a small glancing angle. The vertical bands are not present in diffraction patterns obtained from many layers of molecules; for example, the pattern of Fig. 7 from fifteen layers of stearic acid molecules shows no trace of vertical bands.

Five layers of molecules.—A diffraction pattern from five layers of stearic acid molecules is somewhat sharper and clearer than that from three layers, and better measurements can be made upon it. Measurements upon this pattern, which is not reporduced here, are contained in Table II. In the second and fourth columns are given distances of the sharp horizontal diffraction lines from the center line, those above the center line in the second column and those below in the fourth. Estimated intensities of the lines are written down also. In the first column are indicated the orders of the inclined diffuse bands upon which the diffraction lines appear.

FIG. 7. Pattern from many layers of stearic acid molecules. Dipping direction downward and normal to the primary beam, as in Fig. 6.

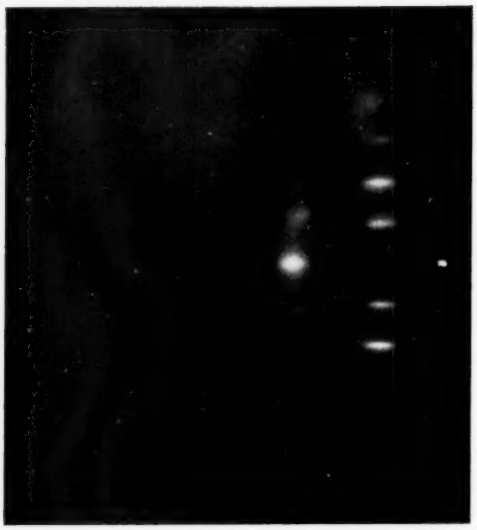

FIG. 8. Pattern from many layers of stearic acid molecules. Primary beam *parallel* to direction of dipping.

In Table II are tabulated distances from the center line of 23 diffraction features. Of these, 15 appear clearly to represent different measurements of the first six orders of a single spacing; these orders are tabulated in the last column. To obtain the best possible value of the fundamental spacing, of which the measured distances represent various orders, we have plotted these spacings against their respective orders. The line drawn through the origin which fits the experimental points as well as possible has a slope corresponding to a fundamental spacing of 3.30 mm. The fit would be slightly poorer if we chose 3.29 mm or 3.32 mm, although we do not imply precision of such a high order for the experimental data.

TABLE II. *Five layers of stearic acid molecules. Specimen in camera with dipping direction downward, and normal to primary electron beam.*

	Horizontal Diffraction Lines				
	Above Center Line		Below Center Line		
Diffuse Bands	Distances from Center Line	Estimated Intensities	Distances from Center Line	Estimated Intensities	h
Zero Order			13.0 mm	2	4
			19.7	1	6
First Order	3.4 mm	5	3.4	10	1
	6.3	4	6.3	3	
	9.9	7	9.9	8	3
	11.3	2			
	14.3	3	14.3	1	
	16.5	2	16.5	4	5
Second Order	6.5	9	6.5	2	2
	11.0	1			
	13.5	4	13.5	1	4
	17.3	1			
	20.2	2			
Third Order	3.5	2	3.5	1	1
	16.8	2			5

Electron beam parallel to dipping direction. Seven layers of molecules.—In order to proceed with analysis of the stearic acid structure it is convenient to measure also a diffraction pattern obtained with the primary electron beam parallel to the dipping direction. Such a pattern, from seven layers of molecules, is reproduced in Fig. 8.

Distances of the horizontal features of this pattern from the center line are written down in the second column of Table III, and estimated intensities in the third column. Most of the distances are approximately multiples of 5.5 mm The best value of this fundamental distance has been obtained from a plot of the measured values of the second column against the integers of the fourth. The data are best fitted by a line corresponding to 5.50 mm, which is in better agreement with the available measurements than 5.45 mm or than 5.55 mm.

Deductions from the reflection experiments.—The diffuse bands of Fig. 8 are vertical, parallel to the specimen surface. This observation, to-

gether with the fact that the bands obtained with the primary beam normal to the dipping direction are inclined to the surface normal, proves that the stearic acid molecules stand with the axes of the hydrocarbon chains inclined to the supporting surface and approximately parallel to the dipping plane, which is defined by the dipping direction and the surface normal. The diffuse bands of Fig. 8 have separations of about 11 mm.

The data of Tables II and III suggest that the molecules are built into crystals of monoclinic form with

$$a=(L\lambda/3.30)\text{ mm}=8.27\text{A},$$
$$b=(L\lambda/5.50)\text{ mm}=4.96\text{A},$$

the crystals being oriented precisely with their a and b axes parallel to the supporting surface and the b axes showing strong preference for the direction normal to the dipping plane. The logical procedure by which these ideas are reached is described in detail in an earlier paper.[2] Reference to this is also necessary to justify other deductions which are made below.

In order to test the suggested values of a and b, as well as the preferred crystal orientation, we have written down measured distances of Tables II and III in the first four columns of Table IV, for the purpose of comparing them with values in the last column calculated from the relation $R=[(3.30h)^2+(5.50k)^2]^{\frac{1}{2}}$. In this expression h and k are any integers, and all values of R are included in Table IV up to $R=27.5$ mm. It is found that the measured distances are in excellent agreement with the calculated values. In some cases either of two, or even three, pairs of values of h and k can be assigned to a measured distance; the correct assignments are, however, obvious from the crystalline orientation which the data establish.

The reciprocal lattice of each stearic acid crystal is made up of points occurring close together along parallel lines which are normal to the supporting surface. Intersections of these lines with the surface are indicated in Fig. 9, reciprocal lattice dimensions in mm^{-1} being multiplied by $L\lambda$ to reduce them to mm. Each point in Fig. 9 represents a section of a diffraction line which is actually observed and written down in Table IV. Points along the vertical line through the center represent reflections the Miller indices of which are of the form $(h\ 0\ l)$ and points along the horizontal line through the center have Miller indices $(0\ k\ l)$. Points indicated by open circles are observed when the primary beam is normal

TABLE III. *Seven layers of stearic acid molecules (Fig. 8). Specimen in camera with primary electron beam parallel to dipping direction.*

	Horizontal Diffraction Lines Above and Below Center Line		
Diffuse Bands	Distances from Center Line	Estimated Intensities	k
First Order	5.5 mm	6	1
	6.75	2	
	10.85	7	2
	16.6	3	3
	21.75	3	4
	22.9	2	
	27.8	1	5
Second Order	6.65	3	
	11.15	2	2
	16.5	1	3

TABLE IV. *Measured separations of horizontal lines from center line.*

Beam Normal to Dipping Direction		Beam Parallel to Dipping Direction				Calculated Separations
Odd Ordered Bands	Even Ordered Bands	First Order Band	Second Order Band	h	k	
3.4 mm 3.5				1	0	3.3 mm
		5.5 mm		0	1	5.5
6.3		6.75	6.65 mm	1	1	6.4
	6.5 mm			2	0	6.6
				2	1	8.6
9.9				3	0	9.9
		10.85	11.15	0	2	11.0
11.3	11.0			3	1	11.3
				1	2	11.5
				2	2	12.8
	13.0 13.5			4	0	13.2
14.3				4	1	14.3
				3	2	14.8
		16.6	16.5	0	3	16.5
16.5 16.8				5	0	16.5
				1	3	16.8
				4	2	17.2
	17.3			5	1	17.4
				2	3	17.8
				3	3	19.2
	19.7			6	0	19.8
				5	2	19.8
	20.2			6	1	20.5
				4	3	21.1
Measurements upon this pattern give $\beta=70°$		21.75		0	4	22.0
				1	4	22.2
				6	2	22.7
		22.9		2	4	23.0
				7	0	23.1
				5	3	23.3
				7	1	23.7
				3	4	24.1
				7	2	25.6
				4	4	25.7
				6	3	25.8
				8	0	26.4
				8	1	27.0
				5	4	27.5
		27.8		0	5	27.5

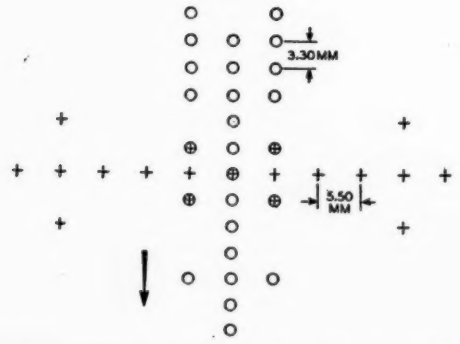

FIG. 9. Cross section of the stearic acid reciprocal lattice, showing only points corresponding to features observed in the reflection experiments. (All distances are multiplied by $L\lambda$ to reduce to mm.)

to the dipping direction; points indicated by crosses are observed with the beam parallel to the dipping direction. The dipping direction is indicated by the heavy arrow.

The monoclinic angle, β, can be determined by direct measurement upon the diffraction pattern which gave the data of Table II. One measures the inclination to the surface normal of a line through the centers of diffraction streaks of the form (h 0 l). We have obtained $\beta=70°$ in this way.

The fact that diffraction features of appreciable intensity occur approximately along the diffuse bands is equivalent to the statement that reflections occur only for values of l in the neighborhood of $l=n(c/s)$, where c is the length of the edge of the unit cell parallel to the c axis and n an integer representing the order of a diffuse band.[2] An interesting observation, which is indicated clearly in Table IV, is that of all reflections of the form (h 0 l) only those with h odd occur on diffuse bands of odd order and only those with h even on diffuse bands of even order. In other words, for reflections of the form (h 0 l) h and n are either both odd or both even. We have not yet succeeded in interpreting this observation in terms of crystal symmetry.

Measurement of the c spacing.—On some diffraction patterns are observed spots corresponding to (0 0 l) reflections for various orders of l. Although we have found and measured 97 such reflections, none are well defined and in no case can we determine value of l unambiguously. The spacing which we determine from these reflections is of the order of 25A, but the precision of this value is very low. We presume that the reflections which are discovered are even orders only of the spacing $c \sin\beta \sim 45$A. That even orders only appear may be due to lack of great difference between the irregularities introduced at carboxyl and at paraffin ends of the molecules. We reported a correspondingly small spacing (20A) in our earlier observations on alpha-stearic acid.[2] It is interesting to note that barium stearate built-up layers yield a c spacing of the order of 50A; in this case the irregularities introduced by the presence of barium atoms are great enough to cause odd as well as even orders to be found.

Transmission experiments

A diffraction pattern from two layers of stearic acid molecules on a Resoglaz foil is reproduced in Fig. 10, and a pattern from six layers in Fig. 11. The diffuse rings which are prominent in the former are due to the supporting Resoglaz foil; the arrays of sharp spots are produced by the layers of stearic acid molecules. Each spot pattern is predominantly that of a single crystal.

Measurements of the separations of spots along the vertical and horizontal directions give, respectively, 3.40 mm and 5.47 mm in Fig. 10, and 3.34 mm and 5.50 mm in Fig. 11. Both sets of values agree well with 3.30 mm and 5.50 mm obtained from the reflection experiments. Thus we conclude that stearic acid molecules built upon a Resoglaz foil form crystals which have the same structure as those formed by building upon a chromium surface. From Fig. 10 we are quite certain that even molecules of the first layer upon Resoglaz fit into the structure of the crystal; Resoglaz seems to have no influence upon the arrangement of the first layer of molecules built directly upon it, as does a metal surface. A similar observation has already been recorded for barium stearate molecules upon metal and upon Resoglaz. In both cases the paraffin ends of the molecules are in contact with an organic foil, whereas the carboxyl or barium ends are in contact with a metal.

Some general observations

Boundary lubrication.—The striking difference between the irregular arrangement of stearic acid molecules in the first layer upon a chromium

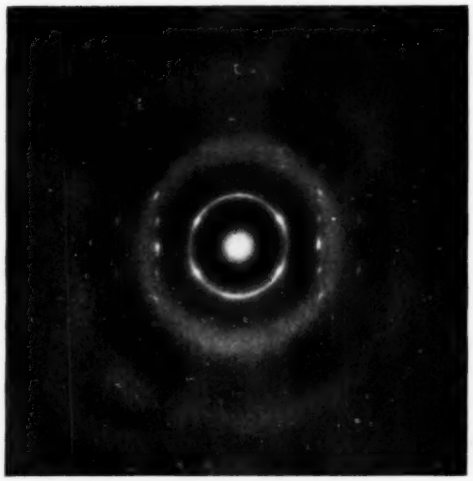

FIG. 10. Pattern from two layers of stearic acid molecules on a Resoglaz supporting foil. Dipping direction downward.

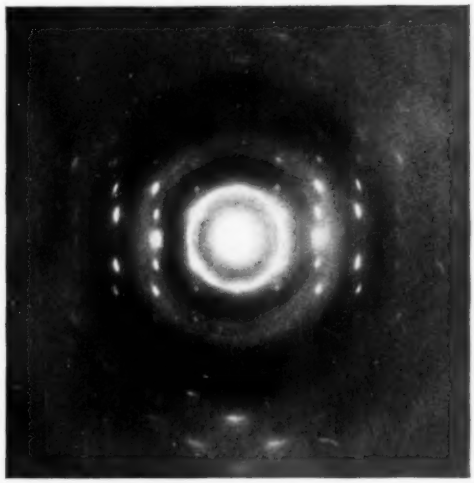

FIG. 11. Pattern from six layers of stearic acid molecules. Dipping direction downward.

surface and the regular structure in subsequent layers proves that the influence of the metal surface does not extend appreciably beyond the first layer. It seemed to us altogether probable that the same difference between the first and subsequent layers would be found if a different metal were substituted for chromium. This we have confirmed by experiments upon a highly polished steel gauge block made by Carl Zeiss; the diffraction patterns from one layer and from seven layers of stearic acid molecules upon this block are sensibly the same as those of Figs. 5 and 7, respectively. We are thus at a loss to account for the observation by Clark, Sterrett and Lincoln[11] that stearic acid deposited by fusion is not oriented upon iron, although it is well oriented upon copper.

The similarity of Figs. 1 and 5 suggests to us that stearic acid molecules of the first layer may react directly with a superficial layer upon a chromium surface to form stearate molecules. Layers of stearic acid molecules on top of the first layer exist in uncombined form. The effect upon its lubricating properties of the addition of stearic acid to a paraffin oil may be due to interaction of the first layer of acid molecules with a metal surface. The results of the present experiments have led us to believe that electron diffraction methods can be successfully applied to fundamental studies of boundary lubrication. We propose to carry out tests upon various compounds which can be added to lubricating oils to increase "oiliness."

Polymorphic forms of stearic acid.—In the first column of numerical values of Table V are written down data regarding the stearic acid structure described above. In the second column are corresponding data from our earlier paper,[2] with a corrected value of the angle β. In the other columns are other published data regarding stearic and palmitic acids. It is evident that our values tabulated in the first two columns represent different crystalline forms, which are also differently oriented with respect to the dipping direction; in the older form (column 2) the axes of the hydrocarbon chains are inclined *downward* from the surface of the supporting block as the block is held during dipping, whereas in the present form (column 1) the axes are inclined *upward*.[12] We are unable to account for the occurrence of these two modifications. The newer form (column 1) has been obtained consistently for many months, although temperature of the water has been varied somewhat and *p*H has been changed over a considerable range; the other form (column 2) appeared with equal

[11] Clark, Sterrett and Lincoln, Ind. and Eng. Chem. **28**, 1318–1322 (1936).

[12] Clark and Leppla [J. Am. Chem. Soc. **58**, 2199–2201 (1936)] have reported that the axes of the hydrocarbon chains of stearic acid in built-up layers are inclined *downward*.

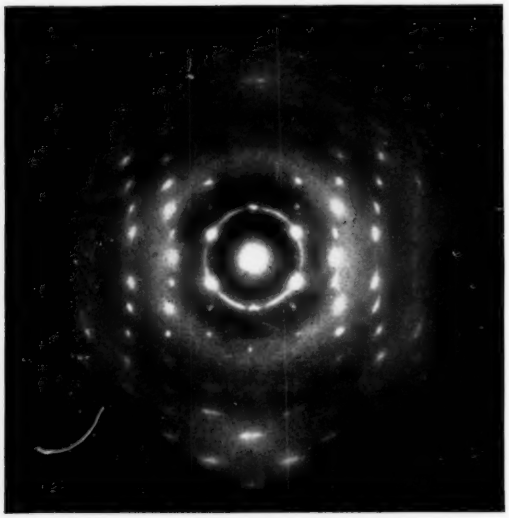

FIG. 12. Pattern from twelve layers of stearic acid molecules. Dipping direction downward.

uniformity a few months earlier. It seems that the surface of the metal block can have nothing to do with the form which appears, because at a given time identical modifications are developed upon chromium and upon Resoglaz. Dr. B. E. Warren has suggested to us that a particular form may be determined by "seeding," the existence of tiny seed crystals about the experimental equipment.

In the second column of Table V we have given 52° for the monoclinic angle β. The earlier value of 57° [2] was incorrectly determined. The correct angle is obtained by measuring the inclination to the surface normal of a line through the centers of diffraction streaks of the form $(h\ 0\ l)$. In our earlier paper we measured not this inclination but the slope of the diffuse bands obtained with the primary beam normal to the dipping direction. If all crystals were precisely oriented with their b axes normal to the "dipping plane" the two measurements would yield identical values; for crystals which are not precisely oriented in this way the earlier measurement yields too high a value, by 5° in the case under consideration.

Values of $c \sin \beta$ obtained by Francis, Piper and Malkin for three different modifications of stearic acid are given at the bottom of Table V It is evident that the form which they describe as "b" is the same as that studied by Müller and

TABLE V. *Comparison of present data on stearic acid with previously published quantities.*

	Germer and Storks		Palmitic Acid	Stearic Acid		
	Stearic Acid					
	Journal Chemical Physics (this paper)	Proc. N.A.S.[2]	"α" Form Thibaud and Dupré la Tour[14]	"α" Form Thiessen and Schoon[15]	Müller[16]	"β" Form Thibaud and Dupré la Tour[14]
a	8.27A	9.4A	9.41A	9.36A	5.546A	5.68A
b	4.96A	5.0A	5.00A	4.95A	7.381A	7.39A
c	—	—	45.9A	—	48.84A	—
β	70° Upward	52°[13] Downward	50° 50′	51.2°	63° 38′	—
$a\ b \sin \beta$	38.6A^2	37.0A^2	36.5A^2	36.6A^2	36.76A^2	—
$c \sin \beta$	—	—	39.5A after c has been adjusted to streaic acid value by adding 5.0A	—	43.76A	43.95A
$(h\,0\,l)$ reflections	h and n both even or both odd	h even				
Francis, Piper and Malkin[17] $c \sin \beta$	Stearic Acid "a" form 46.6A		Stearic Acid "c" form 39.95A		Stearic Acid "b" form 44.0A	

[13] Corrected, as described in text.
[14] Thibaud and Dupré la Tour, J. de Chim. Phys. **29**, 153–167 (1932). Dupré la Tour, Thesis, Univ. of Paris, 1932.
[15] Thiessen and Schoon, Zeits. f. physik. Chemie **38**, 216–231 (1937).
[16] Müller, Proc. Roy. Soc. **A114**, 542–561 (1927).
[17] Francis, Piper and Malkin, Proc. Roy. Soc. **A128**, 214–252 (1930).

by Thibaud and Dupré la Tour and designated as "β" by the latter experimenters. Also our older form (column 2) is the same as that studied by Thiessen and Schoon, and designated by them and by us as the "α" modification because of its similarity with "α" palmitic acid. If we add 5.0A to the c edge of alpha-palmitic acid as determined by Thibaud and Dupré la Tour, in order to make it comparable with the stearic acid edge, we obtain a value of $c \sin \beta$ in agreement with that for the form designated as "c" by Francis, Piper and Malkin; thus the "c" form and the "α" form are identical. It may well be that our new modification of stearic acid (column 1) is that described as "a" by Francis, Piper and Malkin. This cannot be tested as we do not know the length of the edge of the unit cell parallel to the c axis. One might think that this edge would be the same for the different modifications, but this apparently is not so; 5.0A added to the c edge of alpha-palmitic acid gives a value which is definitely in disagreement with the c edge of beta-stearic acid as found by Müller.

It is interesting to observe that all values of $ab \sin \beta$ (line five of Table V) are in rather good agreement, corresponding in every case to the cross section of two hydrocarbon chains. The high value in the first column differs from those in other columns by an amount which is probably not beyond possible experimental error in our measurements. The cross section of a single hydrocarbon chain in barium stearate, 20.4A^2 as determined in the first part of this paper, is distinctly greater than the cross section in stearic acid, 18.4A^2. This may suggest that the modification of column 1 is contaminated by some metal ions. In the case of our earlier measurements (column 2) we were able to rule out such a possibility by producing relatively large crystals in which no significant contamination could occur. Although we have not done this in the case of the new crystal modification, we believe that metallic contamination is unlikely.

Distortion of diffraction patterns.—A curious distortion of some diffraction patterns has been observed. An example of this is exhibited in Fig. 12, a transmission pattern from twelve layers of stearic acid molecules. The spots of Fig. 12 do not fall along straight lines, as do those of Figs. 10 and 11.

A disturbance, which seems to be similar, is often found in reflection patterns from built-up layers. In both Fig. 6 and Fig. 7 horizontal diffraction features are shifted from their "correct" positions by varying amounts along the diffuse bands.

We have attempted to account for these strange phenomena by refraction, by electrostatic charging of the films or by distortion or inhomogeneity of the crystals, but without success.

Barium Myristate Molecules in a Single Layer

It has seemed important to find out just how thin a layer of atoms on a polished metal surface will give a diffraction pattern which can be interpreted. We have been able to build a layer of barium myristate molecules on a metal surface by the Langmuir-Blodgett technique, but we have not been able to build a layer of barium laurate molecules. A diffraction pattern was obtained from the single layer of barium myristate which resembles the pattern of Fig. 1. It seems probable that considerably shorter hydrocarbon chains than those of myristic acid (14 carbon atoms) would give interpretable diffraction patterns, if a single layer of these chains could be prepared.

These experiments have shown that a diffraction pattern can be obtained from a film whose scattering power is probably comparable with that of naturally occurring layers of adsorbed gas molecules; if the electron wave-length were increased to about 0.12A it would seem that this could certainly be accomplished. Thus it seems to us that the study of adsorbed gas films by means of electron diffraction patterns observed photographically waits now only upon improvement in vacuum technique.

We are greatly indebted to Dr. Irving Langmuir for the stimulus to carry out these experiments, and to him and to Dr. Katharine Blodgett and to Mr. Vincent J. Schaefer for assistance with technical details. We wish also to thank Drs. C. J. Davisson and W. Shockley and Mr. W. E. Campbell for helpful suggestions and criticisms.

LETTERS TO THE EDITOR

This section will accept reports of new work, provided these are terse and contain few figures, and especially few halftone cuts. The Editorial Board will not hold itself responsible for opinions expressed by the correspondents. Contributions to this section must reach the office of the Managing Editor not later than the 15th of the month preceding that of the issue in which the letter is to appear. No proof will be sent to the authors. The usual publication charge ($3.00 per page) will not be made and no reprints will be furnished free.

Lifetime of Free CN Radical

By use of a method similar to that described by Oldenberg[1] for his work on OH radicals, the 0,0 band of the $^2\Sigma - ^2\Sigma$ system of CN radical at λ3883 has been observed in absorption at temperatures not far above room temperature. An absorption tube, 150 cm long and 3 cm in diameter was mounted in front of the slit of the 21-foot grating with a tungsten projection bulb behind it as the source of continuous spectra. Cyanogen at low pressure was kept flowing in the tube, and at intervals a discharge was passed through it. The discharge was controlled by a switch mounted on the same shaft with an optical shutter in front of the slit. This cut out all emission from the cyanogen discharge and passed only a short flash of the continuous background. The time between the cut-off of the discharge and this flash was regulated by the angle between the opening of the switch and the open sector in the shutter.

A cylindrical quartz lens was used to increase the speed of the grating as recommended by Oldenberg.[2] Intensity marks were photographed on each plate, using a calibrated step weakener. Microphotometer traces were made of the plates, and from them the relative concentrations of CN radicals were determined for different times after the end of the discharge. To eliminate possible errors in intensities due to poor resolution of the band lines the concentrations were calculated by a method based on the comparison of lines of equal intensities in the different exposures.

The concentrations were observed to fall off approximately linearly with time at pressures below one millimeter, indicating a reaction on the walls of the tube with a rate limited by the rate of diffusion to them. At higher pressures the results are still inconclusive. The rotational temperature of the absorbing gas ranges from 500° to 300°K depending on the time after the discharge. The longest life observed was six-thousandths of a second. Further experiments at higher pressures are in progress. It is expected that the observed lifetime will increase, and that a homogeneous mechanism of recombination will appear.

JOHN UNDERHILL WHITE

Department of Physics,
University of California,
Berkeley, California,
March 19, 1938.

[1] O. Oldenberg, J. Chem. Phys. **3**, 266 (1935).
[2] O. Oldenberg, J. Opt. Soc. Am. **22**, 441 (1932).

Catalysis in the Exchanges of Organic Compounds with Heavy Oxygen Water*

Recent tests[1] of the exchanges of alcohols, aldehydes, ketones, esters and phenols with H_2O^{18} have demonstrated that, in the absence of a catalyst, exchange of oxygen takes place only with aldehydes, ketones, and trichloroacetic acid. Since the exchange reactions of ketones have been shown to be both general acid and hydroxyl ion catalyzed[2] we have performed exchange experiments with a number of organic compounds under conditions of acid and basis catalysis.

The mass spectrograph was used to determine isotopic ratios, the procedure being that of Cohn and Urey. For recovery of the water for analysis in all experiments, fractional distillation was used; in the acetic acid experiment a preliminary addition of metallic sodium was necessary. Methyl alcohol was used as a mutual solvent for the heavy oxygen water and nitrobenzene.

The results are given in Table I.

TABLE I.

SUBSTANCE	CATALYST	TIME (HR.)	TEMP. °C	NUMBER OF OXYGENS EXCHANGED
Methyl alcohol	0.1*N* HCl	24	25	0
Methyl alcohol	0.1*N* NaOH	48	25	0
Nitrobenzene	0.03*N* HCl	24	25	0
Nitrobenzene	0.03*N* NaOH	24	25	0
Potassium acetate		48	25	0
Acetic acid	0.1*N* HCl	40 days	25	2
Benzoic acid		4 hr.	100	2
Benzoic acid	0.1*N* HCl	4 hr.	100	2

The exchange of acetic acid in the presence of 0.1*N* HCl is especially significant when compared with the negative result obtained by Cohn and Urey for butyric acid in neutral solution. It seems probable that in general the exchange reactions of carboxylic acids are acid catalyzed; the exchange of benzoic acid in the absence of HCl may be due to the larger rate of exchange of this compound under the influence of its own acidity.

IRVING ROBERTS

Columbia University,
New York, N. Y.,
April 14, 1938.

* Publication assisted by the Ernest Kempton Adams Fund for Physical Research of Columbia University.
[1] Cohn and Urey, J. Am. Chem. Soc. **60**, 679 (1938); Herbert and Lauder, Trans. Faraday Soc. **34**, 432 (1938).
[2] Cohn and Urey, reference 1; Roberts and Urey, J. Am. Chem. Soc. **60**, 880 (1938).

Raman Effect in Liquid Ethane

Further study of the Raman spectrum of ethane was considered advisable because of current controversy over the question of internal rotation in this molecule and because of variances noted in the reports of previous Raman investigations. We have measured nine Raman shifts in liquid ethane at −120°C. In Table I our values are shown in comparison with those existing in the literature.

Lines 994, 2884, and 2941 cm^{-1} are strong. The latter pair arise from resonance splitting[1] due to the proximity of a fundamental with the first overtone of another. The mean of the observed pair is 2913. This corresponds to the higher fundamental. A pair of weaker diffuse lines are observed by us at 2922 cm^{-1} and 2963 cm^{-1}. These may likewise be attributed to resonance splitting. The mean value here is 2943. Doubly degenerate frequencies[2] 1463 cm^{-1} (Raman active) and 1480 cm^{-1} (infra-red active) respectively could be responsible. It will be noted that the pairs overlap. Now the 2922 cm^{-1} line probably corresponds to that observed by Lewis and Houston[3] at 2940 cm^{-1}. They do not record the presence of a single line corresponding to our 2963 cm^{-1} frequency, but this might well be one of the weak "Stokes lines" which they found in this region.

The diffuse line of medium strength 1463 cm^{-1} is present here; this was not found by Lewis and Houston; it was observed by Bhagavantam[4] but was attributed by him to some impurity. Lewis and Houston's weak shift of 1344 cm^{-1} did not appear. Bartholme and Karweil[2] list 743 cm^{-1} and 1375 cm^{-1} among the Raman active fundamentals of ethane; evidently these were deduced from specific heat data. We did not find experimental evidence for them.

Probably of isotopic origin is the weak line at 979 cm^{-1} which has been attributed to the $C^{12}-C^{13}$ molecule. This separation of 15 cm^{-1} from the corresponding frequency (994 cm^{-1}) of the normal molecule is slightly less than that reported by Bhagavantam.[4] In measurements on four plates [8 pairs of lines] we found no separations differing more than one wave number from our value.

It is of interest to note that our values for the 994 cm^{-1} and 1463 cm^{-1} vibrations are slightly higher in frequency than are the corresponding values in the gaseous state. This reverses the shift normally observed in going from liquid to gas. However, calculations by Glockler and Wall[5] have shown that the force constant for the C−C bond is higher for liquids than for gases.

Raman tubes of 30 cc capacity were employed. The three prism Steinheil spectrograph gives dispersion of 8A/mm at 4358A. Eight concentric mercury-neon lamps furnished radiation. No filters were used. All Raman lines were excited by 4047 and 4358, except for the shift 2768 cm^{-1} in which case near coincidence of lines prevents 4047 from being effective. 4078 excited only the strongest frequencies. There was little background; however, on longest exposures (16–20 hours) several unreported faint lines appeared which we have not been able to explain.

In commercial ethane the strongest lines of ethylene and propane appeared; these were not found in that prepared from EtMgBr and purified.

TABLE I.

Liquid Ethane		Gaseous Ethane	
Glockler Renfrew[7] (1938)	Daure[6] (1929)	Lewis Houston[3] (1933)	Bhagavantam[4] (1929)
979			975
994	990	993	993
		1344	
1463	1460		1460
2733		2744	
2768		2778	
2884	2890	2899	2900
2922		2940	
2941	2950	2955	2955
2963		(Stokes lines)	

GEORGE GLOCKLER
M. M. RENFREW

University of Minnesota,
Minneapolis, Minnesota,
April 6, 1938.

[1] E. Fermi, Zeits. f. Physik **71**, 250 (1931); A. Adel and E. F. Barker, J. Chem. Phys. **2**, 627 (1934).
[2] E. Bartholme and J. Karweil, Naturwiss. **25**, 476 (1937).
[3] C. M. Lewis and W. V. Houston, Phys. Rev. **44**, 903 (1933).
[4] S. Bhagavantam, Ind. J. Phys. **6**, 596 (1931).
[5] G. Glockler and F. T. Wall, J. Chem. Phys. **5**, 813 (1937).
[6] P. Daure, Ann. de physique **12**, 375 (1929).
[7] M. M. Renfrew, duPont Fellow (1937–38).

The Oxygen Exchange Reaction of Glycine Hydrochloride and Water*

The oxygen exchange reaction of acetic acid and some of its derivatives with H_2O^{18} has been studied by Cohn and Urey[1] who observed complete oxygen exchange only in the case of trichloroacetic acid in slightly acidic solution. Recently we have been enabled by a grant from the Rockefeller Foundation to carry on an investigation of the oxygen exchange reaction of H_2O^{18} with various amino acids, their derivatives and with proteins.

We have observed that glycine hydrochloride exchanges its oxygen atoms 100 percent calculated on the basis of two available oxygens per molecule. This exchange took place at 100°C within 24 hr. at a *p*H of 1.9 or slightly less in a solution containing approximately 2 molecules of the hydrochloride to 3 molecules of water. Under the same conditions of time, temperature and molecular ratio no exchange was observable with glycine itself. Analysis of the water samples was carried out by the mass-spectrograph method of Cohn and Urey.[1] These observations are in complete agreement with the results of Dr. I. Roberts, department of chemistry, Columbia University, who has obtained complete exchange of 2 oxygen atoms at room temperature between acetic acid and H_2O^{18} in $N/10$ solution of hydrochloric acid within 30 days.

WHITNEY H. MEARS

The Laboratories of the Mt. Sinai Hospital,
and Department of Chemistry, Columbia University,
New York, N. Y.,
April 5, 1938.

* Publication assisted by Ernest Kempton Adams Fund for Physical Research of Columbia University.
[1] J. Am. Chem. Soc. **60**, 679 (1938).

The Concentration of N^{15} and S^{34}*

Urey, Huffman, Thode and Fox,[1] pointed out that a further increased concentration of N^{15} could be secured by the arrangement of distillation columns in cascade. The first column should be the largest and should increase the concentration by a factor, say β, and should have a total flow β times as great as that of the second unit in the cascade. The product of the first unit is fed to the smaller second unit. This should further increase the concentration by another factor, β, and should have a total flow β times as great as that of the third unit of the cascade. In this way three units should change the ratio of the isotopes by a factor of β^3 and the total transport should be approximately the same in each unit. We have attempted to make β equal to 10 in the apparatus described here.

Our first unit consists of a 50-foot length of 3-inch glass tubing packed with Berl saddles. The second unit is a 40-foot length of 1-inch glass tubes packed with quarter-inch glass spirals of the Fenske type. The third unit is a 25 foot length of $\frac{3}{8}$-inch glass tubing packed with glass spirals. If mounted one above the other these three units would make an apparatus some 115 feet tall. We have built these in sections with a pump lifting the liquid from the first section to the top of the second and with a return tube allowing the gas of the second section to flow to the bottom of the first. In this way the entire apparatus can be mounted on one floor. Our sections are 15 feet long. The pumps consist of a rubber tube lying in a brass band with rollers compressing the rubber tube and forcing the liquid through. In this way there are no valves to cause trouble, the pump handles small amounts of sediment, and there is no "gas or vapor lock" as in piston pumps. Such pumps have worked satisfactorily for long periods of time.

Using the exchange reaction between ammonium nitrate solution and ammonia and the second and third units described above, we have produced a sample of 14.8 percent N^{15} in approximately two weeks time. When the apparatus was stopped the concentration appeared to be rising. This is a 46-fold change in the ratio instead of 100 calculated on the assumption that the number of plates in our long columns would be the same per unit length as in 3 foot and 4 foot lengths which we used for preliminary tests. About 0.15 of a gram of N^{15} was transported per 24 hours.

Using the exchange reaction between sodium bisulfate solution and sulfur dioxide, we have found that S^{34} is concentrated in the solution. In seven days using the third unit only a concentration of 6.8 percent S^{34} was secured, representing approximately a threefold increase in the concentration of this isotope. The simple process fractionation factor is 1.015 as determined from the concentration of S^{34} in the feed liquid and in the escaping sulfur dioxide gas. It thus appears possible to concentrate the sulfur dioxide of mass 34 by this method in appreciable quantities.

The first section of our apparatus has not yet been put in operation. It is designed to give a production of 1.5 grams of N^{15} per 24 hours in concentrations of about 60 percent. The same unit should produce about 3.5 grams of S^{34} in various concentrations above that of normal per 24-hour period.

A detailed report of these experiments will be made after our first unit has been placed in operation. In the meantime we can say that sufficiently increased concentrations and sufficient amounts of the isotopes N^{15} and S^{34} for many researches can be secured with comparatively inexpensive apparatus (some five or six hundred dollars) and in a short time (some two or three months).

HARRY G. THODE
JOHN E. GORHAM
HAROLD C. UREY

Columbia University,
New York, N. Y.,
April 15, 1938.

* Publication assisted by the Ernest Kempton Adams Fund for Physical Research of Columbia University.

[1] J. Chem. Phys. 5, 856 (1937).

The Hydrogen Bond and Infra-Red Absorption

Over a period of years a large amount of chemical evidence has been accumulated, which requires for its interpretation the postulate of some sort of a hydrogen bond. Whenever a hydrogen atom is attached to one of certain other atoms, it is capable of forming a link, which may complete a chelate ring or bring about the association of two molecules. Some have supposed this linkage to be due solely to dipole interaction but it seems probable that other effects, such as resonance, may contribute to the energy of the bond. The first definite test for the presence of a hydrogen bond was reported by Wulf[1] and his colleagues when they observed that the first harmonic of the hydroxyl group was absent in the infra-red absorption spectrum. This discovery has proved to be of fundamental importance because it has opened the way to the quantitative study of this phenomenon, which appears to be of widespread occurrence and significance. Soon after Wulf, *et al.*, published their results the authors began a study of the infra-red absorption of substances likely to show hydrogen bonding. In addition to confirming the results of Wulf and his collaborators we discovered that the fundamental absorption of the hydroxyl group was shifted from a normal value of 2.7μ to the neighborhood of 3.0μ.[2] This fact was fully confirmed by the substitution of deuterium for hydrogen in the hydroxyl group.

Recently Herman and Hofstadter[3] have made a similar use of deuterium in identifying the frequency associated with hydrogen bonding in acetic acid vapor. They were apparently unaware of our work along this line and suggest that the normal hydrogen bond frequency is to be expected at 3.3μ. Actually they obtain for the deuterium frequency 4.3μ which indicates a frequency of 3.1μ for the normal hydrogen bond. This is sufficiently near the frequency that we have reported in other types of molecules. In our first report,[2] however, we noted the variation in the hydrogen bond frequency with the nature of the molecule and there are various reasons why the hydrogen bond in acetic acid may be considerably different from that in the alcohols. For example, the results of electron diffraction indicate a symmetrical ring with two bonds. Another factor of some significance is the ionization constant of the hydrogen.

Gillette and Daniels[4] observed a very complex spectrum in the neighborhood of the C−H band. We believe from our observations upon the carboxylic acids that the hydrogen bond absorption gives a maximum near 3.2μ which is practically the wave-length of the C−H. As a result of this superposition one might expect interaction or resonance effects, which may be lacking in the deuterium substituted compounds. Most of the absorption throughout this region, however, seems to be due to the particular type of hydrogen bonding present. This point will be discussed in detail elsewhere.

A. M. Buswell
W. H. Rodebush

University of Illinois,
Urbana, Illinois,
March 18, 1938.

[1] Hilbert, Wulf, Hendricks and Liddell, J. Am. Chem. Soc. **58**, 548 (1936).
[2] Buswell, Deitz and Rodebush, J. Chem. Phys. **5**, 84, 501 (1937).
[3] Herman and Hofstadter, J. Chem. Phys. **6**, 110 (1938).
[4] Gillette and Daniels, J. Am. Chem. Soc. **58**, 1139 (1935).

A Spectroscopic Study of the Symmetries of the Fields About Ions in Solution

Bethe[1] has shown on general theoretical grounds what groups of levels arise from a particular energy level when an atomic or ionic system is subject to electrical fields of different symmetries. In place of the single line in the spectrum of the unperturbed atom or ion, a group of lines make their appearance and in general, the less symmetrical the field, the more numerous the lines. A particular example of such a "splitting" of the levels by an electrical field is the Stark effect. The general theory has found a natural application in the spectra of crystals of the rare earths. For our present purpose, we shall call attention to one of the recent confirmations. In this work it was found that the monoclinic crystal of praeseodymium $Pr_2(SO_4)_38H_2O$ has 30 lines in the group at 5920A whereas the trigonal crystal $3Mg(NO_3)_22Pr(NO_3)_324H_2O$ has five lines. In the group at 4670A the monoclinic crystal has 27 lines and the trigonal 6. From this it is to be inferred that the microscopic symmetry of the fields about the Pr^{+++} in the trigonal crystal is higher than in the monoclinic.

The unusual sharpness of the spectra possessed by *solutions* of trivalent europium made it appear likely that the groups induced by the fields in solution might be resolved and their component lines counted. We would then be in position to observe whether the groups change their structure when Eu^{+++} is present under different conditions. The number of components would permit attempts to assign definite symmetries. (The basic energy levels of the "unperturbed" Eu^{+++} are regarded as known.)

All of the europium salts we have investigated had as their origin europium oxalate of high purity which Dr. H. N. McCoy had generously presented for our work. He had purified europium from the other rare earths by the methods he has recently described.[3]

The absorption spectra of the solutions we have taken are exceptionally sharp both in the visible and ultraviolet regions. In this note, however, we shall consider a group in the blue only. This group as observed with a solution of europium chloride consists of four components (4640A; 4645A; 4649A; 4658A) with the inner two somewhat diffuse. A solution of the nitrate has three distinct lines in the group (4644A; 4648A; 4654A). These structures persist throughout the whole range of concentrations which we have studied, from about 1 molal to about 0.01 molal. The definiteness of structure and the persistence of both patterns without change of wave-length is especially interesting along side the fact that the freezing point lowering of lanthanum nitrate (a rare earth nitrate isomorphic with europium) at 0.01 molal is from three to four times as great as a non-electrolyte of the same concentration produces. The reference to lanthanum brings out the point that we look upon Eu^{+++} as an indicator for the symmetries of the fields about the other rare earth ions, of more general interest about the spherically symmetrical gadolinium ion Gd^{+++} and lanthanum ion La^{+++}. The latter has the electronic structure of the rare gas xenon and has been a favorite trivalent ion in the thermodynamic chemistry and hence accurate freezing point data are available.

Based on the smaller number of lines in the spectra, we ascribe a higher symmetry to the electric fields about Eu^{+++} in the solutions of the nitrate than about Eu^{+++} as the chloride. When the nitrate was dehydrated and dissolved in anhydrous ether the group stood out as two strong lines. The still greater symmetry of the fields in the ether solution is in keeping with the accepted notion that a higher symmetry is more probable in nonpolar solvents.

To discover whether a redistribution of the fields can be made to occur when another electrolyte is added, we added magnesium nitrate to a dilute solution of europium nitrate in the same molal proportion of magnesium to rare earth as exists in the trigonal crystal of praeseodymium which we have already referred to. Magnesium nitrate itself is completely transparent in this region. With a dilute solution, the familiar triplet of europium nitrate appeared. With a concentrated solution which was really supersaturated, the spectrum was greatly altered. Two strong absorption lines now formed the group instead of the three. It seems then that in the presence of magnesium nitrate, a greater symmetry has been achieved about Eu^{+++} in solution and that the symmetrical arrangement within the crystal does not come into being entirely as the crystal grows.

We are continuing with these researches and we shall discuss in a more complete and detailed paper the particular symmetry about europium in each of the solutions.

Simon Freed
S. I. Weissman

G. H. Jones Laboratory,
University of Chicago,
Chicago, Illinois,
April 9, 1938.

[1] H. Bethe, Ann. d. Physik **3**, 133 (1929).
[2] A. Merz, Ann. d. Physik **28**, 569 (1937).
[3] N. N. McCoy, J. Am. Chem. Soc. **57**, 1756 (1935).

Note on Surface Viscosimetry

Dervichian and Joly[1] have recently corrected an equation of Bresler and Talmud,[2] which describes the viscous flow of a monolayer through a canal above a fluid substrate. While pointing out its qualitative agreement with their experimental results, they express pessimism as to the possibility of an adequate theoretical treatment of the problem. At the same time they dismiss an equation developed by us[3] as inapplicable to surface viscosimeters of current design. This leads us to make several comments on the theoretical and practical aspects of the problem.

The relation between our theory and that of Bresler and Talmud is most easily clarified by a statement of the physical assumptions made in each case. Bresler and Talmud assume complete slip between the substrate and film, introducing a resistance term into the hydrodynamical equation for the film, proportional to its velocity relative to the stationary substrate. We, on the other hand, assume no slip between film and substrate and introduce a resistance term proportional to the normal velocity gradient at the film-substrate boundary. In view of the fact that the substrate is a viscous fluid, our assumption appears to be in better accord with ordinary hydrodynamical ideas. Moreover, since our resistance term depends upon the viscosity coefficient of the substrate, we are not forced to introduce an arbitrary frictional constant as are Bresler and Talmud.

Dervichian and Joly state that our equation applies only to deep canals, but this is not the case. It is only necessary that the bottom of the canal be closed. From the practical standpoint, however, a deep canal needs no bottom. Our equation for the area flux, A, may be written to an adequate approximation as follows,

$$A=\frac{\alpha a^3}{12\eta}\left[1+\frac{a\eta_0}{\pi\eta}\coth\left(\frac{\pi h}{a}\right)\right]^{-1}, \tag{1}$$

where α is the film pressure gradient, a and h the width and depth of the canal, η_0 and η the respective viscosity coefficients of substrate and film. We remark that Eq. (1) predicts the same type of limiting dependence on the canal width, a, as the corrected Bresler-Talmud formula. If both a/h and $a\eta_0/\eta$ are small relative to unity, Eq. (1) reduces effectively to the surface analog of Poiseuille's formula,

$$A=\alpha a^3/12\eta. \tag{2}$$

On the other hand, if the canal is broad and shallow with a/h and $a\eta_0/\eta$ large relative to unity, the limiting form is,

$$A=(\alpha\pi^2 h/12\eta_0)a, \tag{3}$$

in which the flux is proportional to the first power of the canal width and is independent of the film viscosity. These are exactly the features which led Dervichian and Joly to favor the Bresler-Talmud equation.

It does not seem a valid criticism of our equation that it is inapplicable to surface viscosimeters of current design. Rather, the possibility of developing an accurate theory for a special type of canal would seem to be a recommendation for the redesign of the instrument and the abandonment of models for which the integration of the hydrodynamical equations is prohibitively difficult. However, we are in agreement with Dervichian and Joly that there are many practical difficulties to be overcome before the canal viscosimeter can be regarded as an accurate instrument. Turbulence effects, difficult of correction, may be a source of trouble. One might expect them to be particularly dangerous with wide short slits of the type sometimes used by Dervichian. It may also be difficult to prevent some slip of the film at the edges of the canal due to imperfect contact. Compressibility of the film and variation of its viscosity with pressure, by no means negligible factors in many cases, greatly complicate the hydrodynamical equations. Their effect could be minimized by regulating the exit pressure in the canal so that the total pressure drop is small relative to the entrance pressure. Unfortunately, this procedure entails considerable difficulty in the design and operation of the viscosimeter.

W. D. HARKINS
J. G. KIRKWOOD

University of Chicago,
Chicago, Illinois,
April 15, 1938.

[1] Dervichian and Joly, J. Chem. Phys. **6**, 226 (1938).
[2] Bresler and Talmud, Physik. Zeits. Sowjetunion **4**, 864 (1933).
[3] Harkins and Kirkwood, J. Chem. Phys. **6**, 53 (1938).

A Temperature Effect in the Infra-Red Spectrum of Phenol

As part of a research program on various organic compounds,* the infra-red spectrum of phenol, from 1μ to 15μ, was determined at temperatures of 25°C, 42°C, and 101°C. The spectrometer[1] used was a Wadsworth mounting of a rocksalt prism. The absorption cells were made from partially cleaved rocksalt plates and gave a sample thickness of about 0.01 mm.

The transmission curves in Fig. 1 show that the principal effect of a temperature change is a shift in the positions of the three absorption bands found at about 3μ, 7.4μ, and 8.2μ. The band found at 3.1μ in the spectrum of phenol at 25°C (solid phenol) shifts to 2.96μ when the phenol is melted (42°C) and shifts slightly further (2.92μ) when the liquid phenol is heated to 101°C. The position of the ν(O−H) absorption, 2.96μ, in liquid phenol agrees well with the position of this band as found by Gordy and Nielsen[2] in the spectra of concentrated solutions of phenol in various solvents. The small shift of this band when the temperature was raised to 101°C indicates that the degree of association has not been appreciably changed. The shift of this band to 3.1μ in the spectrum of solid phenol may be due to further association of the "hydrogen bond" type mentioned by Gordy and Nielsen or to forces involved in the crystal structure.

The bands, found at 7.33μ and 8.16μ in solid phenol, shift to longer wave-lengths as the temperature is increased. These shifts are approximately continuous with temperature as contrasted with the shift in the 3μ band. In addition to the wave-length shift, the 8.16μ band increases markedly in intensity and breadth when the sample is melted. The changes in the 8.16μ band mentioned above

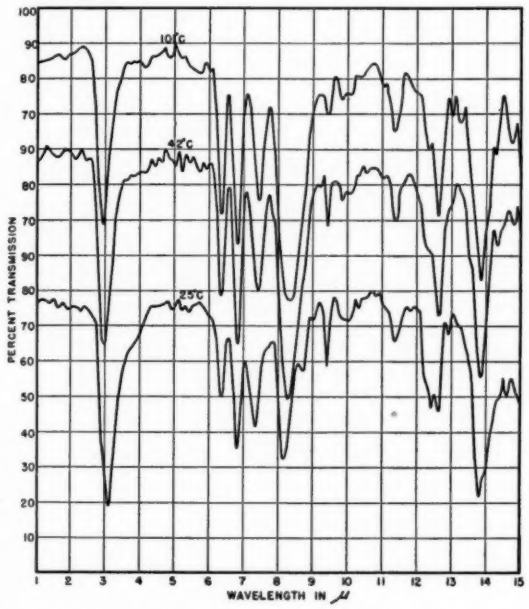

FIG. 1. The transmission spectra of phenol at various temperatures. Cell thickness approximately 0.01 mm.

and the fact that bands at approximately this wave-length are found in the spectra of a large number of compounds containing OH constitute evidence that this band is connected with the hydroxyl group.

R. ROBERT BRATTAIN

Princeton University,
Princeton, N. J.,
April 12, 1938.

* In collaboration with Research Department, Calco Chemical Co. Inc.

[1] R. B. Barnes, R. R. Brattain and F. Seitz, Phys. Rev. **48**, 582 (1935).

[2] W. Gordy and A. H. Nielsen, J. Chem. Phys. **6**, 12 (1938).

Effect of Deuterium Substitution on Color*

Although it is well known that substitution of a deuterium for a hydrogen atom in a compound modifies the physical properties of the compound, still there is no case recorded in the literature where such a substitution changes the color of the compound. Such a color change has been observed by us with nitroethane under special conditions.

When an equivalent quantity of $Ba(OD)_2$ is added to about $0.02N$ proto-nitroethane in heavy water, a proton is removed from the nitroethane to yield the ion $CH_3CH=NO_2^-$ according to the equation:

$$2CH_3CH_2NO_2+Ba^{++}+2OD^- = 2CH_3CH=NO_2^-+Ba^{++}+2HOD. \quad (1)$$

If to this solution be added now an equivalent quantity of D_2SO_4, a deuteron is reintroduced into the nitroethane to yield:

$$2CH_3CH=NO_2^-+Ba^{++}+D_2SO_4 = 2CH_3CHDNO_2+BaSO_4\downarrow. \quad (2)$$

Throughout these operations the solution remains perfectly colorless.

However, if an equivalent quantity of $Ba(OD)_2$ be again added, the solution turns *light yellow* very rapidly. In this case the reaction involved is:[1]

$$2CH_3CHDNO_2+Ba^{++}+2OD^- = 2CH_3CD=NO_2^-+Ba^{++}+2HOD. \quad (3)$$

The color can be discharged and brought back by repeated alternate additions of D_2SO_4 and $Ba(OD)_2$.

These same operations with $CH_3CH_2NO_2$ in light water and with $Ba(OH)_2$ and H_2SO_4 yield no colored solutions.

It will be observed that the only difference between the products in Eq. (1), where there is no color, and Eq. (3), where the yellow color appears, is in the nitroethane ion. In the former the ion is $CH_3CH=NO_2^-$, while in the latter it is $CH_3CD=NO_2^-$, the difference being in the substitution of a deuterium for a hydrogen atom on the carbon α to the nitro group.

From these observations in both H_2O and D_2O it can be concluded that $CH_3CH_2NO_2$, CH_3CHDNO_2, $CH_3CD_2NO_2$ and $CH_3CH=NO_2^-$ are colorless, while the ion $CH_3CD=NO_2^-$ is colored a light yellow in solutions about $0.02N$ with respect to nitroethane. Preliminary absorption measurements indicate that absorption starts at 5000–5200A and continues into the ultraviolet.

Because of the possible connection between the development of color and ease of proton and deuteron transfer in conjunction with acid-base catalysis and acid strength ultraviolet and visible absorption spectra are being investigated.

SAMUEL H. MARON
VICTOR K. LAMER

Department of Chemistry,
Columbia University,
New York, N. Y.,
March 29, 1938.

* Publication assisted by Ernest Kempton Adams Fund for Physical Research of Columbia University.

[1] Wynne-Jones, J. Chem. Phys. **2**, 381 (1934).